

118

MARTIN MARIETTA ENERGY SYSTEMS LIBRARIES



3 4456 0361389 1

CENTRAL RESEARCH LIBRARY
DOCUMENT COLLECTION

ORNL-2745
Controlled Thermonuclear Processes
TID-4500 (15th ed.)

PROCEEDINGS OF SYMPOSIUM ON MAGNETIC FIELD DESIGN
IN THERMONUCLEAR RESEARCH
HELD AT GATLINBURG, TENNESSEE
DECEMBER 11 AND 12, 1958

**CENTRAL RESEARCH LIBRARY
DOCUMENT COLLECTION
LIBRARY LOAN COPY
DO NOT TRANSFER TO ANOTHER PERSON**

If you wish someone else to see this document, send in name with document and the library will arrange a loan.



OAK RIDGE NATIONAL LABORATORY
operated by
UNION CARBIDE CORPORATION
for the
U.S. ATOMIC ENERGY COMMISSION

Printed in USA. Price \$2.25. Available from the
Office of Technical Services
Department of Commerce
Washington 25, D. C.

LEGAL NOTICE

This report was prepared as an account of Government sponsored work. Neither the United States, nor the Commission, nor any person acting on behalf of the Commission:

- A. Makes any warranty or representation, expressed or implied, with respect to the accuracy, completeness, or usefulness of the information contained in this report, or that the use of any information, apparatus, method, or process disclosed in this report may not infringe privately owned rights; or
- B. Assumes any liabilities with respect to the use of, or for damages resulting from the use of any information, apparatus, method, or process disclosed in this report.

As used in the above, "person acting on behalf of the Commission" includes any employee or contractor of the Commission, or employee of such contractor, to the extent that such employee or contractor of the Commission, or employee of such contractor prepares, disseminates, or provides access to, any information pursuant to his employment or contract with the Commission, or his employment with such contractor.

ORNL-2745
Controlled Thermonuclear Processes
TID-4500 (15th ed.)

Contract No. W-7405-eng-26

PROCEEDINGS OF SYMPOSIUM ON MAGNETIC FIELD DESIGN
IN THERMONUCLEAR RESEARCH
HELD AT GATLINBURG, TENNESSEE
DECEMBER 11 and 12, 1958

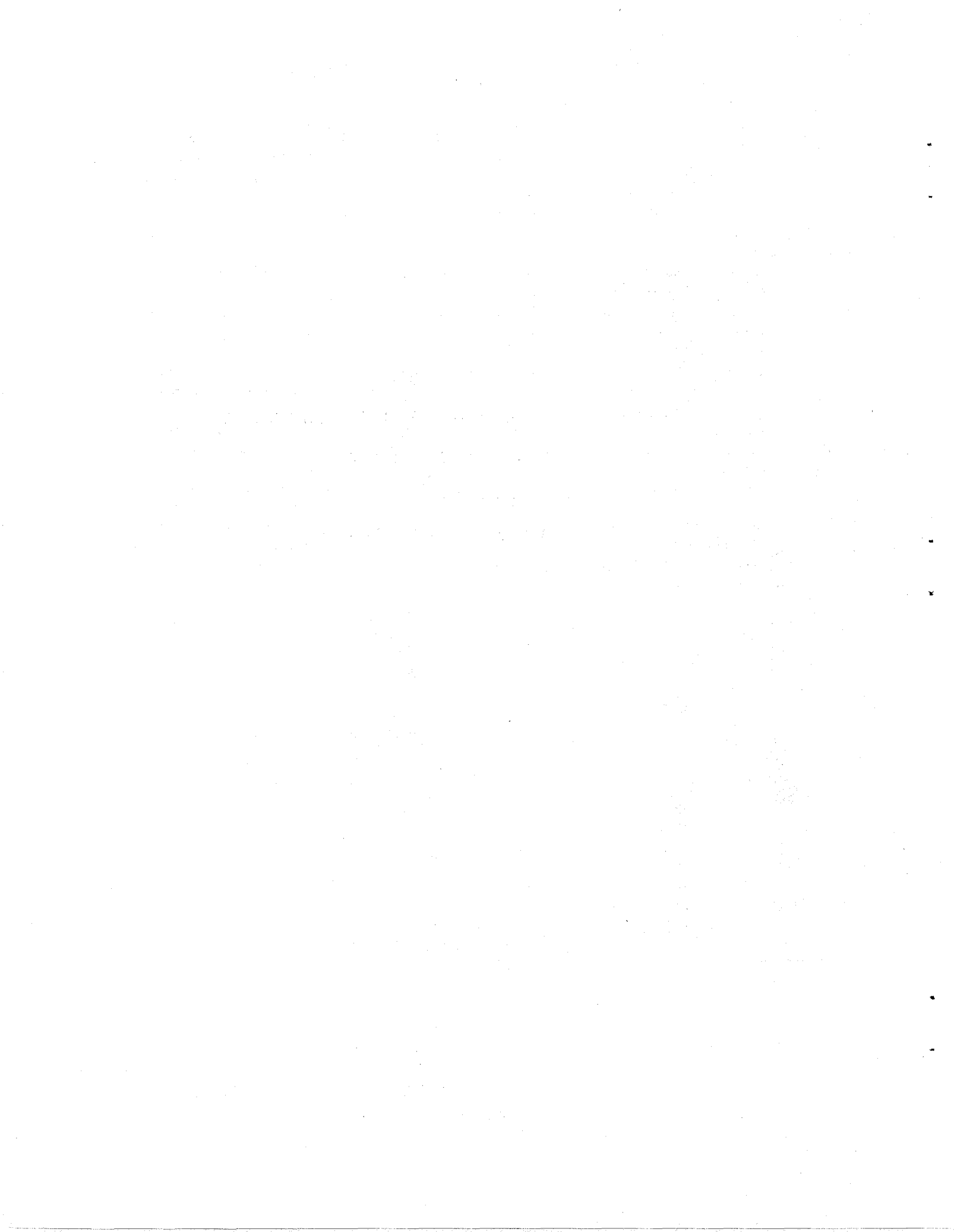
DATE ISSUED

SEP 23 1959

OAK RIDGE NATIONAL LABORATORY
Oak Ridge, Tennessee
operated by
UNION CARBIDE CORPORATION
for the
U. S. ATOMIC ENERGY COMMISSION



3 4456 0361389 1



FOREWORD

Arthur H. Snell
Assistant Director
Oak Ridge National Laboratory

The demands of the varied thermonuclear experiments that are appearing around us have led to the design of magnetic fields of novel configurations, often with carefully-controlled field contours and conforming to exacting specifications. A classical realm of physics emerges today with new importance and new interest. On a wide scale, physics also today demands magnetic fields of greater intensity and of longer duration than ever before, so that limiting problems of mechanical strength in windings and of heat dissipation insist upon solution. The importance of conferences of this kind ranges beyond Project Sherwood alone; accelerator technology and cryogenics are only two of the many allied branches of science that are directly interested in magnet development. When one thinks of the wealth that is presently being invested in large magnets throughout the world, an economic importance adds itself to the scientific in requiring examination and re-examination of the fundamentals of magnet engineering. It is in this framework that this symposium was conceived, and the papers that follow show that the ingenuity of physicists and engineers is capable of rising to the occasion. Although this particular symposium has been organized at the instance of the Oak Ridge National Laboratory, it is to be hoped that this will be only the first of a series of meetings within the Sherwood Project devoted to a subject that we all hope will develop swiftly until magnetic fields of new intensities and configurations are within easy technical grasp.

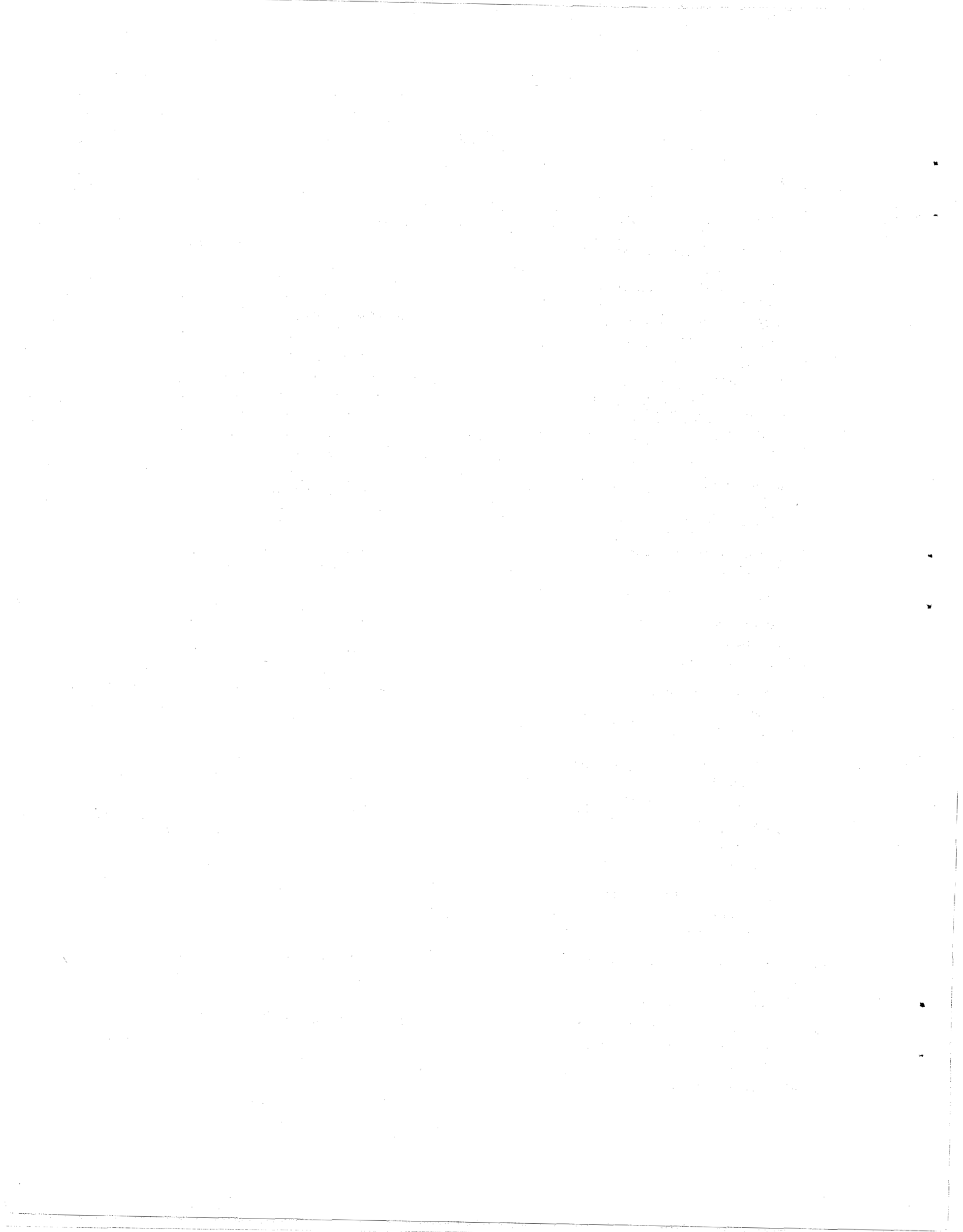
Chairman of Symposium: W. F. Gauster

Chairman of 1st Session: E. D. Shipley

Chairman of 2nd Session: R. Carruthers

Chairman of 3d Session: R. G. Mills

Chairman of 4th Session: P. R. Bell



CONTENTS

Foreword.....	iii
A. H. Snell Oak Ridge National Laboratory	
1. Brief Review of Heat Transfer Problems Encountered in the Production of Magnetic Fields	1
L. G. Alexander Oak Ridge National Laboratory	
2. Some of the Thermal Problems Involved in the Design of the Confining Field Coils for the C Stellarator	1
F. J. Arnaud Princeton University	
3. Computations of Magnetic Fields from Tabulated Data	7
C. E. Bettis Oak Ridge National Laboratory	
4. Magnetic Coil Design for DCX-1	8
E. S. Bettis Oak Ridge National Laboratory	
5. Magnetic Switching Devices	10
R. Carruthers Atomic Energy Research Establishment, Harwell	
6. An Analog Board for Time-Varying Axial Symmetrical Fields	13
U. Christensen Princeton University	
7. Pulsed Magnetic Fields	15
S. Foner Massachusetts Institute of Technology	
8. Boiling Burnout with Vortex Coolant Flow	19
W. R. Gambill Oak Ridge National Laboratory	
9. Magnetic Field Design for DCX-2 Experiments	21
W. F. Gauster Oak Ridge National Laboratory	
10. Some Basic Concepts in Magnetic Field Theory	22
W. F. Gauster Oak Ridge National Laboratory	
11. Construction and Fabrication Features of Some Magnet Coils Used in Fusion Studies	22
E. I. Hill University of California	
12. Design and Development Experiences with High-Temperature Stabilizing Windings for Project Matterhorn B-3 Machine	25
H. G. Johnson Princeton University	

13. The Generation of Higher Continuous Fields	41
H. H. Kolm Massachusetts Institute of Technology	
14. Refrigeration of Magnet Coils	44
H. L. Laquer Los Alamos Scientific Laboratory	
15. The Production of Pulsed Magnetic Fields at AFCRC	48
M. A. Levine Air Force Cambridge Research Center	
16. Magnetic Field Design and Construction Experience at Princeton	51
R. G. Mills Princeton University	
17. Proximity Effect and Its Importance to the Pulsed Field Designer	59
F. Tenney and D. R. Wells Princeton University	
18. The Use of Analog Computers in the Design of Magnetic Field Systems	61
K. E. Wakefield Princeton University	
19. Optimization of D-C Coil Design with Respect to Coil Fabrication Cost and Cost of Installed D-C Power	68
A. F. Waugh University of California	
20. Some Aspects of Heat Dissipation from Aluminum-Foil Coils	72
A. F. Waugh University of California	
21. Synthesis of Inhomogeneous Magnetic Fields	74
D. R. Whitehouse Massachusetts Institute of Technology	
22. Magnetic Field Problems Associated with the Los Alamos Thermonuclear Experiments.....	79
F. L. Ribe Los Alamos Scientific Laboratory	
The Role of Magnetic Fields in Fusion Research (presented but not published)	
A. Simon Oak Ridge National Laboratory	

1. BRIEF REVIEW OF HEAT TRANSFER PROBLEMS ENCOUNTERED IN THE PRODUCTION OF MAGNETIC FIELDS¹

L. G. Alexander
Oak Ridge National Laboratory

ABSTRACT

The design of internally cooled electrical coils for the production of high-intensity magnetic fields presents many new aspects and combinations of the familiar modes of heat transfer. However, the customary methodology appears to be sufficient for preliminary analysis and understanding of the problems. This methodology comprises the derivation of a qualitative, approximate equation expressing the relative performance of the various parts of a system, followed by an examination of this equation in order to locate the limiting features of the system. These features are then investigated by more rigorous methods, which in turn provide guidance for development research in the laboratory.

¹L. G. Alexander, *A Brief Review of Heat Transfer Problems in the Production of Magnetic Fields*, ORNL CF-59-5-87 (to be published).

2. SOME OF THE THERMAL PROBLEMS INVOLVED IN THE DESIGN OF THE CONFINING FIELD COILS FOR THE C STELLARATOR

F. J. Arnaud
Project Matterhorn - Princeton University

INTRODUCTION

The model C-1 Stellarator will be a large thermonuclear experimental device to be built at the James Forrestal Research Center for the Project Matterhorn. The device may be best described as a race-track-shaped vacuum vessel enclosing an ionized gas (plasma), which is surrounded by confining coils. This race track will be threaded by a large magnetic field whose purpose it is to confine the plasma to the central region of the vacuum vessel.

Confining Field Coils. - The axial field in the vacuum vessel will be produced by a number of coils known as confining field coils placed along the axis (472 in. in length) of the race track. These coils are designed to produce a field of 55,000 gauss in the volume enclosed by the vacuum vessel (approximately 24,000 in.³).

Energy Consideration. - The maintenance of a 55,000-gauss field through a length of 472 in. requires 52 million ampere turns. It is also desired to bring the flux to this level in approximately one second, maintain the level for one second, and then bring the current to zero in approximately $\frac{1}{2}$ second. Generator capacity to supply the energy for this field and for ohmic losses will be approximately 200 million watts.

COIL DESIGN

Obviously 200,000 kw in coils as small as these will produce thermal problems. The hottest spot temperature is one of the major elements that limit the capability and lifetime of any electrical equipment. In working to optimize the coil design it is essential to be able to calculate

with reasonable speed and accuracy the hottest spot temperature in order to be able to evaluate the desirability or practicality of various conductor sizes, shapes, and cooling means. For the temperature ranges here considered water coolant has been selected. The conductor will have a central longitudinal hole for a water circulatory path.

This introduces several independent variable parameters such as:

1. size and shape of central conductor hole,
2. the number and length of water paths,
3. the velocity and direction of flow.

These parameters will influence the temperature of the conductors as follows:

1. Increasing the size of the hole will reduce the net area of the conductor and thus increase the resistance and therefore the I^2R loss. This will increase the heat to be stored while reducing the weight of copper in which this heat must be stored. Thus the size of the hole will doubly influence the cyclical transient of stored heat.
2. The shape of the hole will influence the length of the heat conduction path between the most distant part of the copper and the copper-water dividing surface and thus the temperature drop between them.
3. The shape of the hole will also influence the area of the water-copper dividing surface and thus the temperature drop through the thin film of stagnant water which adheres to the surface.
4. The velocity of the water will affect the thickness of the film of stagnant water and thus the temperature drop through this film.
5. The velocity of the water and the cross-sectional area of the hole will determine the quantity of water which will flow to the cooling path. A water velocity of 10 fps was selected to be used in order to ensure turbulent nonlaminar flow to as great extent as possible and at the same time to minimize the possibility of cavitation. This velocity was used throughout all studies of temperature rises. The number and length of the water paths will determine the heat to be removed when the water flows through each cooling path.
6. The direction of water flow will determine which copper is in contact with the coolest water and which copper is in contact with the hottest water.

The complete problem can be stated as follows:

Given a conductor width W_{Cu} (maximum dimension) and net copper cross-sectional area A_{Cu} having a central water hole with a width W_H (in same directions as the W_{Cu}), net area A_H , and transverse perimeter P_H . This conductor is worked at a current density which gives a watt loss per pound of W/lb for a repetitive equivalent square wave pulse duration of t seconds at duty cycle $D.C.$ Water circulates in the water path L ft long at a velocity of V ft/sec. What is the hottest spot temperature?

This problem can be greatly reduced in complexity if the following assumptions are made:

1. Assume that no heat is conducted along the length of the copper. A quick calculation of the heat conducted along the copper due to the slight gradient along the length of the copper shows this to be infinitesimal compared to the heat generated per unit length.

2. If the problem is broken down into separate elements where the temperature drop in the copper is calculated as one element and the temperature drop in the film of stagnant water at the copper-water dividing surface another element, then two merely balancing interrelated assumptions can be made. First, to calculate the internal temperature drop in the copper, assume that the conductor is changed to annular cylinder of revolution with an ID equal to the maximum diameter of the hole and an outer diameter equal to W_{Cu} . All copper is at the same watts per pound as in the original conductor. This is the same as assuming that the path of heat flow along the greatest length of copper path is radial to the center of the copper. This is pessimistic and results in this temperature drop being too large. The second assumption is that at the copper-water dividing plane the heat flow lines are perpendicular to the dividing surface and equally spaced. This implies that each unit area of the copper-water dividing surface carries the same heat and has the same temperature drop. By itself this last statement is a trifle optimistic but the net resulting calculation of temperature drop between the water and the most distant hottest-spot copper is very nearly accurate. In the coils of the C Stellarator the value of these two elements of temperature rise were small; therefore any error will be negligible.

In investigating the influence of various parameters on the temperature of the hottest-spot copper it is convenient to divide the total temperature of the copper at any location into separate elements as follows:

$$t^{\circ}C = a^{\circ} + b^{\circ} + c^{\circ} + e^{\circ} - f^{\circ}$$

where

a° = ambient temperature in $^{\circ}C$ (temperature of incoming water),

b° = water rise in $^{\circ}C$ from inlet to the location considered,

c° = temperature rise in $^{\circ}C$ through the surface film at the copper-water dividing surface,

d° = rise in $^{\circ}C$ through the copper from the duct to the hottest point of the exterior surface (in a plane normal to the conductor),

(All the above four elements are calculated on a time-average basis.)

e° = cyclical transient rise in $^{\circ}C$ due to heat stored during the pulse (this element is calculated on a pulse basis),

f° = decrement in $^{\circ}C$ by which the hottest copper is below the time-average at the beginning of the pulse.

This last element compensates for the fact that the first four elements are computed on an average basis.

The evaluation of each one of these elements separately is much easier than trying to evaluate the whole problem at once and introduces less error than the errors that are beyond control—such, for example, as the roughness of the interior surface of the copper or the wandering of the hole.

These elements can be evaluated as follows:

Ambient Temperature

a° = the temperature of the incoming water and is not influenced by any of the parameters under consideration here.

Water Rise

$$b^{\circ} = \frac{0.321}{4.187 \times 12 \times 2.54 \times 6.45} \times \frac{W/lb \times L \times A_{Cu} \times D.C.}{V \times A_H}$$

where

0.321 = density of copper in lb/in.³,

4.187 = cal/joule,

12 × 2.54 = cm/ft,

6.45 = cm²/in.²,

W/lb = I²R loss in watts/lb,

L = distance from water inlet in in.,

A_{Cu} = net conductor area in in.²,

D.C. = duty cycle,

V = velocity of water in ft/sec,

and

A = area of water in hole in in.².

This reduces to

$$b^{\circ} = 3.90 \times 10^{-4} \times \frac{W/lb \times L \times A_{Cu} \times D.C.}{V \times A_H}$$

Surface Film Rise

$$c^{\circ} = \frac{0.321}{8} \times \frac{A_{Cu} \times W/lb \times D.C.}{P}$$

where

8 = thermal conductivity of the surface film in w/in.²/°C. This is a fairly conservative value for the average range of velocities, Reynolds numbers, and Prandtl numbers for the conditions existing in these cooling circuits.

P = the transverse perimeter of the cooling duct in in.

This reduces to

$$c^{\circ} = 4.01 \times 10^{-2} \frac{A_{Cu} \times W/lb \times D.C.}{P}$$

Internal Copper Rise

$$d^{\circ} = \frac{0.321}{4.187 \times 0.918 \times 2.54} \times W/lb \times D.C. \times \frac{1}{16} (W_H^2 - W_c^2 + 2W_c^2 \log_e W_c/W_H)$$

where

0.918 = thermal conductivity of copper in $\text{cal}\cdot\text{sec}^{-1}\cdot\text{cm}^{-2}\cdot^{\circ}\text{C}^{-1}\cdot\text{cm}$,

2.54 = cm/in.,

W_c = maximum cross-section dimension of the copper in in.,

W_H = dimension of the hole in in. in the same direction as W_c , and all others as previously defined.

This reduces to

$$d^{\circ} = 2.05 \times 10^{-3} W/lb \times D.C. (W_H^2 - W_c^2 + 2W_c^2 \log_e W_c/W_H) .$$

Cyclical Transient

$$e^{\circ} = \frac{1}{175.8} (1 - D.C.) W/lb \times t ,$$

where

175.8 = thermal capacity of copper in $\text{w}\cdot\text{sec}\cdot\text{lb}^{-1}\cdot^{\circ}\text{C}^{-1}$,

t = equivalent square-wave pulse time in sec, and all others as defined before.

This reduces to

$$e^{\circ} = 5.688 \times 10^{-3} (1 - D.C.) W/lb \times t .$$

Decrement

Under continuous pulsing, each temperature involved in this problem will have a cyclical transient which will consist of two exponential curves. During the pulse the temperature will follow a rising exponential. Since the pulse is of a very short duration this portion of the temperature curve will be essentially a straight line. The decreasing temperature curve will also follow an exponential. Because of the greater cooling time this curve will depart much more from a straight line. The magnitude of this transient will vary with the location within the copper or the water. Thus, the farther along in the path from the heat source to the heat sink the smaller will be the transient due to the attenuation analogous to that of an electrical impulse wave traveling through an RC network. Figure 1 shows the relation between average and final temperatures vs the length of the cooling period expressed in time constants. The difference between the average and the final temperatures is also plotted against the time of the cooling period. Thus this curve can be used to evaluate the approximate value of the decremental temperature item f° . Since for most of these coils the system thermal time constant is of the order of 72 sec and the cooling period is 37 sec, the period is approximately one-half a time constant. Therefore, the decrement is approximately 20 to 25% the sum $b^{\circ} + c^{\circ} + d^{\circ}$. This factor f° could have been used as a multiplier on the factors b° , c° , and d° , in which case it would have the value of T final/ T average of

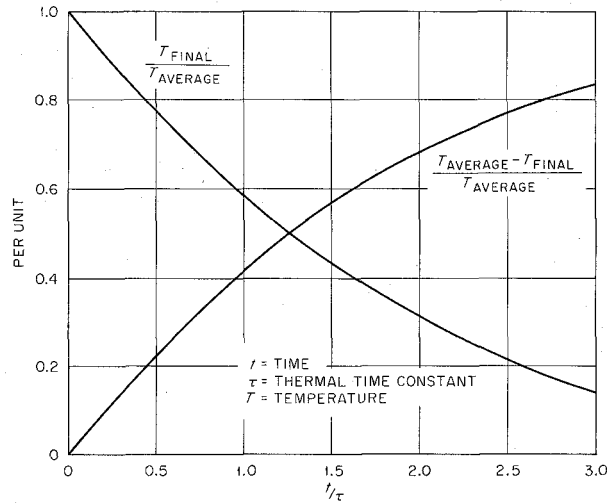


Fig. 1. Relation of Average and Final Temperatures vs Cooling Time.

Fig. 1. However, from a practical angle it is simpler to calculate b° , c° , and d° , ignoring f° and later to apply f° as a correctional decrement; or if f° is small enough it may be ignored and taken as a factor of safety – the procedure used in all preliminary design work when copper sizes and shapes were being selected.

CONCLUSIONS

The applicability of this method to an accurate determination of hot-spot temperature requires a semiaccurate determination of the thermal time constant of the coils. At first it was believed that the use of lumped parameters in the determination of the time constant of the coils would so poorly represent the distributed parameters as to cast serious doubt on the accuracy of the time constant values and, therefore, on the final answers. However, when the coil designs for certain of the coils for the C-1 Stellarator were sufficiently established, computer studies of their temperatures were made. The computer studies did not lump the parameters but distributed them exactly as they are distributed in the actual copper except for the assumptions outlined above which circularized the copper cross section. A comparison of the computer study vs this short method indicates approximately a 2% error.

3. COMPUTATIONS OF MAGNETIC FIELDS FROM TABULATED DATA

C. E. Bettis
Oak Ridge National Laboratory

It is well known that the magnetic field for circular loops can be expressed by means of elliptic functions of the first and second kind. Tables^{1,2} are available from which such fields can be computed. The field of a cylindrical current sheet requires the integration of these elliptic functions over the length of the sheet. Müller³ and Foelsch⁴ have shown that such fields can be expressed in closed forms involving elliptic functions of the first and third kind. Foelsch published formulas and tables⁵ which simplify considerably the computation of the field of cylindrical current sheets. This work was not available in the U.S.A.; however, it was possible to secure it on microfilm from the Bavarian State Library.

From Foelsch's tables the field strengths for a semi-infinite current sheet were calculated and the results put in graphical form. The graph consists of a family of curves showing axial field strength vs normalized distance from the face of the semi-infinite current sheet. Each curve of the family represents the field strength at a given distance from the axis of the current sheet.

The application of the graph data to specific coil problems generally requires the plotting of the axial field strength vs distance from the cylinder axis at a given distance from the face of the coil in question. The field at the plane selected is the field resulting from a semi-infinite current sheet whose face coincides with the nearer face of the given coil, minus the field resulting from a semi-infinite current sheet whose face coincides with the farther face of the coil in question. The value of the axial field strength in each case is normalized to the axial field at the center of the face of the semi-infinite current sheet. Thus the two values for the two faces can be subtracted directly.

A. C. Downing of the ORNL Mathematics Panel is using the Oracle (Oak Ridge Automatic Computer and Logical Engine) to calculate from fundamental formulas the values of B_z , B_u , A , and rA for semi-infinite current sheets. This compilation of data will be published as an ORNL report and will, no doubt, extend the possible applications of the methods described above.

¹J. P. Blewett, *J. Appl. Phys.* 18, 968-76 (1947).

²C. L. Bartberger, *J. Appl. Phys.* 21, 1108-14 (1950).

³K. P. Müller, *Arch. Elektrotech.* 17, 336 (1926).

⁴K. Foelsch, *Arch. Elektrotech.* 30, 139 (1936).

⁵K. Foelsch, *Tabellen und Kurven zur Berechnung des Magnetfeldes von kreiszylindrischen Spulen*, K. Triltsch, Würzburg, 1936.

4. MAGNETIC COIL DESIGN FOR DCX-1

E. S. Bettis

Oak Ridge National Laboratory

The failure of previous attempts to solve the problem of cooling the DCX-1 mirror-field coils (which were potted in an epoxy resin to form a monolithic unit) by rifle drilling to provide for axial water flow led to the development of a new design. Figure 2 shows the new coil - 28 in. OD \times 18 in. ID \times 12 $\frac{3}{4}$ in. long - without its stainless steel case and leads.

The coil is made up of four layers, each consisting of 40 turns of edgewise-wound 1- \times $\frac{1}{4}$ -in. copper. The winding was preformed by a winding machine and the layers were accurately dimensioned by being tightened around a machined mandrel. Glass tape was then wound between the spaced turns, and the coil was compressed on the mandrel by a hydraulic press. The layer of coil thus formed was vacuum-impregnated with class H varnish and baked. The dipping and baking were then repeated, and the interior and exterior were hand sanded. No machining was done to the coil layers after winding.

A separator pad was made by placing a 0.030-in. glass cloth in a die which was vacuum-filled with an air-setting epoxy resin. The finished spacer provided a ribbed semiflexible sheet with $\frac{3}{8}$ - \times $\frac{1}{4}$ -in. ribs connected by a glass resin-impregnated web approximately 0.030 in. thick joining the center of all the ribs. When placed between layers of the coil these spacers provided mechanical separation and insulation between the layers with water coolant passages so that water could be circulated across the inner and outer edge surfaces of the conductors.

The four layers with the spacers were then nested and electrically connected in series. On the ends of each layer a hoop of Micarta was cemented, after one surface of the hoop had been machined to conform to the helical end of the coil. These Micarta hoops or rings serve to square the coil ends and to insulate the coils from the case.

The cases for the coils were made of stainless steel with rubber-gasketed top plates which carried two sets of diametrically opposed holes for water connections and electrical leads. Ribbed inserts for the ends of the cans were arranged to direct the water flow so that four longitudinal passes of the coil are made by the water.

Approximately 495 gpm flows through the coil, and the temperature rises 16°F in flowing through the complete coil. The maximum copper temperature is calculated to be some 41°F above the water temperature at the maximum hot spot. The film drop is calculated to be about 16°F.

These coils have given no trouble in operation for some months, and the design seems to have been satisfactory for coils running at a current density of 24,000 amp/in.².

UNCLASSIFIED
PHOTO 33625

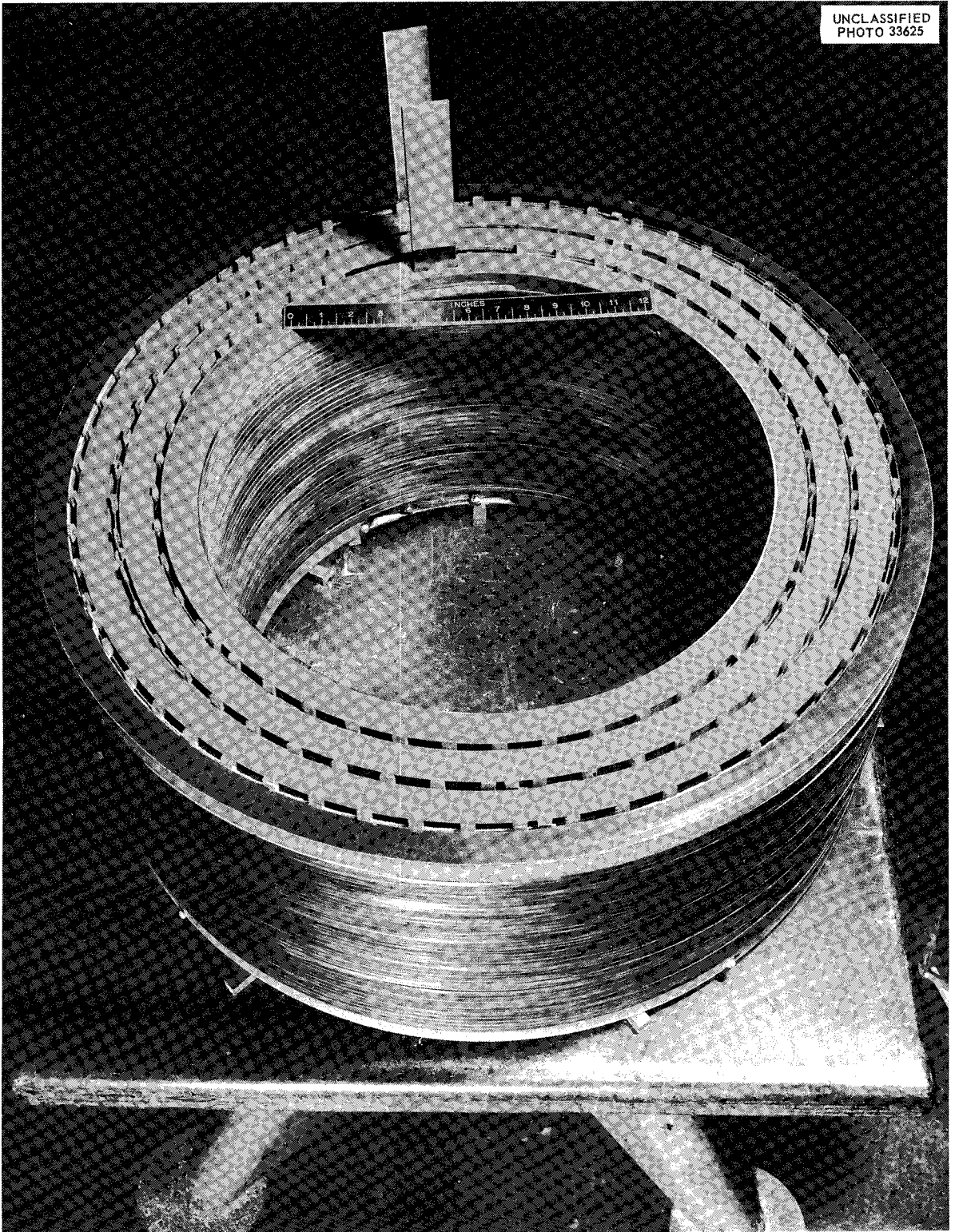


Fig. 2. Coil for Establishing Magnetic-Mirror Field in DCX-1.

5. MAGNETIC SWITCHING DEVICES

R. Carruthers - AERE

INTRODUCTION

Magnetic switches in the form of saturable reactors have found considerable use as aids to commutation in such applications as mechanical rectifiers and high-voltage mercury-pool rectifier installations. There is little information on the design of such devices, and when an application arose in connection with switching the main discharge circuit of Zeta we investigated these design problems. Some basic relationships were established which are of great help in making an initial appraisal of the practicability of magnetic switching for a specific duty.

BASIC PROBLEM

Magnetic switches cannot be used alone in switching a d-c circuit since, given time, the core flux will eventually reach a steady value. They are therefore used in conjunction with other switches - mechanical or electronic.

In the case of Zeta a magnetic switch was used to limit the circuit current until the contacts of a series mechanical switch were firmly closed. Another use is to control the rate of change of current before the opening of a circuit and the rate of rise of inverse voltage immediately after opening.

Such requirements can all be reduced to a specification of three quantities:

1. the impressed voltage,
2. the time for which the impressed voltage is to be withstood before saturation of the core ("hold-off time"),
3. the maximum value of incremental inductance which can be tolerated in the switch when saturated.

DESIGN PROCEDURE

Let

E = impressed voltage,

t = hold-off time,

L_s = the incremental inductance of the switch when saturated,

ΔB = flux swing in the core necessary to just saturate it,

ΔH = M.M.F. change required to produce ΔB ,

I = current in the switch immediately prior to saturation.

Let us assume that the winding of n turns is uniformly distributed over a magnetic circuit of area A and length l .

Then we may write:

$$E = nA \frac{dB}{dt} \times 10^{-8} \quad (1)$$

$$L_s = 4\pi \times 10^{-9} \frac{n^2 A}{l} \quad (2)$$

If the applied voltage is sensibly constant during the hold-off time we may write (1) as:

$$E = \frac{nA \Delta B}{t} \times 10^{-8} ; \quad (3)$$

$$\therefore \text{core area } A = \frac{Et}{n \Delta B} \times 10^8 . \quad (4)$$

From (2) we obtain

$$lA = \frac{4\pi n^2 A^2}{L_s \times 10^9} ; \quad (5)$$

and, substituting for A^2 from (4), the core volume

$$lA = \frac{4\pi E^2 t^2}{\Delta B^2 L_s} \times 10^7 . \quad (6)$$

This clearly indicates that the core volume is not greatly dependent on the material used since all suitable magnetic materials have much the same saturation flux density. Also, the volume is not affected by the shape of the unit or the number of turns on the winding.

The core material is of most importance in determining the value of current flowing in the switch immediately prior to saturation.

This current is obtained from the relation:

$$\Delta H = \frac{4\pi n l}{10 l} .$$

From (2) and (3),

$$\frac{4\pi n}{10 l} = \frac{L}{nA} \times 10^8 = \frac{L \Delta B}{Et} ;$$

$$\therefore \Delta H = \frac{L \Delta B l}{Et} ,$$

$$I = \frac{\Delta H Et}{\Delta B L_s} .$$

This relation indicates where the magnetic characteristics of the core are of significance. For a given ΔB , ΔH can vary over several orders of magnitude for different materials, small values (0.1 oersted) being obtainable only with very expensive alloys.

THE ZETA SWITCH

The mechanical switch used for closing the circuit had an arcing time of 300 μ sec at the peak working voltage of 25 kv. In this time the current would rise to several kiloamperes and there would be considerable contact erosion requiring maintenance after only a few hundred operations. It was expected that arcing currents of up to 100 amp would not give any trouble.

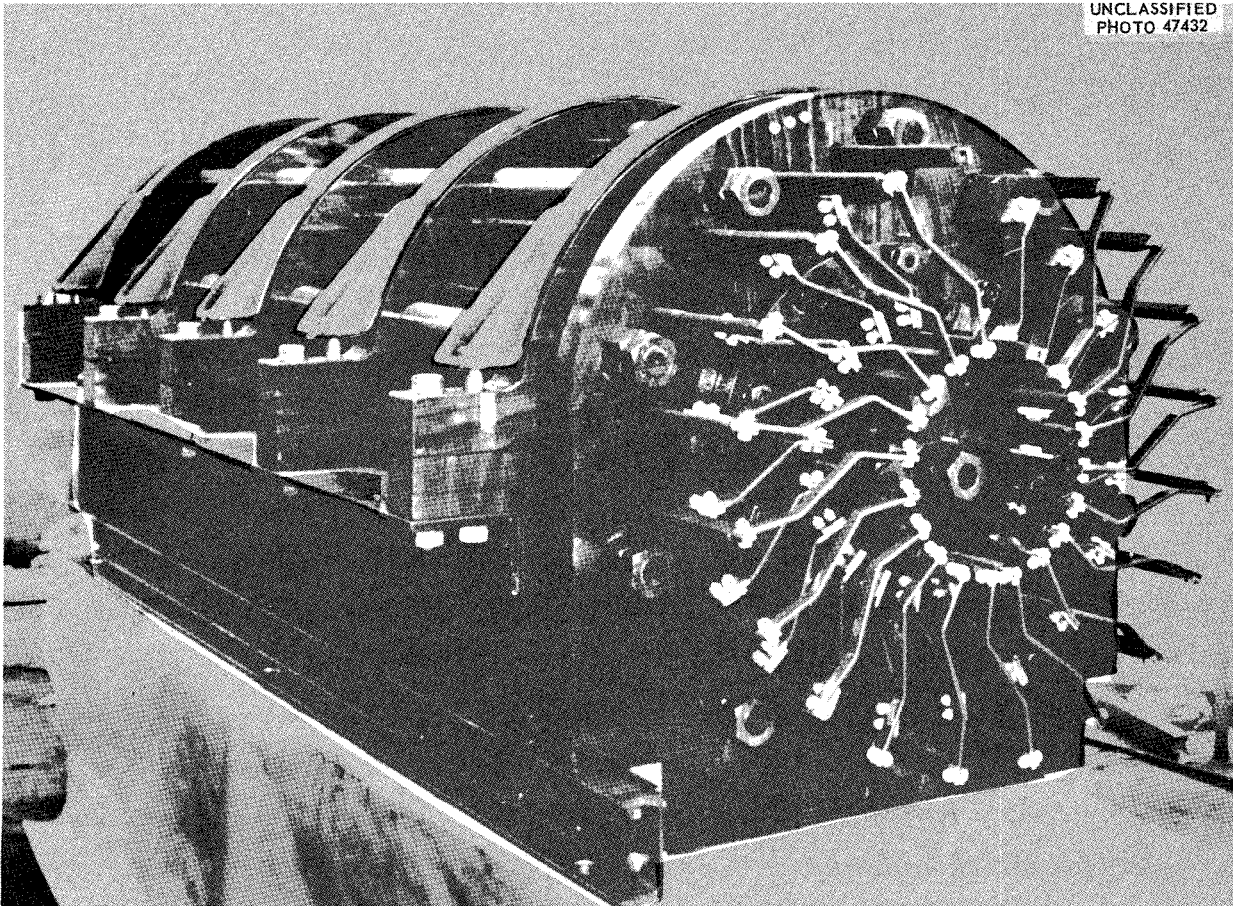


Fig. 3. Zeta Magnetic Switch.

A magnetic switch (see Fig. 3) was designed to meet this requirement; it comprises a core of cold rolled steel – 38 toroids 12 in. ID and 25 in. OD of 2-in.-wide strip. A 19-turn winding – made from copper bar wound with Micanite tape and resin impregnated – is mounted very close to the core after the manner of an alternator stator winding.

To obtain optimum performance the core is biased by another 19-turn winding energized through a suitable isolating choke.

This magnetic switch, which weighs over $2\frac{1}{2}$ tons, holds off 25 kv for 600 μ sec without the current rising above about 50 amp, and when saturated its inductance is only 70 μ h – of the order of 10% of the total circuit inductance.

CONCLUSIONS

For a given switching duty it is a straightforward matter to calculate the size of the magnetic switch because of the small difference in peak flux swing available with suitable core materials. The core is then constructed from the lowest grade – and cheapest – material that will have a presaturation current within the capacity of the other circuit elements.

A magnetic switch designed for use with Zeta reduced the electrical wear on the contacts of the associated mechanical switch to such a level that in the course of many tens of thousands of operations the wear was largely due to mechanical rubbing.

6. AN ANALOG BOARD FOR TIME-VARYING AXIAL SYMMETRICAL FIELDS

U. Christensen

Project Matterhorn, Princeton University

ABSTRACT

An analog board has been contemplated that will simulate the electromagnetic response of any system consisting of axial symmetrical conductors. These conductors can be either shorted, opened, or energized by a time-varying voltage. On such a board one can, with the proper equipment, measure any desired magnetic or electrical quantity of the system.

There are two types of electrical networks that would be accurate analogs for any axial symmetrical fields, one a discretizing of the actual space elements and the other a simple transform of the first one.^{1,2}

DISCRETIZING OF THE ACTUAL SPACE ELEMENTS

The space element considered in the axial symmetrical system is a ring concentric with the z axis and with a rectangular cross section (Δr , Δz).

The permeance of this element in the z direction is:

$$\Delta P_z = \int_{r_1}^{r_2} \frac{\mu 2\pi r dr}{\Delta z} = \frac{\mu\pi}{\Delta z} (r_2^2 - r_1^2) = \frac{\mu 2\pi}{\Delta z} r_{av} \Delta r,$$

and the reluctance of the element in the r direction is:

$$\Delta R_r = \int_{r_1}^{r_2} \frac{dr}{\mu 2\pi r \Delta z} = \frac{1}{\mu 2\pi \Delta z} \ln \left(\frac{r_2}{r_1} \right);$$

so the permeance in the r direction is then:

$$\Delta P_r = \frac{1}{\Delta R_r} = \mu 2\pi \Delta z \frac{1}{\ln(r_2/r_1)} \sim \frac{\mu 2\pi r_{av} \Delta z}{\Delta r}$$

We can now simulate the entire space by a two-dimensional network consisting of many inductors with an inductance $\Delta L = |\Delta P|$ where the mutual inductance between them must be zero.

When a space element is superimposed by an element of conducting material, the network must be modified as shown in Fig. 4. With the notations in Fig. 4, we have:

$$\Delta L_r = |\Delta P_z|,$$

$$\Delta L_z = |\Delta P_r|,$$

and

$$\Delta R = \frac{\rho 2\pi r_{av}}{\Delta r \Delta z}.$$

¹W. T. J. Atkins, *Proc. I.E.E.*, 1958, p 151.

²W. J. Karplus, *Analog Simulation*, McGraw-Hill, New York, 1958.

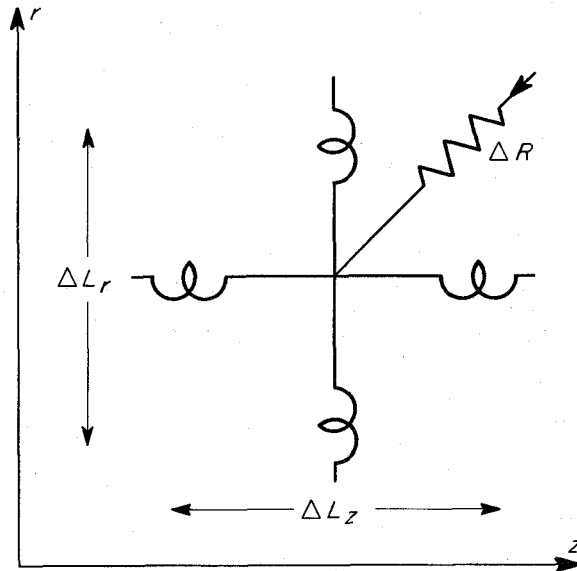


Fig. 4. Network Used in Analog Board for Time-Varying Axial Symmetrical Fields.

The reversal of the indices is due to the fact that a flux flow is perpendicular to the current flow. To simulate a circular conductor with a cross section that consists of many elements, all the ΔR resistors must be connected to a common bus. This configuration will be the equivalent of a solid ring that has been slotted to prevent current flowing in the " θ " direction. The simulation of a solid ring that has not been slotted is accomplished by connecting the bus to the axis. In simulating a one-turn coil that is energized, a generator is connected between the bus and axis.

For a coil with more than one turn, each turn must have its own generator with the voltage so adjusted as to deliver the identical current both in magnitude and phase.

TRANSFORM OF BOARD IMPEDANCES

In the network discussed the space permeance was simulated by a multitude of small inductors. Since an analog board made up of such components would become very expensive and bulky, another less expensive network would be preferred. In this network the inductors are replaced by resistors and the resistors replaced by capacitors. This transform can best be demonstrated by the following simple analogy of equations:

$$e = Ri + L \frac{di}{dt} ,$$

and integrating this with respect to time we have:

$$\int e dt = \int Ri dt + Li ,$$

or

$$V_b = \int \frac{1}{C_b} i dt + R_b i ,$$

where index b indicates board values.

From this analogy it is evident that the generator voltage V_b energizing the board must be the time integral of the actual voltage, and likewise any voltage vs time recorded on the board must be differentiated before obtaining the actual voltage.

This analog board without the feed-in capacitors would be identical to an analog board described elsewhere,³ and would be capable of solving problems involving static magnetic fields.

³K. E. Wakefield, *A Resistance Analogue Device for Studying Axially Symmetric Magnetic Fields*, Princeton University, Project Matterhorn Report PM-S-23, 1958.

7. PULSED MAGNETIC FIELDS

Simon Foner
Lincoln Laboratory,¹ M.I.T.

The need for high magnetic fields in solid state research led to the development of pulsed-field magnets at Lincoln Laboratory. The pulsed field technique is most useful when extremely high fields are desired over small volumes, and when experimental observations can be made in a short time. Under such conditions efficient coils can be employed with no provision for external cooling. When continuous fields are desired, provisions for cooling require extensive modifications of coil design (see Papers 4 and 13). The characteristics of two pulsed field coils are summarized below; a helical design² useful for experiments in relatively small volumes, and a flux-concentrator, designed by B. Howland,³ which may be applicable to high field generation over the large volumes required by thermonuclear machines. Although these developments were not directed toward thermonuclear research, some of the results may prove useful here. As an example the possibilities of a pulsed field Maser are described.

HELICAL PULSED FIELD COILS

Reproducible fields of as much as 750 kilogauss have been obtained with suitable helical coils.² The coil (see Fig. 5) comprises a machined, hardened, beryllium-copper helix which is insulated by a helical mica structure between turns, and which is mechanically supported by a

¹Operated by Massachusetts Institute of Technology with the joint support of the U.S. Army, Navy, and Air Force.

²S. Foner and H. H. Kolm, *Rev. Sci. Instr.* **27**, 547 (1956); **28**, 799 (1957).

³To be published. A brief discussion of this design was presented by B. Lax at the Symposium on High Magnetic Fields held during the Kammerlingh Onnes Conference on Low Temperature Physics at Leiden, Netherlands, June 1958.

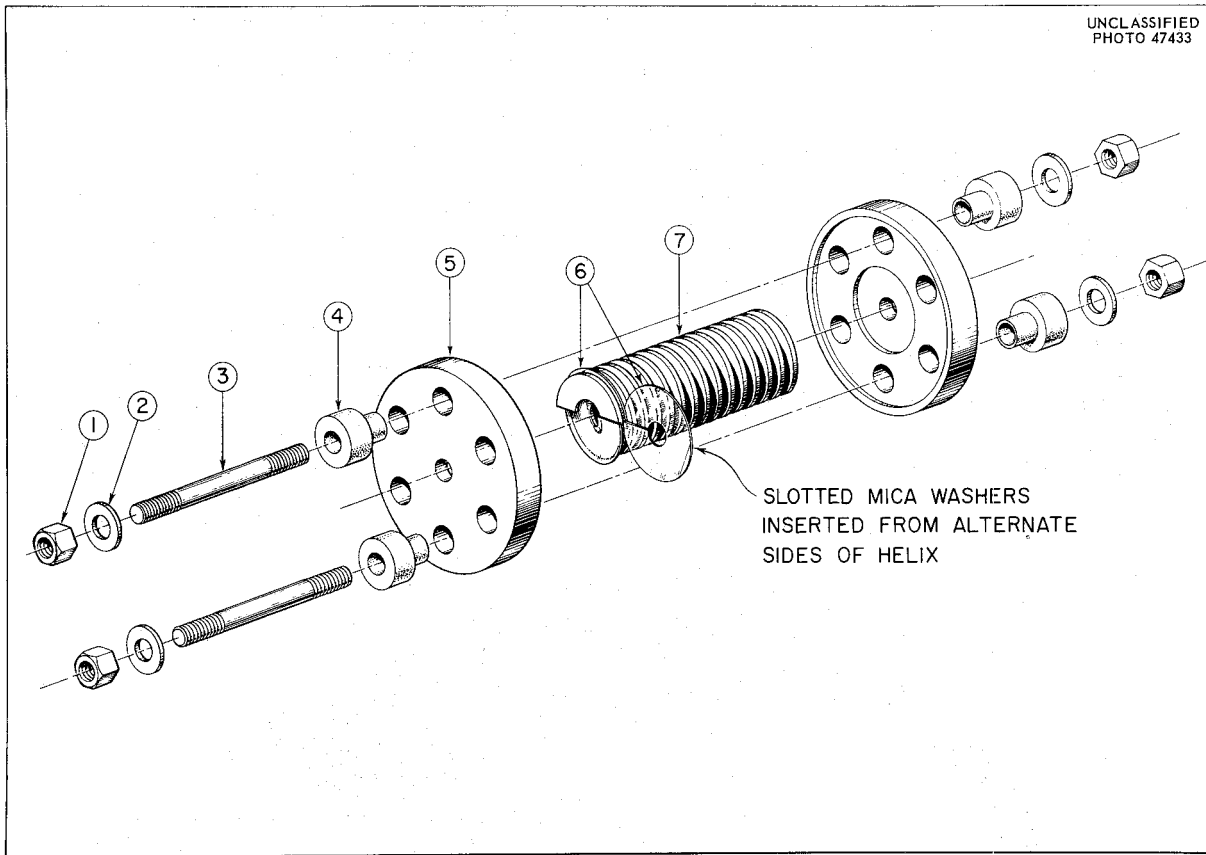


Fig. 5. Helical Pulsed-Field Coil. (1) Steel nut, (2) brass nut, (3) phosphor bronze stud, (4) cloth-bonded plastic insulator, (5) brass face plate, (6) slotted mica insulating washers used to generate two spirals of mica, (7) magnet coil - machined continuous spiral of beryllium-copper.

reinforced ceramic structure. Coils varying from $\frac{3}{16}$ in. to 1 in. ID, from 1 in. to 2 in. OD, and with up to 40 turns have been used. The highest field obtainable is at present limited by the high temperatures and pressures produced in the helical conductor. The problem of machining probably will limit usable field volumes to several cubic inches.

High efficiency is attained by discharging a high-voltage (3000 v), low-capacitance (2000 μ f) pulse circuit through the helical coil. By this means an oscillatory discharge is obtained through the strong, high-resistance, beryllium-copper alloy coil which operates at room temperature. With the above capacitor bank, a field of 750 kilogauss is produced over a useful volume of about 0.1 cm^3 with a half period of 120 μsec , and a field of 150 kilogauss is produced over a useful volume of about 20 cm^3 with a half period of 500 μsec . Characteristics of various coils are given in ref 2.

Numerous experiments have been carried out with this pulsed field system over a wide range of frequencies and temperatures. These include cyclotron resonance⁴ and magnetoband effects at

⁴R. J. Keyes *et al.*, *Phys. Rev.* **104**, 1804 (1956).

infrared,⁵ antiferromagnetic resonance,⁶ ferromagnetic resonance, and paramagnetic resonance⁷ at millimeter wavelengths. The flexibility and wide range of available pulsed fields has proved most useful for surveys of many solid state systems which involve large internal fields.

FLUX-CONCENTRATOR PULSED FIELD COIL

B. Howland of our laboratory has developed a flux-concentrator type of pulsed field coil³ of a novel design (see Figs. 6 and 7). It is equivalent to a pulse transformer which has a multitem

⁵S. Zwerdling *et al.*, *Phys. Rev.* 104, 1805 (1956).

⁶S. Foner, *Phys. Rev.* 107, 683 (1957).

⁷A summary of these various pulsed field magnetic resonance experiments at millimeter wavelengths and applications was presented by S. Foner at the International Conference on Magnetism, Grenoble, France, 2-5 July 1958 and is to be published in the *Journal de Physique* January 1959. Additional references will be found in this article.

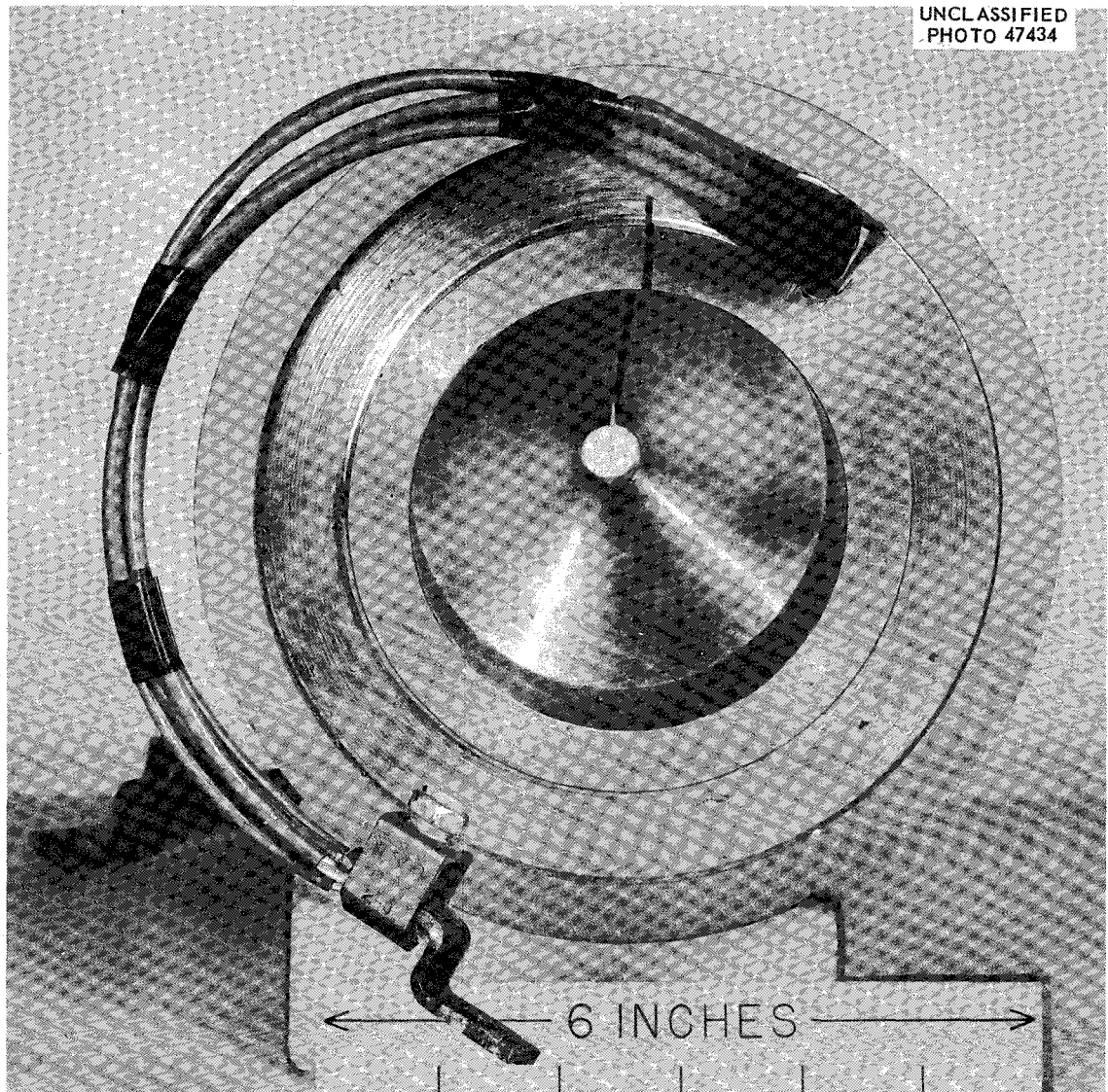


Fig. 6. High-Efficiency Flux Concentrator - End View.

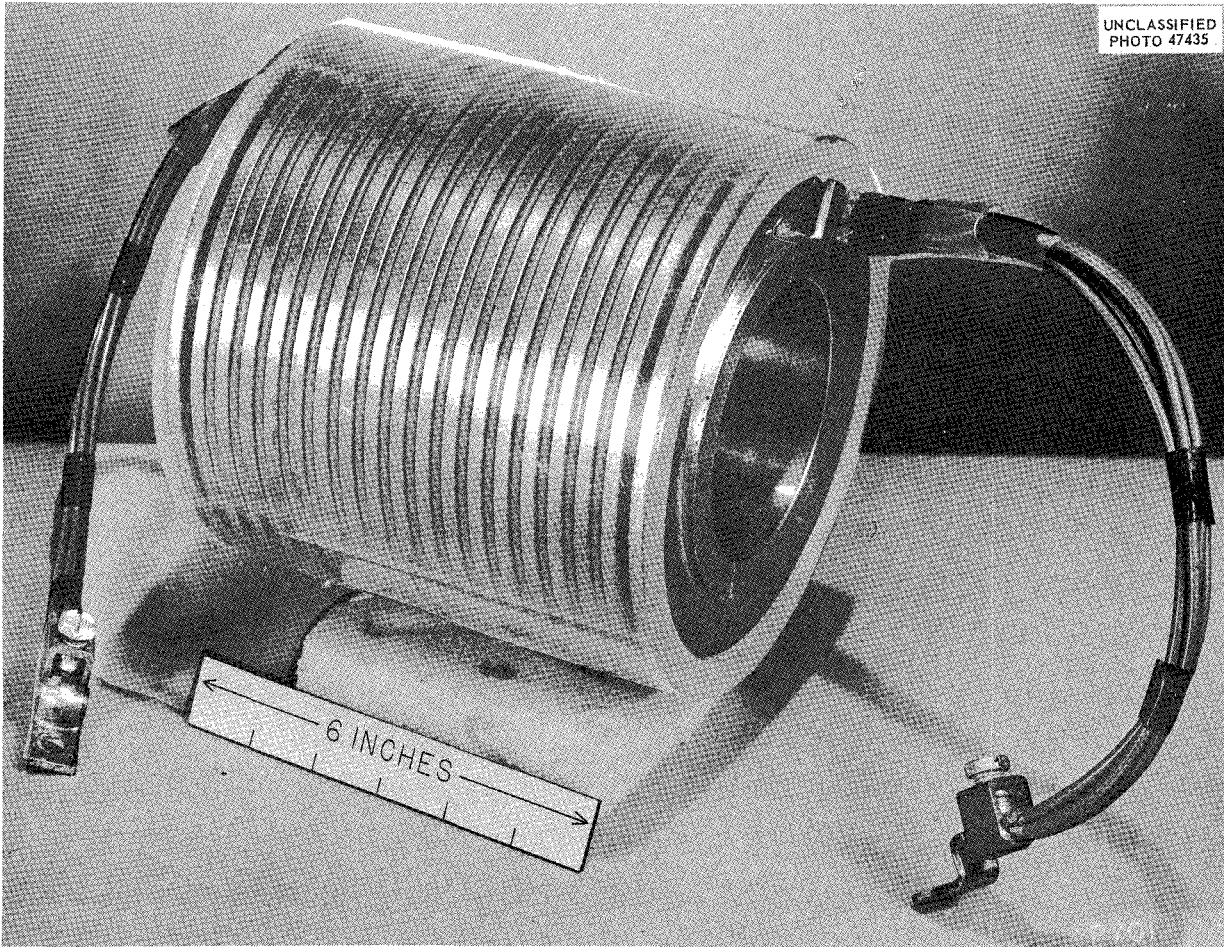


Fig. 7. High-Efficiency Flux Concentrator – Side View.

primary winding and a secondary single-turn winding. Mechanical forces and leakage inductances are minimized by embedding the primary winding in a deep helical slot which is machined on the outside surface of a large cylindrical block. A radial slot to a central hole permits currents to flow in the single-turn secondary. The conductor surrounding the central hole (where the high field is generated) is rigidly supported by the massive conductor structure. The coil is readily machined, and various simple windings are suitable for the primary winding. Because the intricate machining is limited to the outside surface of the conductor, the design can readily be adapted to large field volumes. Most of the currents flow within a skin-depth of the bounding surfaces, and external cooling can be provided throughout the bulk of the structure if a high duty cycle is to be maintained. For very large coils, high efficiency can be obtained with large pulse times, since the penetration depth varies as the square root of the applied frequency. Use of noncontacting, threaded, interchangeable inserts permits the field configurations inside the coil to be modified easily. Leakage inductance losses at the radial slot can also be reduced by careful corrugation of this region.

Tests of such a flux-concentrator have been made with the 2000- μ f, 3000-v surge supply. No mechanical or electrical failure of the primary winding has been observed with the maximum energy available, although sufficiently high fields (450 kilogauss) were generated in the concentrated region to mechanically deform copper or brass inserts.

If small field volumes are required, this flux concentrator is less efficient than the corresponding helical coil unless the pulse half-period is reduced. On the other hand, large field volumes will permit high-efficiency operation of the concentrator even with long pulse times. It appears that the internal structure of the concentrator is stronger than that of the helical coil, so that higher fields should be possible. So far we have not been able to test this possibility with available energy. It appears that this design will be very useful in large-volume, high-field devices of various kinds.

APPLICATION OF SOLID STATE INSTRUMENTATION TO THERMONUCLEAR RESEARCH

To date there has been only limited interchange of ideas in high-field thermonuclear research. Many high-field investigations, in solid state for instance, may prove valuable to the art of thermonuclear research.

As an example, high-temperature plasma diagnostics may require a source at millimeter wavelengths. We are at present examining the possibility of generating such high frequencies with a pulsed field Maser. If we produce an inverted spin population in a paramagnetic salt, and then apply a pulsed field in a time short compared to the spin-lattice time, the electronic spin energy-level separation, $h\nu$, will vary with the applied field. By placing the salt in a dual-mode cavity with an inverting pump frequency, ν_p , much less than the output frequency, ν_0 (corresponding to the higher cavity mode), the pulsed field can be used to tune the paramagnetic system so as to emit radiation at $\nu_0 \gg \nu_p$. The system converts magnetic energy, μH , (where μ is the Bohr magneton of an electron) to radiation energy $h\nu_0$. Estimates indicate that for 10^{19} electron spins, and for a peak pulsed field of 100 kilogauss, average powers of about 0.1 w should be obtained at 1 mm wavelength with such a pulsed Maser. Suitable multiple spin systems will probably reduce the field requirements. Tests of such a device are in progress.

8. BOILING BURNOUT WITH VORTEX COOLANT FLOW

W. R. Gambill
Oak Ridge National Laboratory

Motivations for vortexing a boiling coolant in a high-performance device include: (a) higher velocity for equal flow rate, (b) inward radial vapor transport under the action of centrifugal acceleration, and (c) greater radial turbulent fluctuations. Burnout heat fluxes with vortex water flow as large as 17,300 w/cm² have been reported in a paper giving full details of this study.¹ When compared on a basis of equal superficial velocity, vortex burnout heat fluxes are much larger than for

¹W. R. Gambill and N. D. Greene, *Chem. Eng. Prog.*, p 68-76, October 1958.

straight flow. Some of the advantage is retained when comparison is made on the basis of equal pumping power.

A generalized correlation which has been prepared since the publication of ref 1 is shown as Fig. 8. This plot follows the form used by Lowdermilk *et al.*,² for burnout with net boiling of water in straight flow. The notation is as follows:

$(q/A_1)_b$ = burnout heat flux based on internal surface area, Btu/hr·ft² ,

D_1 = internal tube diameter, ft ,

L/D = length-to-diameter ratio of heated tube ,

G_{SA} = superficial axial mass velocity, lb/hr·ft² .

²W. H. Lowdermilk, C. D. Lanzo, and B. L. Siegel, NACA-TN-4382, September 1958.

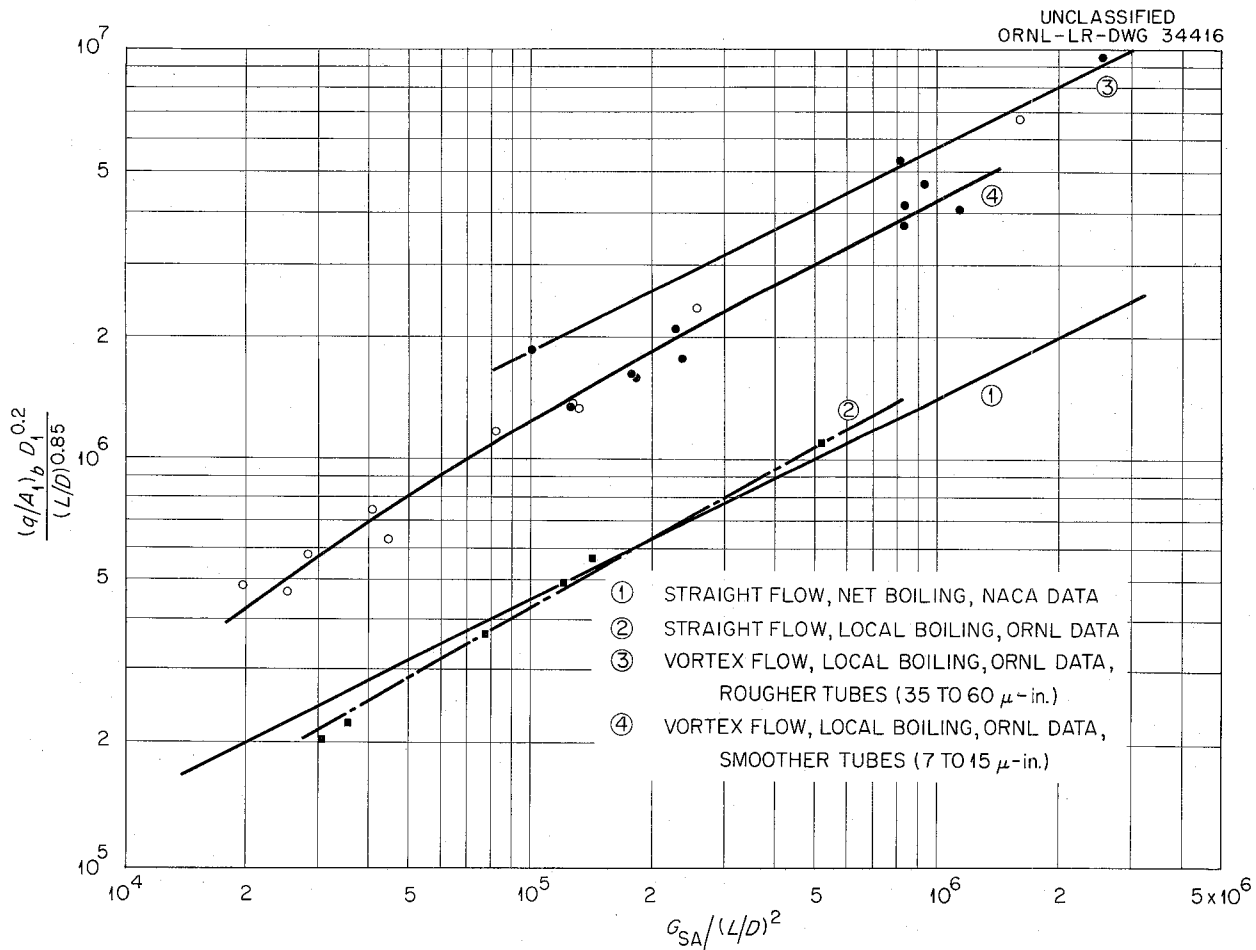


Fig. 8. Boiling Burnout Heat-Flux Correlation. $(q/A_1)_b$ = burnout heat flux based on internal surface area, Btu/hr·ft², D_1 = internal tube diameter, ft, L/D = length-to-diameter ratio of heated tube, G_{SA} = superficial axial mass velocity, lb/hr·ft².

Use of a tangential-slot vortex generator at the beginning of the heated channel limits application of vortex flow to relatively small L/D ratios. This limitation may possibly be removed by using a twisted tape running the entire length of the circular heated channel. A small study of burn-out with twisted tape vortex generators is presently being conducted, and a short series of such tests (with promising results) has already been made at Argonne National Laboratory.³

Some recent applications^{4,5} of boiling liquids to the cooling of d-c magnets have been noted, and it is possible that the vortex flow principle might be applied to some future high-field design.

³R. J. Weatherhead, Reactor Engineering Division, private communication, January 1959.

⁴S. G. Sydorik, and T. R. Roberts, *J. Appl. Phys.*, p 143-48, February 1957.

⁵H. H. Kolm, *J. Appl. Phys.* p 489-91, 1958.

9. MAGNETIC FIELD DESIGN FOR DCX-2 EXPERIMENTS¹

W. F. Gauster
Oak Ridge National Laboratory

ABSTRACT

The magnetic mirror field of the first DCX machine is not supposed to contain thermonuclear reaction products. The DCX-2 will be designed with a stronger magnetic field and a higher mirror ratio. It is hoped that with this device a self-sustained thermonuclear reaction will be demonstrated.

In order to get, first, an approximate idea about the dimensions of the DCX-2, a simple computation scheme starting with a containment calculation was worked out. It was assumed that the thermonuclear reaction products are alpha particles with an energy of 5 Mev. Only the particle movement in the mid-plane of a magnetic mirror was considered. Furthermore, it was assumed that the volume in which thermonuclear reactions will occur is relatively small, so that the alpha particles will start approximately from the mirror center.

As a starting point, symmetrical coils with tapered ends and with current density $i = \text{constant}$ were assumed.

With a mirror ratio 3.5 the following data are obtained:

Inside radius of the coils, $a_1 = 12$ in.

Outside radius of the coils, $a_2 = 28$ in.

Distance from coil middle to the mirror center, $z_0 = 20$ in.

Flux density in the mirror center, $B_{\min} = 16$ kilogauss

Flux density at the coil center, $B_{\max} = 56$ kilogauss

Current density, $i = 1.37 \times 10^4$ amp/in.²

This current density is relatively low (DCX-1 coils have a current density of 2.4×10^4 amp/in.²).

By means of a simple scaling law, data for a DCX-2 machine with other linear dimensions can be found. For an alpha particle with constant energy of 5 Mev, the product of the radius of curvature at any point and

¹W. F. Gauster, "Magnetic Mirror Fields for DCX-2", *Thermonuclear Project Semiann. Prog. Rep.*, Jan. 1959, ORNL-2693, p 109-11 (May 5, 1959).

the magnetic field strength at this same point has to be a constant. Therefore, scaling down any length a to a/k requires the flux density B to be increased to kB . P also has to be scaled up to kP . Finally, it is easy to show that the current density i is scaled up to k^2i . This point of view is important because with larger mirror ratios a power of 15 Mw would require excessively high copper volume and have an unnecessarily low current density. By scaling down the machine and therefore increasing the power, copper volume and current density can be brought to reasonable values.

The numerical example shown was calculated assuming a simple coil shape with constant current density. By changing the coil shape and the current-density distribution it is hoped to find sensibly better data for a DCX-2 machine; however, much further study is needed. It should be kept in mind that space for instrumentation must be provided.

10. SOME BASIC CONCEPTS IN MAGNETIC FIELD THEORY

W. F. Gauster
Oak Ridge National Laboratory

A detailed presentation has been submitted for publication.

11. CONSTRUCTION AND FABRICATION FEATURES OF SOME MAGNET COILS USED IN FUSION STUDIES

E. I. Hill
University of California Radiation Laboratory

The need for high-voltage, fast-rising pulse coils as used in magnetic mirror machines and for highly concentrated z field coils as used in certain pinch experiments has led to the development of some interesting types of coil construction.

The specific problems involved, once the desired field pattern has been established, include cooling, high mechanical forces, size, weight, and insulation. In most cases, the cooling can be simplified by the use of a hollow conductor through which is pumped a heat transfer medium. Soft water is usually used, although a coil has recently been built that will eventually be cooled with liquid nitrogen. Pressure drop-off, when long lengths of water-cooled conductor are used, must be kept to a minimum. One way to do this is to place sections of conductor in series electrically while keeping the cooling of these sections in parallel.

The conductor used at UCRL is of square-cross-section, 98%-conductivity copper. The bore size has been determined to give optimum cooling and electrical properties. Conductor sizes most frequently used are 0.255, 0.340, 0.467, and 0.640 in. Three of the sizes are purchased in 120-ft lengths and shipped in coils. The largest size (0.640) is purchased in straight 60-ft lengths.

Where the need for a high-resistance conductor is indicated, copper refrigeration tubing has been successfully employed.

High fields create tremendous mechanical forces within the coil windings, requiring a construction material which has high mechanical strength. The high voltage encountered requires good

insulation. Cost and other practical considerations dictate that the material lend itself to hand construction.

One of the newest materials, epoxy resin reinforced with Fiberglas, was selected for the job. In addition to meeting the above-mentioned requirements, it has the added advantages of adhering tenaciously to most materials and being relatively light in weight.

Combinations of epoxy with woven Fiberglas and with filament winding using Fiberglas roving give directional strengths not possible with most materials. Recent developments in the fabrication of high-pressure vessels utilizing these materials have shown that directional strengths of 155,000 psi or higher are attainable. There are no limitations on size other than those set by the winding equipment. Since the density of such a structure is about $\frac{1}{4}$ that of steel, it is easy to visualize the advantages of its use in the construction of very large pulsed coils.

Problems of insulating a coil firmly imbedded in a glass-reinforced epoxy structure are simplified by the fact that most of the work can be done by hand using ordinary shop equipment.

It is imperative in pulse coil construction that there be no voids (which can cause arcing, with consequent breakdown of the materials and coil failure) adjacent to any conductor within the coil. Because hand construction methods are dependent on the skill of the workman, good layup techniques and close supervision of each stage of construction are necessary to minimize failures.

Many variations in the design of magnet coils are possible with this type of construction. An example of a one-unit mirror assembly used on the Table Top experiments at UCRL was constructed in the following manner.

A split steel mandrel $7\frac{1}{2}$ in. in diameter was covered with a sheet of 7.5-mil Mylar. This served as a parting film for a laminate of glass cloth and epoxy resin wrapped around the mandrel. The laminate was of sufficient thickness to allow $\frac{1}{8}$ -in.-deep spiral grooves to be machined after curing. Copper conductor (0.640 in. square) was wound into the grooves under a tension of 800–1000 lb to make a coil layer of 50 turns.

Roving saturated with epoxy resin was wound in between the turns and to a depth of about $\frac{1}{16}$ in. over the conductor. Next the outer diameter was machined so that more glass cloth and epoxy resin could be built up. Grooves were cut and eight turns of conductor were wound at each end.

It was desired to have all the copper conductor in both layers in one continuous piece. This was accomplished by storing extra conductor at each end of the assembly while winding the first layer. By winding this extra conductor in a loose coil of fairly large diameter around the shaft supporting the mandrel, it was possible to keep it out of the way of subsequent machining. The stored conductor was later unwound and hooked to the tension machine for winding the second layer.

Because the lengths of conductor were 60 ft long and the total coil required approximately 141 ft, it became necessary to join three lengths. This was done with a flash butt welder set up for the purpose. The resulting outside flash was removed by hand grinding. The inside flash was removed with a drill slightly smaller in diameter than the conductor bore. The drill had previously

been welded to a 61-ft length of $\frac{5}{16}$ -in.-dia steel rod. A $\frac{1}{2}$ -in. electric drill and some muscle provided the necessary power.

To ensure that the joints were sound, the conductor bore was filled with Freon at 20 psi, and a halide leak detector used to probe for leaks. A water flow test based on a 60-psi pressure drop showed that the conductor and joints had no restrictions.

Copper terminals drilled and pipe tapped for water connections were silver soldered to the conductor ends. These were 3 in. square by $1\frac{1}{8}$ in. thick and had a curved flange. The flange was later firmly imbedded in the glass and plastic which was to surround the windings.

Layers of Fibreglas cloth and epoxy resin were wound over the first layer windings between the built-up end sections. Fibreglas roving saturated with epoxy resin was then wound over the entire length of the coil. An attempt was made to level-wind the strands in the same way a spool of thread is wound. This resulted in a glass-epoxy structure approximately $1\frac{3}{8}$ in. thick over the conductor windings.

After the ends were machined, the split mandrel was removed. Canvas-backed phenolic mounting plates were cemented to the ends of the coil for installation in the apparatus.

The physicist's log book shows that this coil has been pulsed 14,000 times. It has created a field of 50,000 gauss in a rise time of 600 μ sec. The power was supplied by a capacitor bank of 10^6 joules at approximately 18 kv.

A z field coil for a linear pinch experiment was recently made which has some interesting features. With an ID of $5\frac{5}{8}$ in., an OD of $12\frac{3}{4}$ in. and a length of 31 in., it contains 615 lb of liquid-cooled conductor.

Four layers of 0.340-in. square copper conductor and four layers of 0.467-in. square copper conductor were laid up on a $\frac{1}{16}$ -in.-thick core of epoxy-glass laminate. Each layer was wound with separate lengths of conductor to which cooling connections were soldered at each end. With the exception of the start of the first turn and the end turn on the last layer, all of the conductor ends were silver soldered together. This made all of the windings in series electrically.

The parallel arrangement of the layers for cooling resulted in 16 connections for the cooling medium but created a more efficiently cooled coil due to less pressure drop.

Because the voltage requirements were low, the insulation between turns consisted of glass sleeving drawn over the conductor. This was thoroughly wet with epoxy resin when the windings were made. A layer of glass cloth was placed between each layer. Two layers of Fibreglas tape with 50% overlap were wrapped over the outside windings. This was done more for mechanical strength than for insulation value.

Two nonmagnetic stainless steel lifting lugs were placed 180° apart near one end of the coil. Fibreglas roving wet with epoxy resin was wound over a portion of the lugs to securely fasten them to the outside diameter.

Each end of the coil assembly was potted with a plasticized epoxy resin to protect the windings in handling.

The coil shapes attainable with the methods described are practically unlimited. The advancements in dielectric materials made in recent years have made it possible to build larger and more powerful coils with greater ease and at lower cost.

12. DESIGN AND DEVELOPMENT EXPERIENCES WITH HIGH-TEMPERATURE STABILIZING WINDINGS FOR PROJECT MATTERHORN B-3 MACHINE

H. G. Johnson
Project Matterhorn, Princeton University

ABSTRACT

This paper describes the design and construction of several types of electrical windings which produce a helical magnetic field around the vacuum (plasma) tube of the B-3 thermonuclear research machine. These windings are constructed as an integral part of the vacuum tube and are designed to withstand the required vacuum tube bakeout temperature of 850° F.

In 1957 the Machine Development Division of Project Matterhorn undertook the problem of producing special electrical windings for use on the B-3 experimental thermonuclear research machine. These windings produce a stabilizing magnetic field in addition to the normal confining field around the plasma (vacuum) tube of the machine. This paper describes the engineering design, development, and test of these windings which were constructed in the Matterhorn shops. They are presently installed and operating in the B-3 machine. Several types of higher performance winding designs are also described. These will replace the present windings upon completion of the current experimental tests.

Figure 9 is a photograph of the B-3 machine with the confining coils and stabilizing windings in place. This photograph was taken during the high-temperature bakeout of the vacuum system. The stabilizing windings and vacuum tube are completely hidden by the confining field coils and their holders. It should be pointed out that need for stabilizing windings was not anticipated in the original design (in fact, the concept of stabilizing windings is a recent "discovery"), and consequently the space limitations imposed many design restrictions and installation problems.

Five basic requirements for the stabilizing windings define the design specifications:

1. The windings must be capable of withstanding 850° F vacuum tube temperatures during bakeout servicing of the system for purposes of outgassing in order to achieve the ultrahigh vacuums of 10^{-9} to 10^{-10} mm Hg required. This operation requires about 12 hr and is carried out several times monthly.
2. The conductors must be cooled by some means to dissipate the I^2R heating during the operating pulse. The cooling must be sufficient to permit a duty cycle of one pulse each 30 seconds.

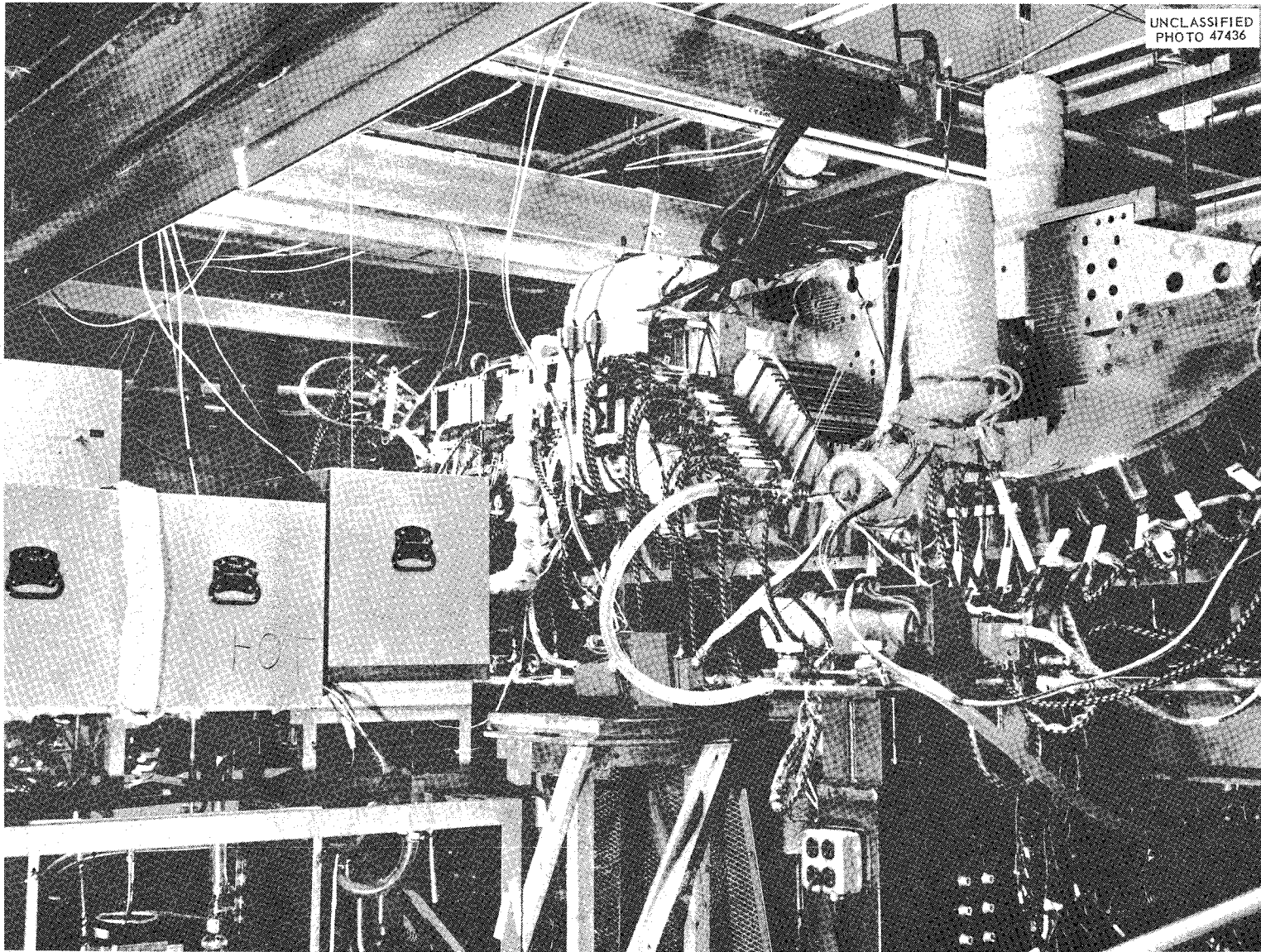


Fig. 9. B-3 Machine with Confining Coils and Stabilizing Windings in Place.

3. The electrical insulation of the windings must withstand 100 v turn-to-turn and 10 kv to ground. An adequate safety factor must be included for fabrication errors, creep, thermal strains, life service, etc.
4. The winding assembly and individual conductors must be structurally secure to prevent any movement due to the electromagnetic forces developed during the rated current pulse of 10,000 amp and also during confining-field fault conditions.
5. The winding conductors should be located radially as close to the plasma tube as possible.

DESIGN AND CONSTRUCTION DETAILS

Type I Winding Design

The Type I design was selected primarily because it was made of more conventional materials and could be constructed within the short time allotted in the experimental schedule. It was believed that this was a very conservative design which would not subject the electrical insulating materials to excessive hot-spot temperatures. Figure 10 is a sketch showing in outline the four various windings of the Type I design that were fabricated and installed in the machine. Figure 11 is a cross section of the Type I design construction. From the standpoint of optimum magnetic

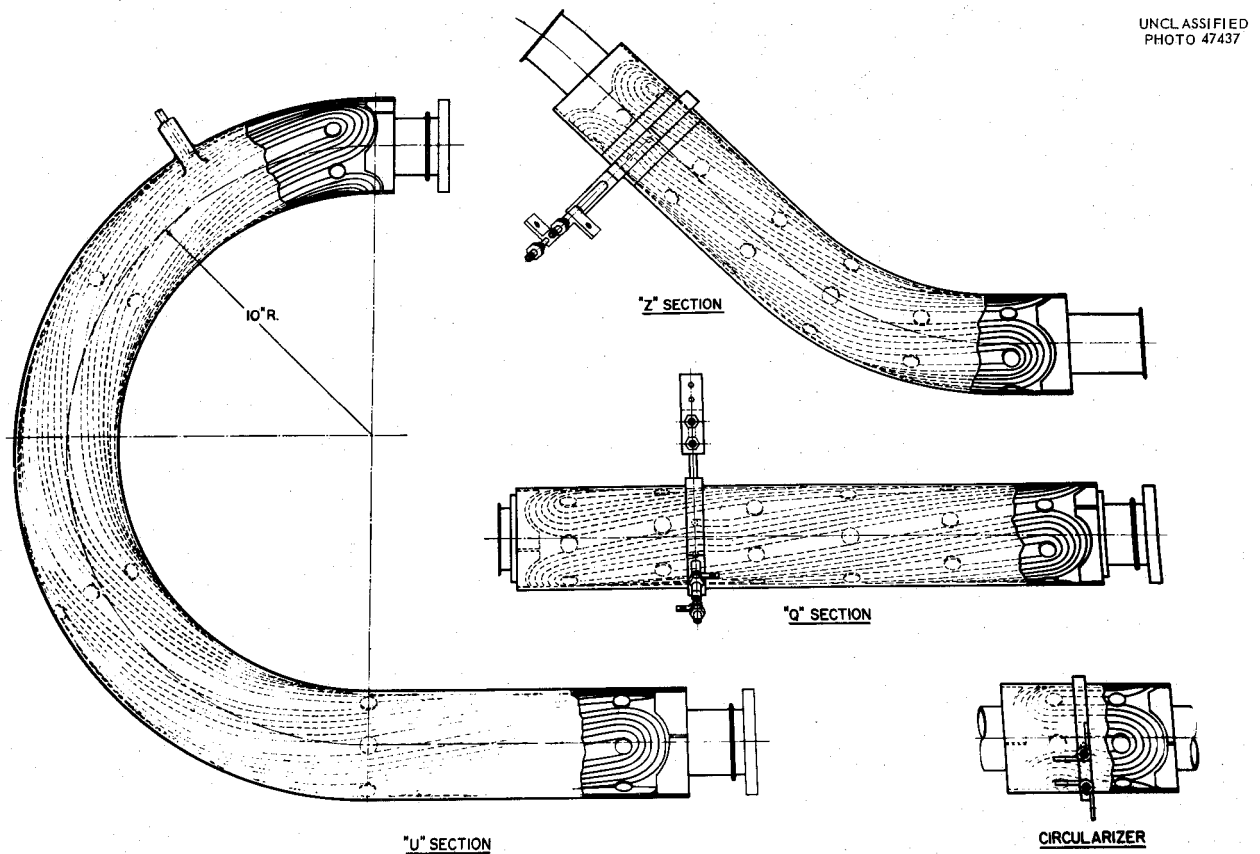


Fig. 10. Typical Stabilizing Winding Assemblies for B-3 Machine (Type I).

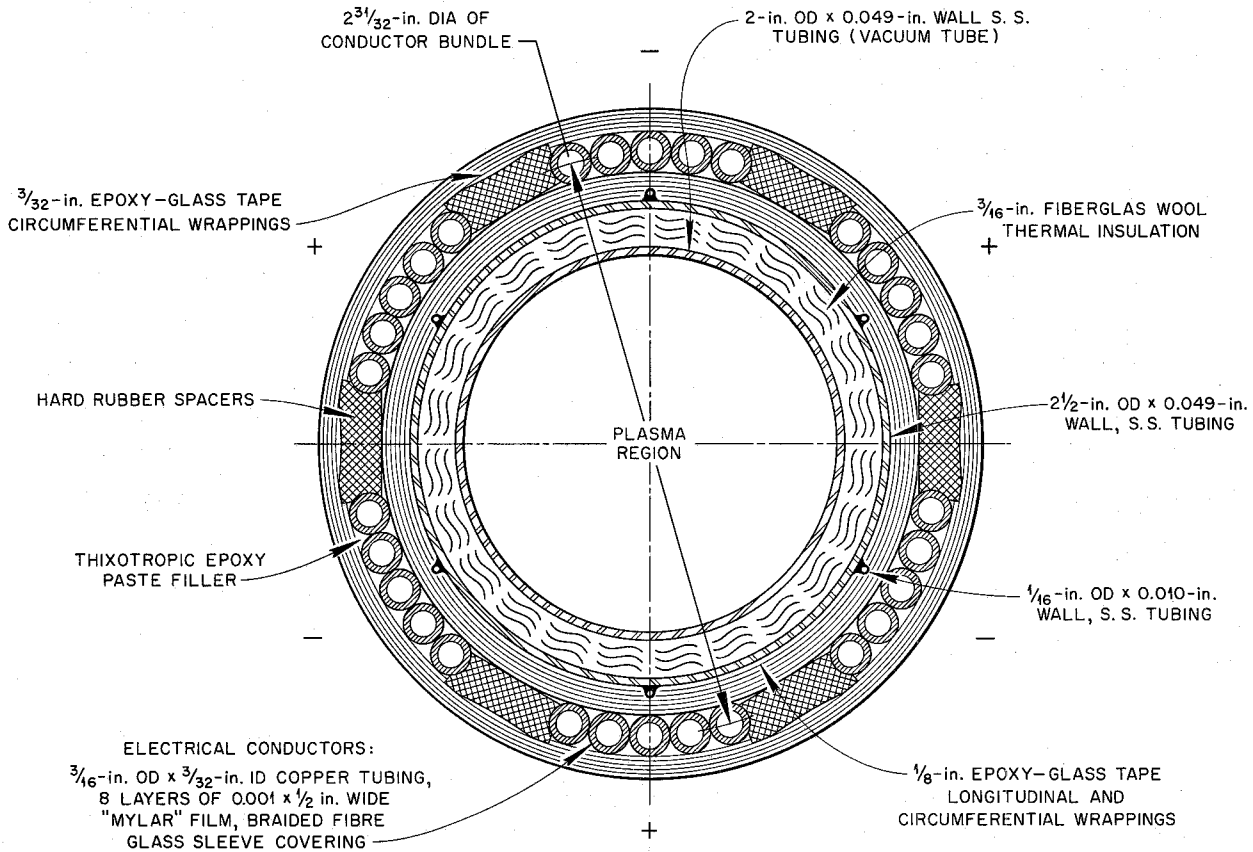


Fig. 11. Section Through Present Design (Type I) Stabilizing Winding.

performance the conductors should be positioned as close to the vacuum tube as possible. Calculation of temperature distributions throughout the cross section indicated that the minimum radial location of the conductors should be $1\frac{3}{64}$ in. in order to keep the hot-spot temperatures within safe limits. For this radial location the magnetic design group then calculated the optimum arrangement of the windings. The values determined were 5 conductors, 6 poles, helical pitch of 0.122 radian/in., and a winding period of 17.18 in.

During bakeout a current of ~ 400 amp is passed through the 2-in.-OD \times 0.049-in.-wall stainless steel vacuum tube. The ohmic heating effect of this current raises the inside wall temperature to the required bakeout temperature, 850° F. Cooling water is circulated through the hollow conductors and the $\frac{1}{16}$ -in.-OD capillary tubes soldered to the $2\frac{1}{2}$ -in.-OD \times 0.049-in.-wall stainless steel winding support tubing. This cooling maintains the outer regions containing the conductors and their associated electrical insulations at acceptable temperatures.

Both the 2-in.-OD and $2\frac{1}{2}$ -in.-OD stainless steel tubes used for the curved sections were precision formed by a tube-bending contractor using a "ball sizing" method. The $2\frac{1}{2}$ -in.-OD tube was then cut in short lengths and slid over the 2-in.-OD tubing and Heliarc welded at the butt

joints in a welding fixture. Thermal insulation was packed in the annulus progressively in sections as the outer tubing lengths were added. The thermal insulation used was a high grade glass wool batting, "Thermo-causti," manufactured by H. I. Thompson Fiber Glass Co., having a density of 3.7 lb/ft³. Rings of this batting, 1½ in. wide × ¾ in. thick were packed and compressed into the annulus to a density of approximately 10 lb/ft³. Conductivity test results on a mockup section with packing densities 50% greater and 50% less gave approximately 25% greater thermal conductivities, which indicated that the packing density used was near the optimum.

Six ¼-in.-OD × 0.010-in.-wall stainless steel capillary tubes, equally spaced, were soldered to the 2½-in.-OD tubing for purposes of reducing the structural tube wall temperatures. Longitudinal layers and circumferential wrappings of glass fiber tape, 0.005 in. thick × 1 in. wide, were then built up over the structural and capillary tubes. These wrappings were "wet" wrapped using liquid epoxy resin impregnation. The subassembly was then cured. The particular epoxy used was Shell Chemical's Epon No. 828 with "Z" curing agent. This is a thermal-setting type requiring 250° F bake to cure. This grade has proved to be very satisfactory for this application—we have subjected it to temperatures as high as 400° F for many hours without observing any serious deterioration in mechanical and electrical insulating strengths. For the windings of this type under normal bakeout conditions, the maximum hot-spot epoxy-glass temperature measured was 275° F.

The conductors are ⅜ in. OD × ⅜ in. ID OFHC (oxygen-free, high-conductivity) copper tubing, annealed dead soft. The conductor is insulated with 8 layers of Mylar polyester tape, 0.001 in. thick by ½ in. wide. The tape is spirally wrapped and butt-lapped, with the direction of the spiral reversed every two layers. A glass fiber braid sleeving is applied by the commercial insulator; this serves to hold the wrappings intact. Before winding, the insulation has a minimum voltage breakdown strength of 15,000 v. However, after winding, especially in the return bend sections, weak spots often develop which show only 5,000 v dielectric strength.

The conductors were wound on a mandrel from which they were transferred to the "cured" subassembly. The conductor bundle was aligned on the subassembly by a row of spirally positioned pins and spacers. The voids between the conductors were filled by working in a thixotropic epoxy paste. The conductor bundle was then wet-wrapped with glass tape — each wrap impregnated with epoxy — until the outside diameter was built up to the specified size. The assembly was then oven-cured at 275° F for two hours.

Figure 12 is a photograph of a typical conductor winding mandrel used for a U-section stabilizing winding. This particular photograph was taken of an early design conductor with a square cross section. Winding and forming difficulties with a bare conductor of this cross section made it obvious that even greater difficulties would be encountered with the insulated conductor, so it was decided to change to the round conductor.

Figure 13 is a photograph of the finished conductor bundle in place on a "cured" U-section ready for the final filling and wrapping. The bundle spacers are in place.

UNCLASSIFIED
PHOTO 47438

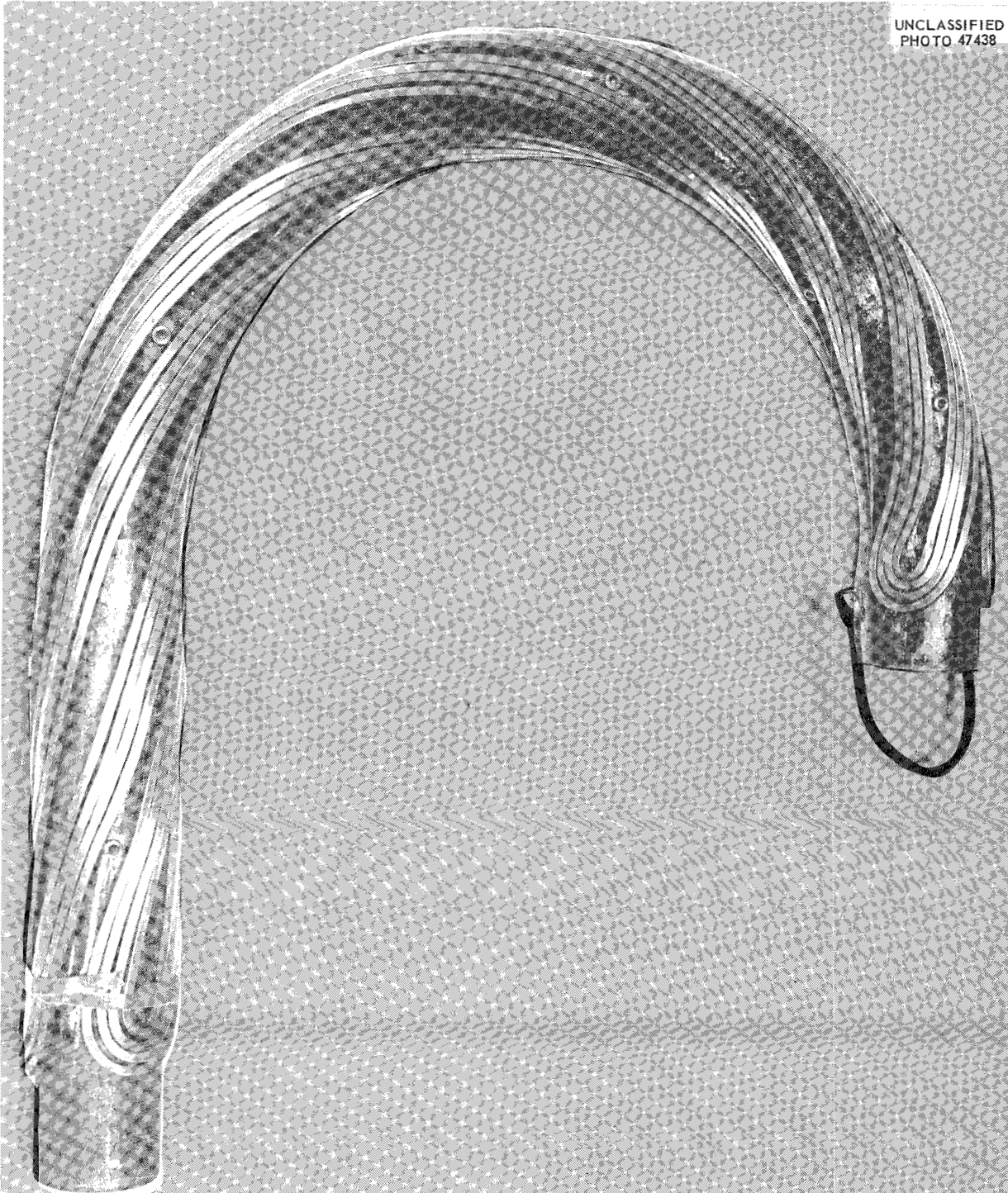


Fig. 12. Early Experimental Square-Conductor U-Section Winding on Forming Mandrel.

UNCLASSIFIED
PHOTO 47439

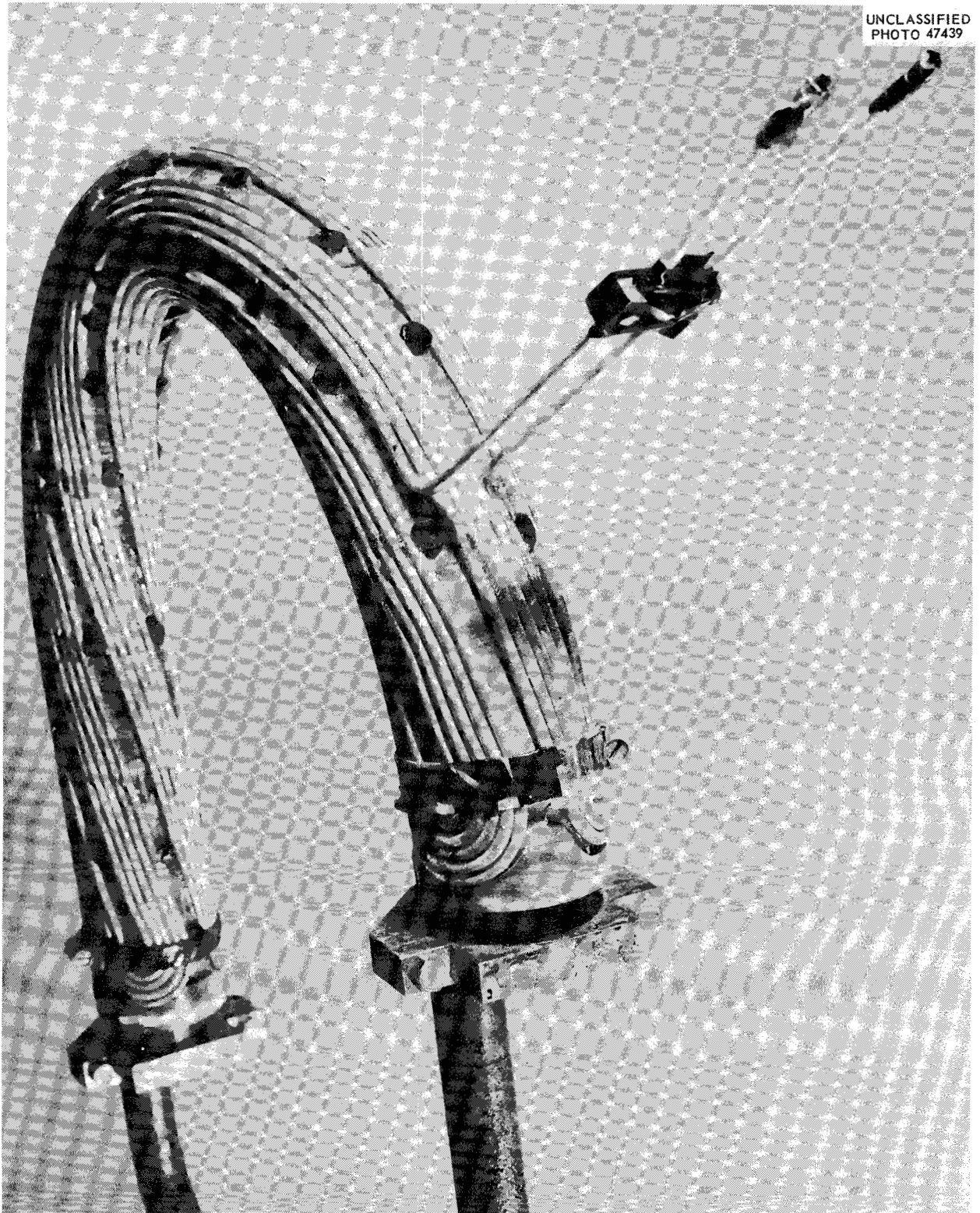


Fig. 13. U-Section Stabilizing Winding with Conductor Bundle in Place Before Potting and Curing.

Figure 14 is a photograph of a finished U-section stabilizing winding in an inspection fixture after curing the final glass-epoxy wrappings and before welding on the vacuum tube flanges and building up the electrical leads terminal block. The outside surfaces are subsequently hand ground down to size, since the radial clearance between the winding and confining field coils is very small.

Modified Type I Winding Design

Figure 15 is a cross section through the modified Type I design which was used in fabricating the spare sections for the original stabilizing windings. In order that the two types of windings

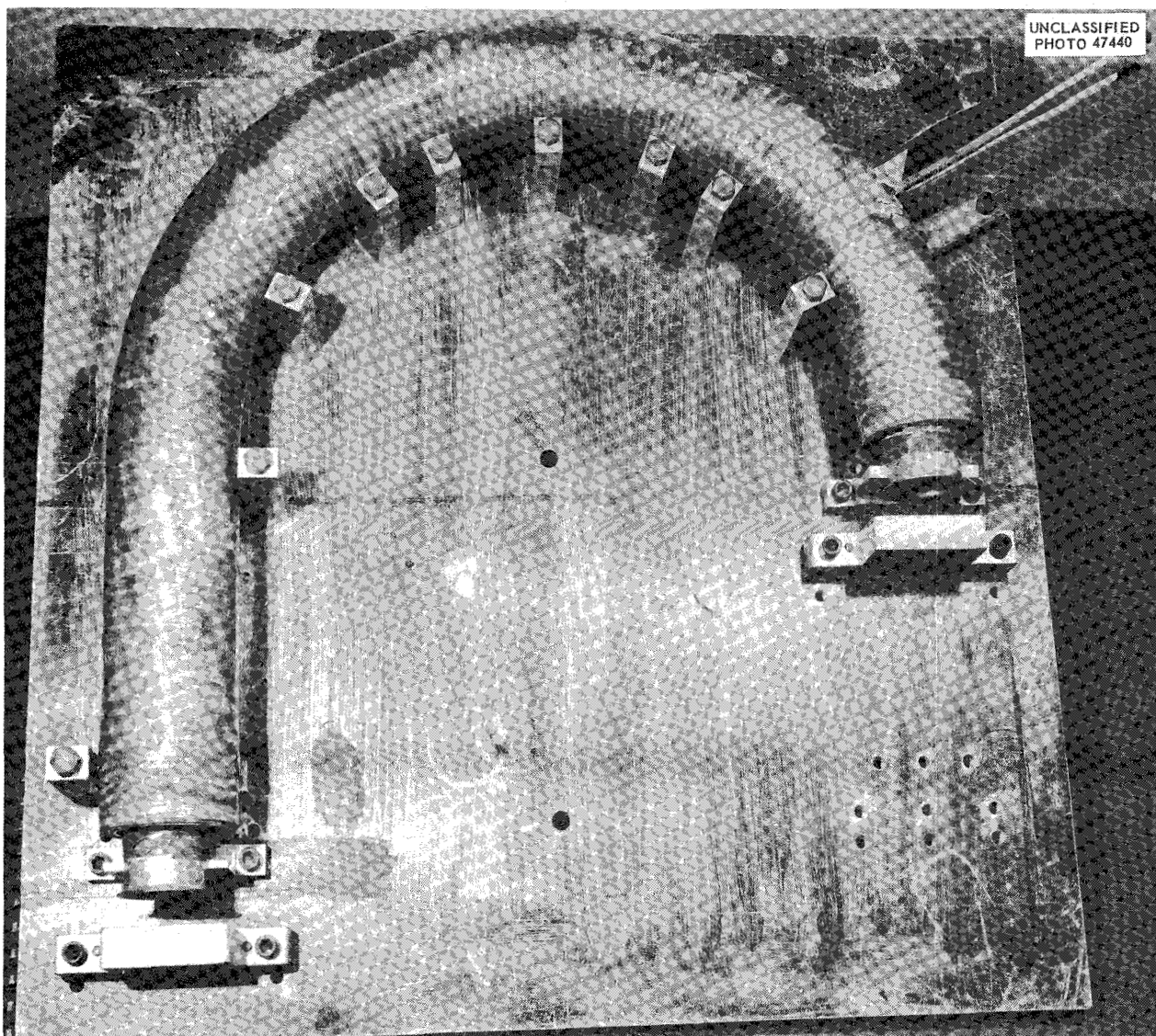


Fig. 14. Completed U-Section Stabilizing Winding in Inspection Fixture Before Welding On the Vacuum Tube Flanges.

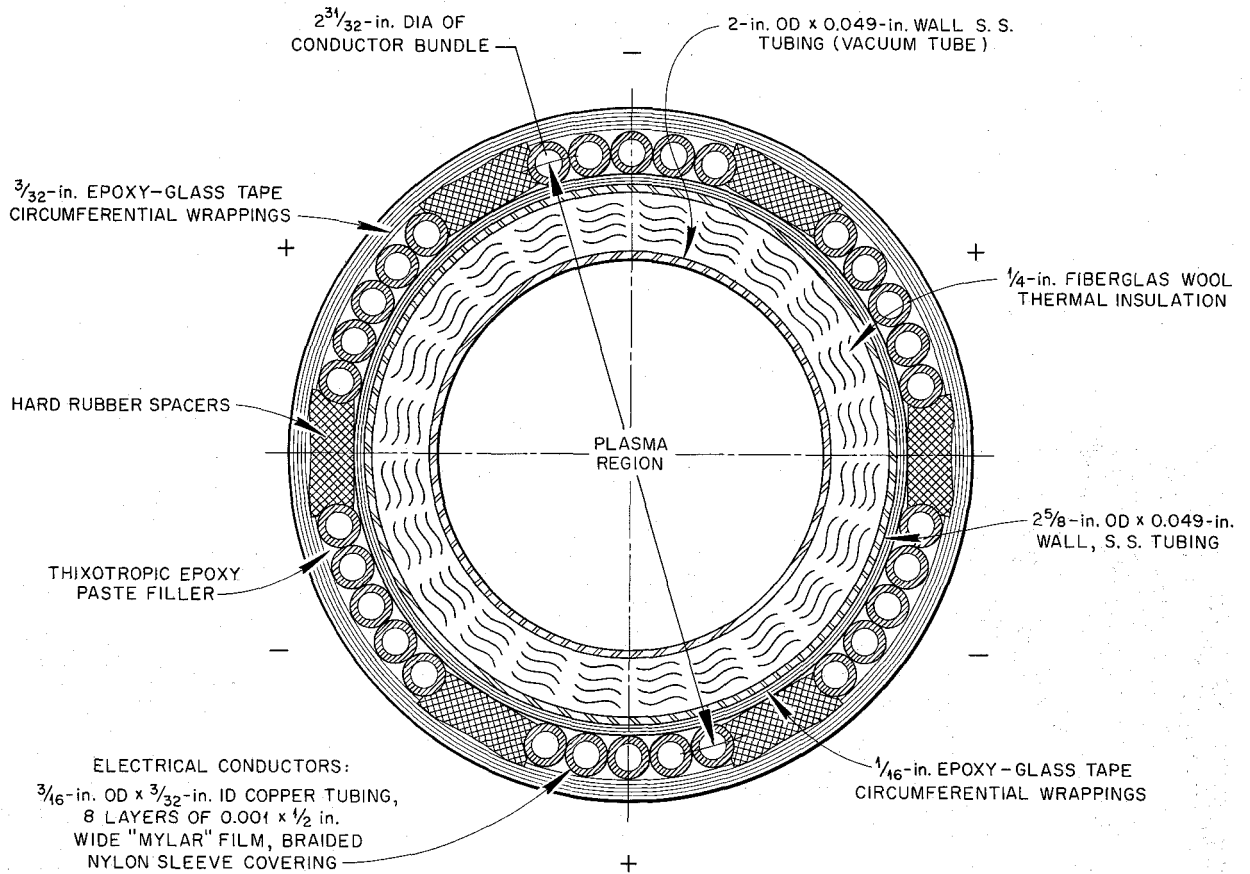


Fig. 15. Section Through Present Replacement Design (Modified Type I) Stabilizing Winding.

be interchangeable, it was necessary to maintain the same conductor radius and helix. This design differs from the original in the following respects:

1. The 1/16-in.-OD auxiliary capillary cooling tubing was removed, since performance tests of the original design showed that the resulting increase in electrical insulation temperatures without cooling water in these tubes could be tolerated. We do not require as great a service life as would be required of industrial electrical equipment.
2. Rather than replace this gap with glass-epoxy which would only unnecessarily increase the dielectric strength to the structural tube, the diameter of the structural tube was increased from 2 1/2 in. OD to 2 5/8 in. OD. This permitted the thickness of the thermal insulation to be increased 1/16 in., which had the twofold advantage of decreasing the hot-spot temperatures in the winding to offset the loss of auxiliary cooling and allowing a greater flexibility of the vacuum tube (which improved the leak tightness of the vacuum seals at the flanges by reducing the bending moments). The seal at the vacuum flanges is a critical item, and it is desirable to reduce bending moments to a minimum.

3. The glass fiber braid around the conductors was replaced by nylon braid which proved much stronger and greatly reduced insulation breakdown in the turn-around bends. The smallest bend radius made in the conductor bundle is approximately $1\frac{1}{2}$ conductor diameters. This bend is so severe that the insulation wrappings wrinkle on the inside of the bend and frequently break the glass braid. When this occurred the insulation wrapping wrinkles were not constrained, and breaks through the insulation appeared. With the nylon braid no breaks of this nature were ever encountered.
4. Thermocouple leads were installed and carried out through the annulus, replacing the wells which were not satisfactory.

Type II Winding Design

Figure 16 is a cross section through the ultimate design which is currently being developed. This design places the conductors essentially on the vacuum tube wall and will give the maximum magnetic performance. In this design the OD surface of the vacuum tube is coated with a porcelain enamel or ceramic-type coating to provide a ground dielectric strength of 4,000 v minimum. Two types of coating have been applied on the U-section vacuum tubes and have been tested. One type was a 0.010-in.-thick commercial porcelain enamel modified by the addition of lithium and

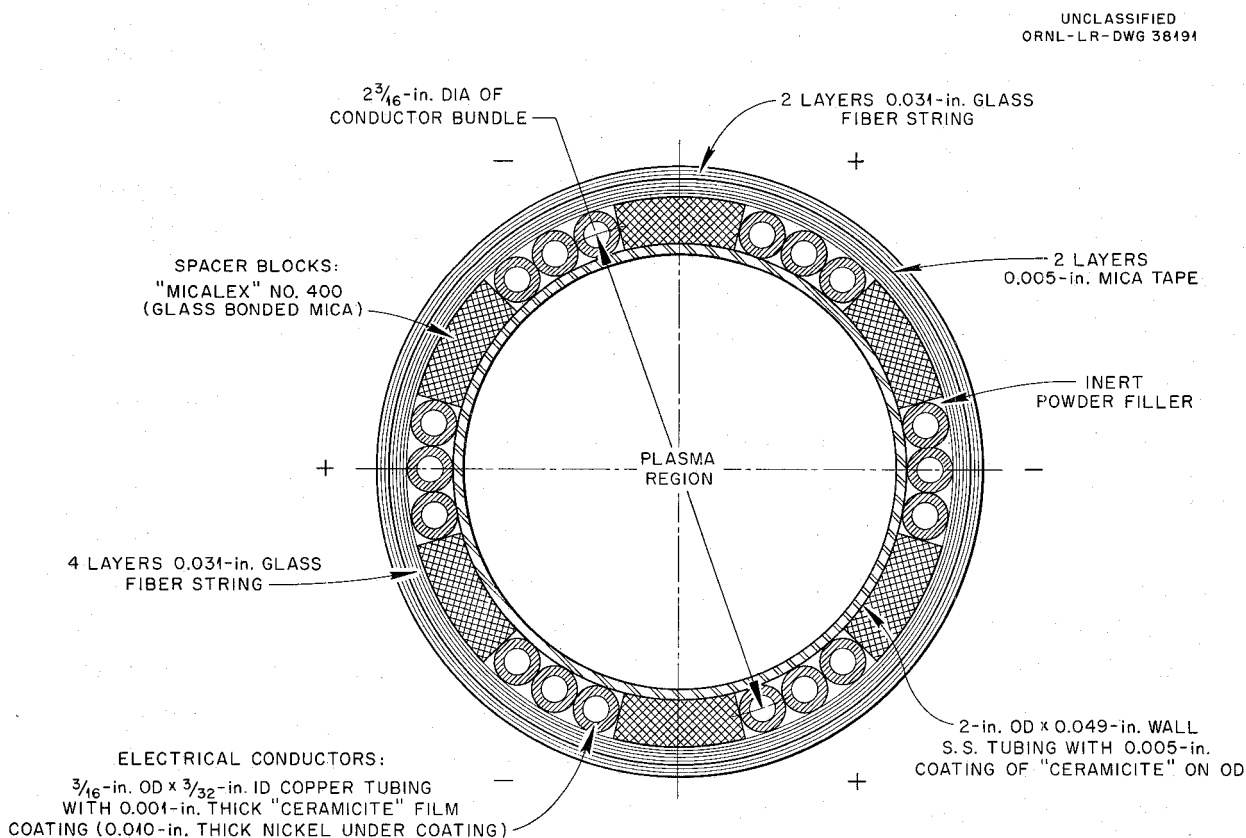


Fig. 16. Section Through Ceramic-Coated Wire Design (Type II) Stabilizing Winding.

fired at 1,400°F. The second was a ceramic-vitreous enamel (0.004 in. thick), identified as "Ceramicite No. C-200" and applied by the Consolidated Electrodynamics Corporation. Both coatings have withstood 4,000-v breakdown tests after a large number of simulated bakeout cycles. The conductors are to be coated with a Ceramicite film for turn-to-turn insulation. This coating is presently being applied to smaller-gage copper wires, and samples we have tested show excellent film adhesion and voltage breakdown strengths after severe bending and twisting. However, the two concerns who are licensed to apply the coating have not coated wires as large in diameter as we require. We are presently negotiating with these concerns to produce sample wires for test evaluation. To produce a satisfactory bond it is necessary to apply the coating to nickel, which requires that the copper conductor be nickel clad. The Superior Tube Company has produced nickel-clad copper conductors by swedging a 0.015-in.-wall nickel tube over a $\frac{3}{16}$ -in.-OD hollow copper tube. If the samples prove satisfactory, an experimental winding will be fabricated. It is planned to add mica sheet between the windings as an additional dielectric barrier in the event relative movement of the conductors causes abrasion.

The conductors will be separated by Mycalex No. 400 (glass-bonded mica) and the complete assembly secured by a number of tension-wound layers of glass fiber string. Outer dielectric insulation will be provided by several layers of mica tape as shown in the cross section. No cooling water is circulated during bakeout, and the whole assembly effectively is at 850°F.

Another high-temperature wire coating is being considered as a substitute for the Ceramicite wire coating. This is a phosphate-and-powdered-mica impregnated, glass-served wire which is serviceable to 950°F that has been developed by the Westinghouse Electric Corporation. It is claimed that this insulation coating has sufficient flexibility to meet the severe bending requirements for forming the windings. Arrangements are being made to secure a specimen winding of this type of insulation for evaluation testing.

Type III Winding Design

Figure 17 is a cross section through a compromise design which will locate the conductors nearer the vacuum tube than the present (Type I) windings, and is considered a backup for the Type II design in the event the ceramic wire coating is not successful. This design has been constructed and tested in a short straight section test assembly. As shown in the cross section, the vacuum tube is coated with a ceramic coating, identical to Type II, for ground electrical insulation. Alternating layers of glass fiber string and tape are tension wound over the vacuum tube to form a $\frac{5}{32}$ -in. thermal insulating layer. Over this Teflon tape wrapped copper conductors are placed. Spacers made of an asbestos insulation board with silicone saturant are inserted between conductors and the assembly over-wrapped with glass fiber string, 2 layers of Teflon tape, and an outer jacket of glass epoxy. During bakeout, cooling water is circulated through the conductors to hold the Teflon hot-spot temperatures below 450°F, which is considered a maximum safe operating temperature for this material.

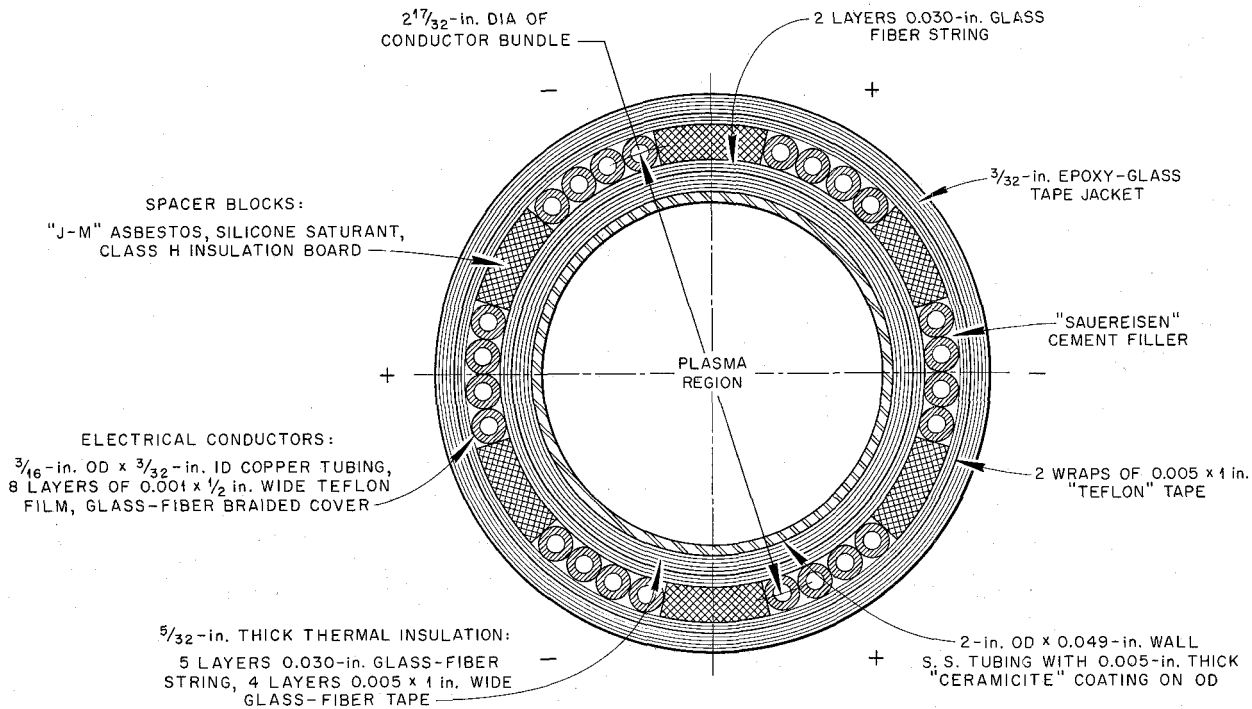


Fig. 17. Section Through Teflon-Coated Wire Design (Type III) Stabilizing Winding.

Figures 18 and 19 are photographs of the test winding which was fabricated for this design. Figure 18 shows the conductor bundle in place with the spacers before filling and wrapping. Figure 19 shows the cutaway assembly after thermal testing. Test results showed that the design was satisfactory.

Hot-spot temperatures directly under the spacers were 500°F maximum. Temperatures directly under the conductors against the string wrappings varied from 350°F to 450°F. Heating current of 650 amp was required to maintain the vacuum tube at the bakeout temperature. Examination and electrical test of the Teflon insulation on the conductors showed no measurable deterioration after 60 hr at normal bakeout and 20 hr at an over-temperature of 950°F. From this we concluded that the insulation hot-spot temperatures were below approximately 450°F, since a measurable deterioration would have been found if any hot-spot temperatures had existed above this value.

HEAT TRANSFER TEST RESULTS

Over-all heat transfer coefficients were measured for several designs, which are summarized in Table 1. These coefficients were taken for vacuum tube wall temperatures ranging between 800 and 850°F. Temperature distribution data are not reported in this paper.

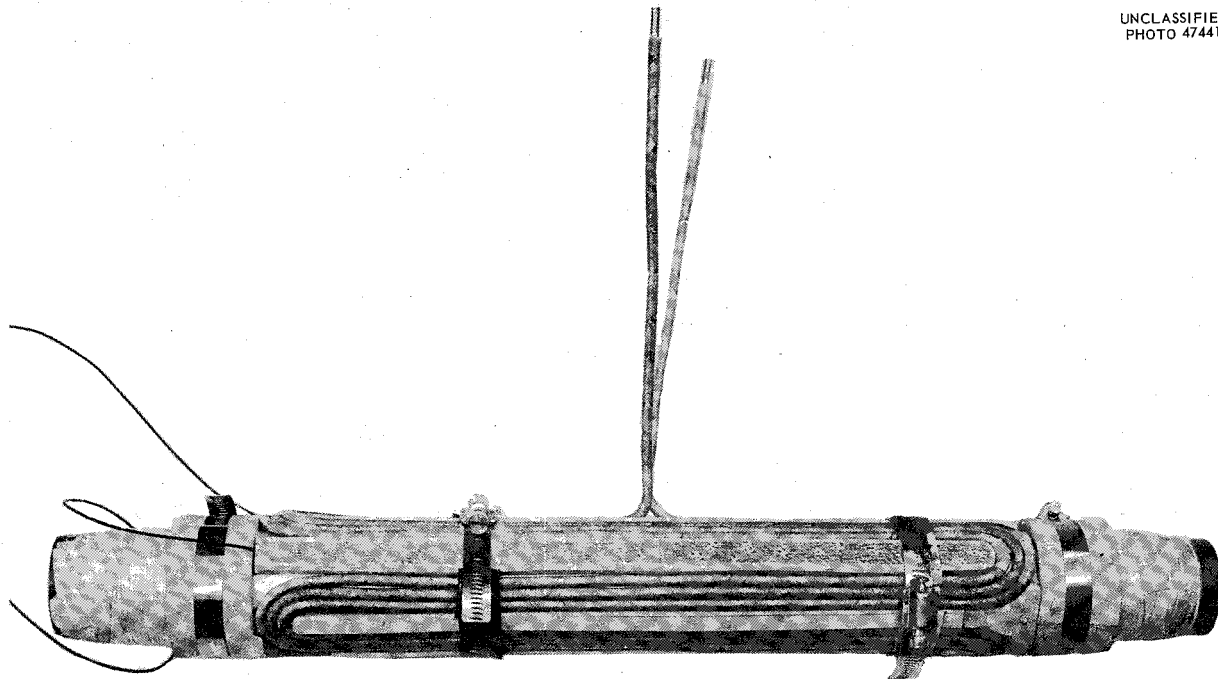


Fig. 18. Teflon-Insulated (Type III) Winding – Conductor Bundle in Place Before Wrapping and Filling.

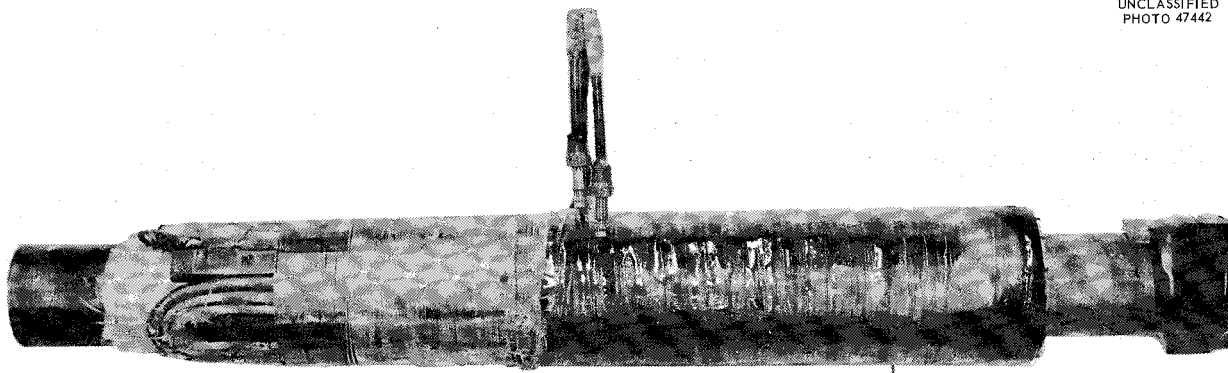


Fig. 19. Cutaway Assembly of Teflon-Insulated Design (Type III) After Thermal Testing.

ELECTRICAL TESTS

One spare Type I U-section stabilizing winding which had been subjected to extensive bake-out and thermal testing – 100 hr at 850° F and 20 hr at 950° F – was used for electrical testing. The electrical tests were designed to simulate normal and overload machine pulse and magnetic fault conditions. For these tests the winding was installed in a special coil test stand with standard B-3 confining field coils as shown in Fig. 20. This photograph shows the stabilizing

Table 1. Overall Heat Transfer Coefficients for Several B-3 Stabilizing Winding Designs

Winding Design	Vacuum Tube Heating Current (amp)	Cooling Water Temperature ($^{\circ}$ F)		Over-all Heat Transfer Coefficient (Btu/hr/ $^{\circ}$ F/ft 2)
		Inlet	Outlet	
Type I, U-section with cooling water flowing in conductors and auxiliary capillary tubes	425	60	110	2.42
Type I, U-section with cooling water flowing in conductors, none in auxiliary capillary tubes	375	60	150	2.07
Modified Type I U-section	360	60	130	1.82
Type III Q-section (3 conductors per pole)	690	60	170	6.15

winding in position with approximately one-half of the winding surrounded by confining coils. The stabilizing winding was wired in series with the 10 confining coils. This arrangement simulates a magnetic fault condition in the confining field, which subjects the stabilizing winding to the most severe mechanical loadings. Cooling-water hoses and connections are to be noted in the photograph. Cooling water is deionized and supplied at 300 psi.

Using the B-3 condenser bank as a power supply, the winding was subjected to approximately 2,000 current pulses of 16-msec duration with peak currents ranging from 5,000 amp (50% rated field) to 17,000 amp (170% rated field). Peak voltages across the winding for the test arrangement were more than twice those that will exist in the actual machine arrangement at the same field. Maximum voltage applied across the stabilizing winding was 750 v corresponding to 150 v turn-to-turn. Typical test voltage and current traces are shown in Fig. 21.

The winding was examined after the tests and there was no evidence of electrical insulation breakdown or loosening of the conductor or epoxy-glass wrapping cover.

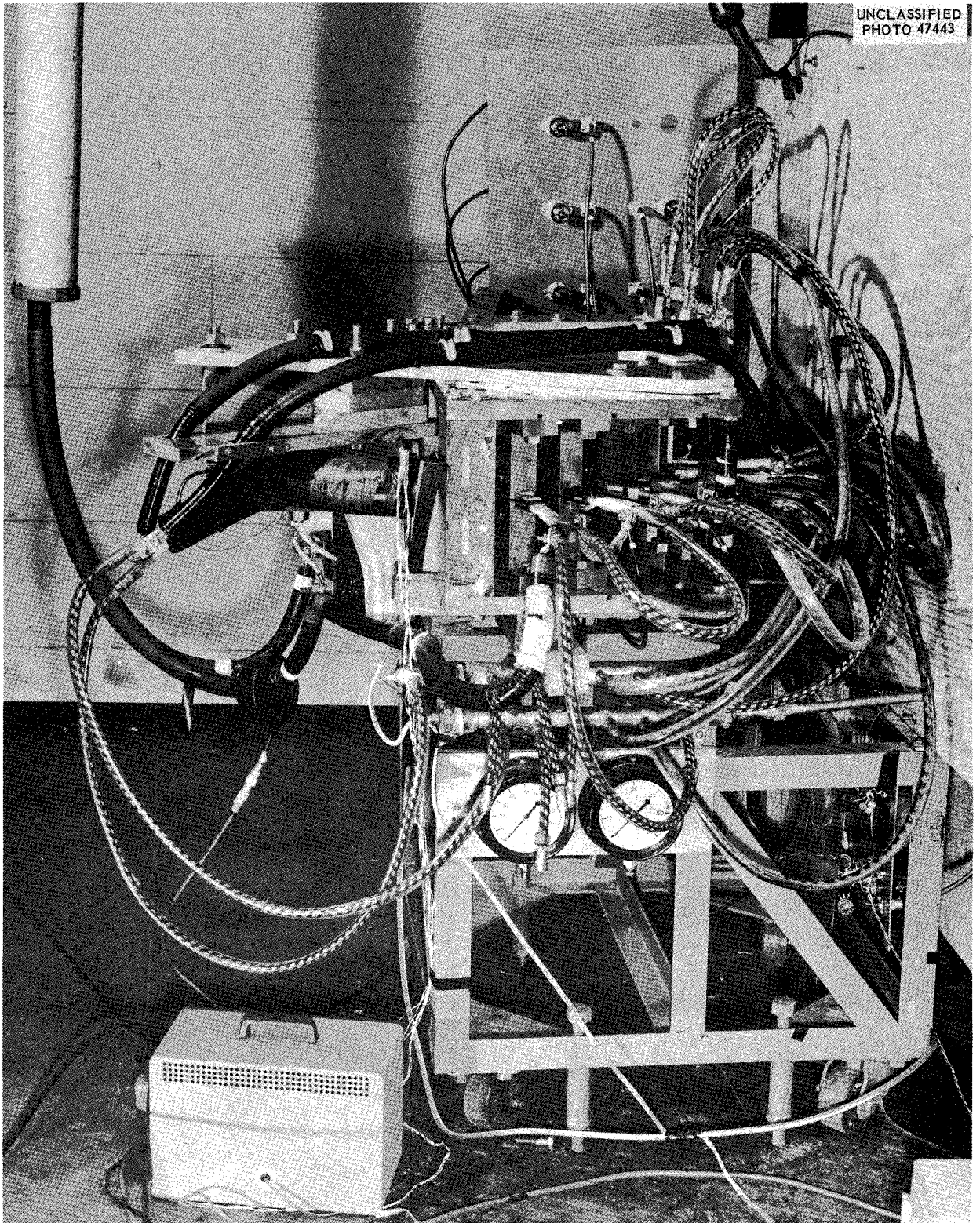


Fig. 20. Pulse-Current Test Stand for U-Section Stabilizing Winding.

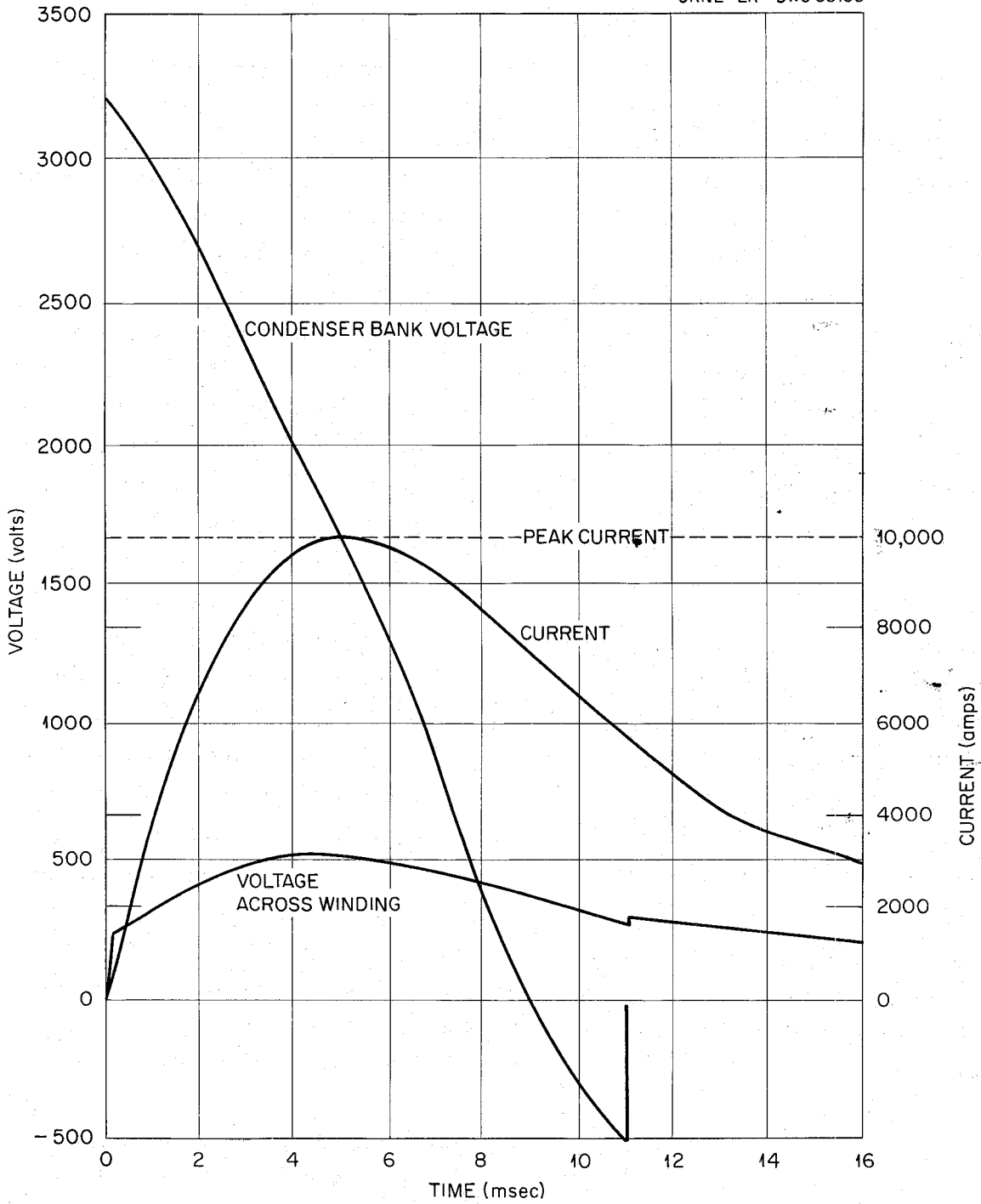


Fig. 21. Typical Stabilizing Winding Test Current-Voltage Pulse.

13. THE GENERATION OF HIGHER CONTINUOUS FIELDS

H. H. Kolm

Lincoln Laboratory, Massachusetts Institute of Technology

Certain experiments in solid state physics of current interest require magnetic fields of modest volume but of substantial intensity, preferably in the several hundred kilogauss range. Some such experiments can be performed in pulsed fields of microsecond duration (see Paper 7), but others require essentially continuous operation. The art of high-field generation was therefore re-examined at Lincoln Laboratory, with a view to designing continuously operating solenoid magnets of minimized volume, with particular emphasis upon access at the largest possible angular aperture, a feature of importance in connection with work in the far infrared.¹

The most advantageous coolant was found to be water under nucleate boiling conditions. Appropriate heat transfer experiments showed that it is possible to transfer 2500 w/cm^2 from copper at 114°C to water at 15°C forced through a flow channel only 0.010 in. thick at a pressure of 70 lb/in.². This is more than ten times the rate of 200 w/cm^2 which served as the basis of Bitter's design in 1936. It represents a performance of 215% in the comparative rating introduced by Laquer² of the Los Alamos Group, in which freely boiling liquid hydrogen rates 100%.

Several new Bitter solenoids were designed to take advantage of this new possibility by reducing their length in order to gain angular aperture, in some cases at a cost in performance. One solenoid has been operating successfully at an average transfer rate of 1250 w/cm^2 (see Fig. 22). A Bitter solenoid does not lend itself to substantial size reduction or high-performance operation due to the circularity of the cooling channels (which are already of minimum practical diameter) and their relatively large separation. Under forced operation substantial thermal gradients force the current progressively outward. A new type of solenoid was therefore designed which represents the first attempt to realize "case 5" considered in Bitter's analysis³ – namely a plane spiral rather than a helical solenoid with tapered ends, in which the current density is also proportional to the radius as in a helix. This design is the logical choice if extreme volume reduction and maximum performance are to be achieved: it provides tremendous heat transfer area without sacrifice of high space factor and mechanical strength. A solenoid of this type (see Figs. 23 and 24) having inside and outside diameters of 0.5 and 2.75 in., respectively, is in principle capable of dissipating 1.7 Mw (the power available in the M.I.T. magnet laboratory) and generating 142 kilogauss.

The first such solenoid was wound of tapered copper foil 0.010-in. thick, consecutive turns being separated by a 0.010-in. interval occupied alternately by axial cooling ducts and spacer ribs. The spacer ribs are partly copper-soldered to the tape and only the minimum fraction of their

¹H. H. Kolm, *J. Appl. Phys.* 29, 489 (1958).

²H. L. Laquer, *Proc. Instr. Soc. Am.* 56, 16 (1956); *Rev. Sci. Instr.* 28, 875 (1957).

³F. Bitter, *Rev. Sci. Instr.* 7, 482 (1936).

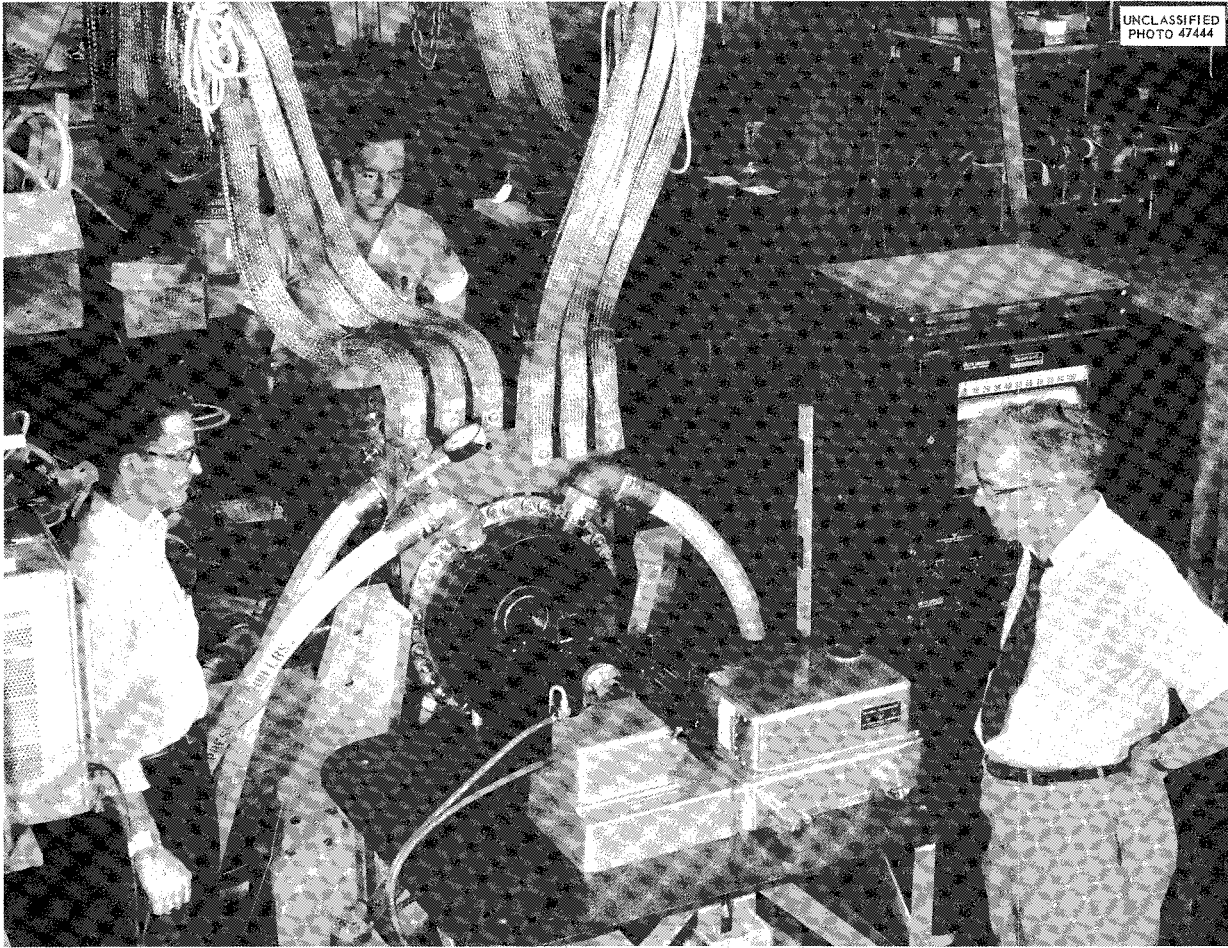


Fig. 22. New Wide-Aperture Bitter Solenoid with Infrared Spectrometer. Left to Right: R. Brown, H. H. Kolm, and F. Bitter.

thickness is insulator; this feature improves space factor and reduces heat generation in the uncooled regions. The spacer ribs are aligned along radii like the spokes of a wheel so as to transmit the radial magnetic forces directly outward to a strong confining envelope. The unsupported segments of tape between adjacent spacers can be kept as narrow as required to achieve adequate strength. Axial constraint is provided by compressing the spacer ribs between insulated spokes protruding from the end housings which serve simultaneously as cooling manifold and inner electrode connection. Solenoids as small as the one described above are limited in operation by flow volume, particularly in the critical region near the center, and a high-pressure cooling system is required to realize their maximum capability. The best performance achieved to date with the existing cooling system (head of 68 lb/in.^2) is 80 kilogauss at a dissipation of about 700 kw. A program is in progress to mechanize the construction of these solenoids and optimize their design. The next solenoid built is to be of 1-in. caliber and should generate about 115 kilogauss with the existing facility.

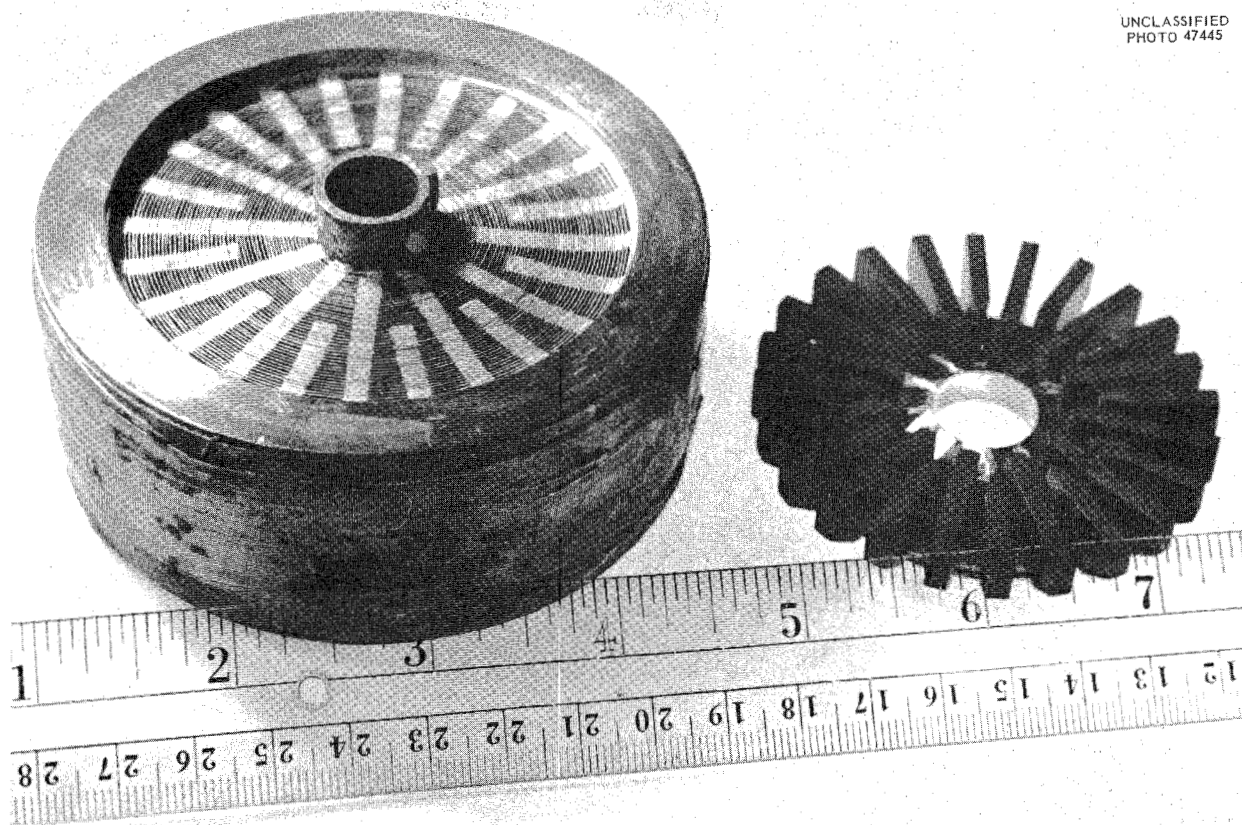


Fig. 23. Core and End Support of 1.7-Mw Solenoid of New High-Performance Design. Manufacture developed under contract at High Voltage Engineering Corp., Burlington, Mass.

Two promising possibilities in the art of high-field generation are to be investigated in the near future. One of these is the use of thermoelectric cooling to remove heat from the most critical parts of a solenoid. This might make operation at liquefied gas temperatures feasible since it is the only heat transfer mechanism which diminishes less rapidly than the resistivity of conductors as the temperature is lowered. The second promising method is that of generating direct current within the solenoid unit by the use of a brushless homopolar generator driven by a coolant turbine. Such a structure is topologically possible and would utilize the remarkable advantages of this type of generator for magnet purposes: a ripple-free output of very high current at very low voltage.

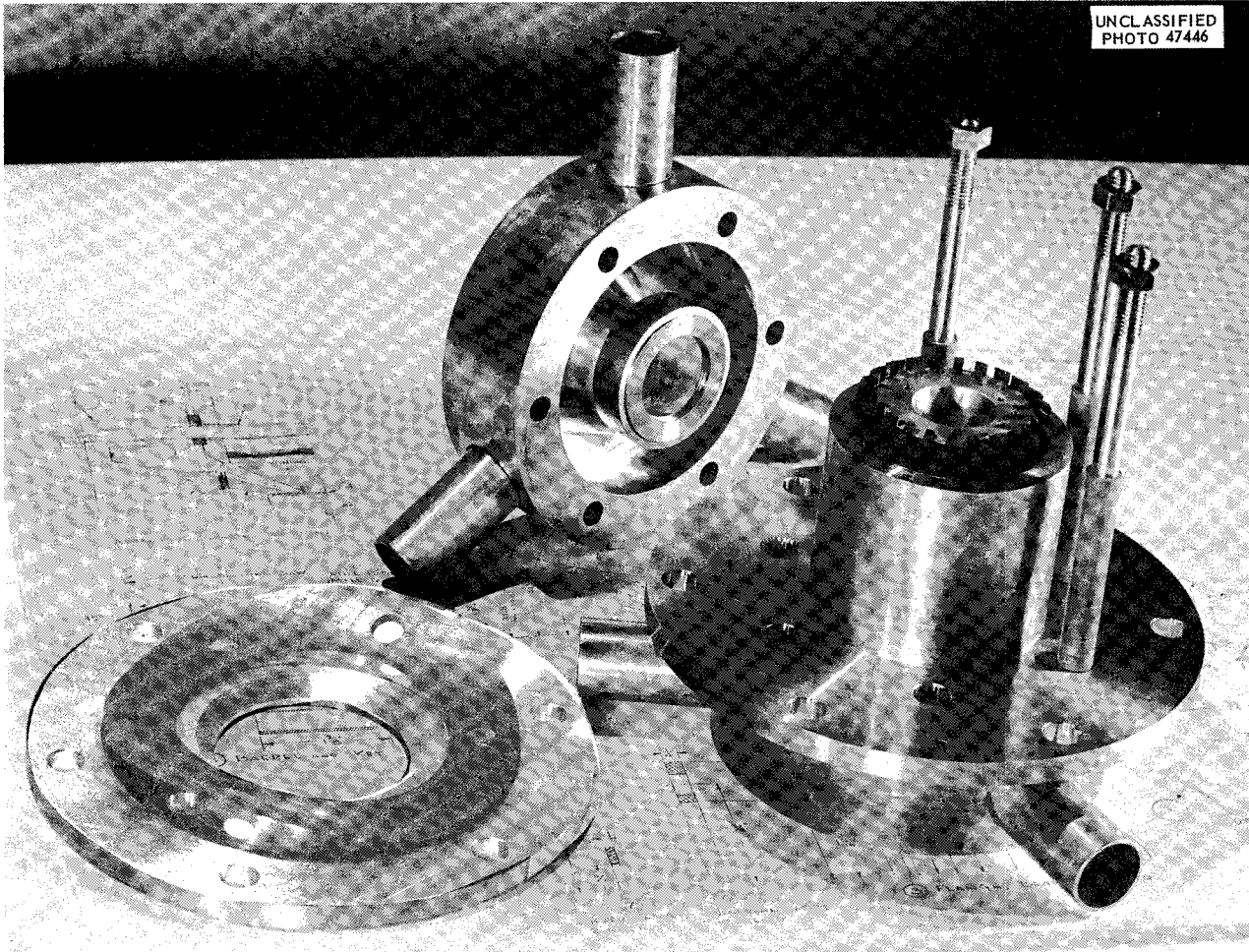


Fig. 24. Assembly View of New High-Performance Solenoid.

14. REFRIGERATION OF MAGNET COILS¹

H. L. Laquer
Los Alamos Scientific Laboratory

Development of steady-field refrigerated magnets has been going on in the cryogenics group of the Los Alamos Scientific Laboratory since January 1955. Feasibility experiments using both liquid nitrogen and liquid hydrogen were reported some time ago.² A maximum steady field of 62 kilo-oersteds was achieved with a coil of 5-in. length, 2.5-in. ID, and 7.5-in. OD immersed in freely boiling hydrogen. Power dissipation was 15 kw. To produce the same field in a similar coil at room temperature would require 1.5 Mw.

¹This invited paper was not received in time for presentation at the meeting.

²H. L. Laquer and E. F. Hammel, *Rev. Sci. Instr.* 28, 875 (1957).

Our recent efforts have been directed toward:

1. Obtaining an installation in which personnel did not have to stand next to the Dewar containing the boiling hydrogen. We now have the magnet coils and dewars in a separately vented concrete vault (Fig. 25) with the high-field regions accessible through holes in the floor of a "nonhazardous" laboratory (Fig. 26).
2. Obtaining long-term operational experience. A coil similar to Coil II (ref 1) has been operated for several periods, each in excess of $\frac{1}{2}$ hour at fields of about 60 koe. The primary emphasis however has been and still is on attendant cryogenic engineering problems such as liquid hydrogen transportation and transfer lines, valves, flow meters, and level indicators.
3. Preliminary work on magnetoresistance. Voltage taps have been attached to two coils so that the average resistivity of various coil sections could be determined as a function of the current and hence of the magnetic field. Figure 27 shows some of the results. The innermost turn seems to have a high "zero" current resistance, but this includes the contact resistance, and we do not know at present whether the excess resistivity is entirely from contact resistance or partially from strains. The remainder of the coil has a low-current resistance of around 8×10^{-9} ohm-cm when immersed in liquid hydrogen. The increase in resistance with increasing current

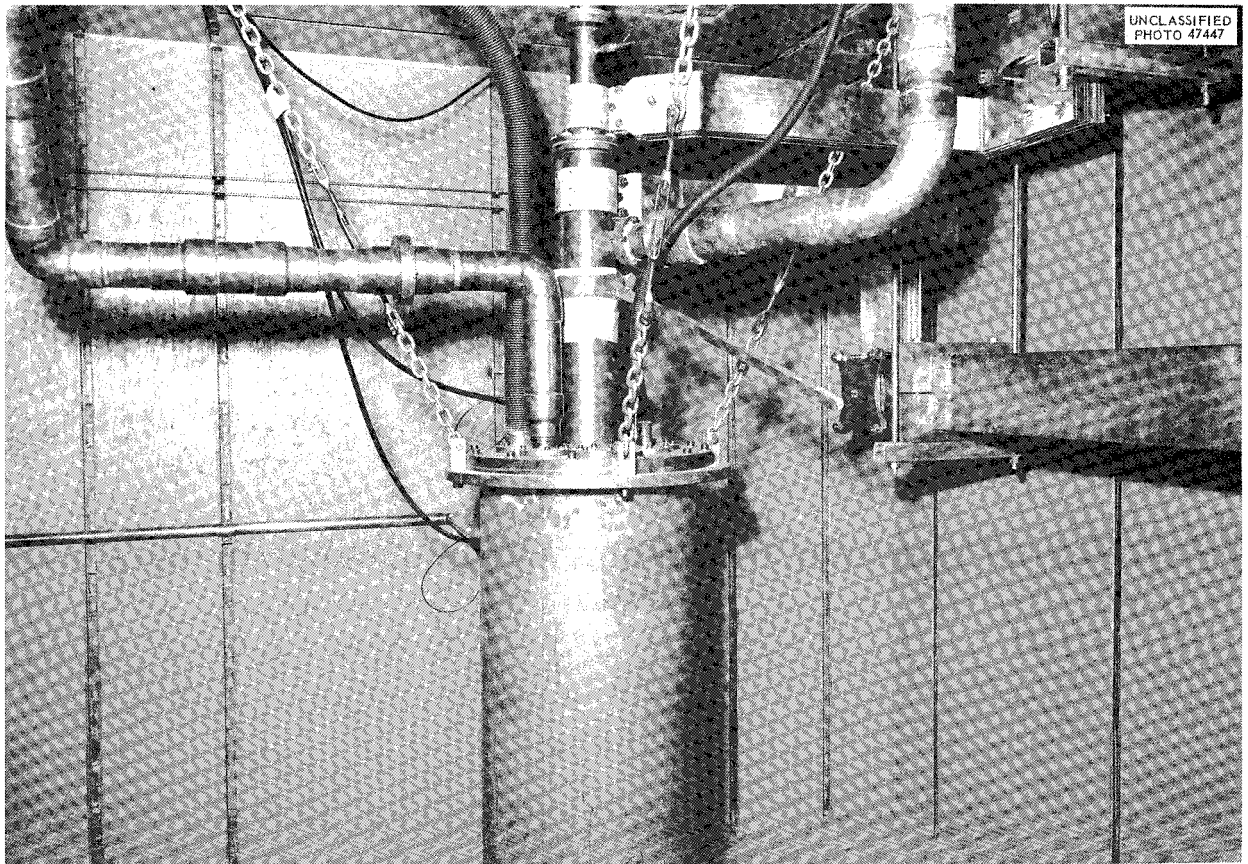


Fig. 25. Coil-Refrigerating Equipment.

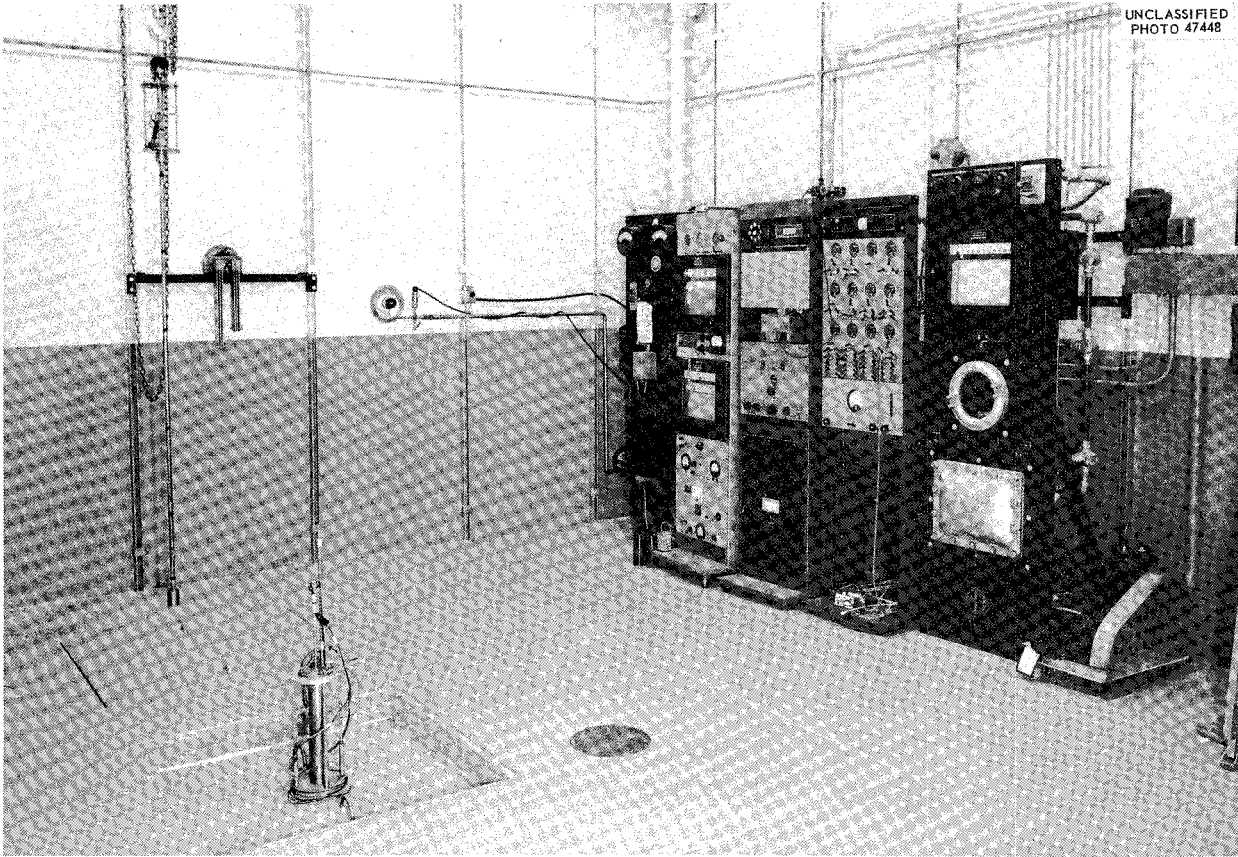


Fig. 26. "Non-Hazardous" Section of Cryogenics Laboratory, Showing Floor Access to High-Field Region.

and its radial variation are clearly apparent and in reasonable agreement with published data on the transverse magnetoresistance of copper.³

Our immediate plans include forced flow experiments, with the hope of going beyond the heat transfer limitations present under free boiling conditions,⁴ and an investigation of the problems of aluminum coil construction with the expectation that magnetoresistance will be considerably less with this conductor than it is with copper.

³J. L. Olsen and L. Rinderer, *Nature* 173, 682 (1954).

⁴S. G. Sydoriak and T. R. Roberts, *J. Appl. Phys.* 28, 143 (1957).

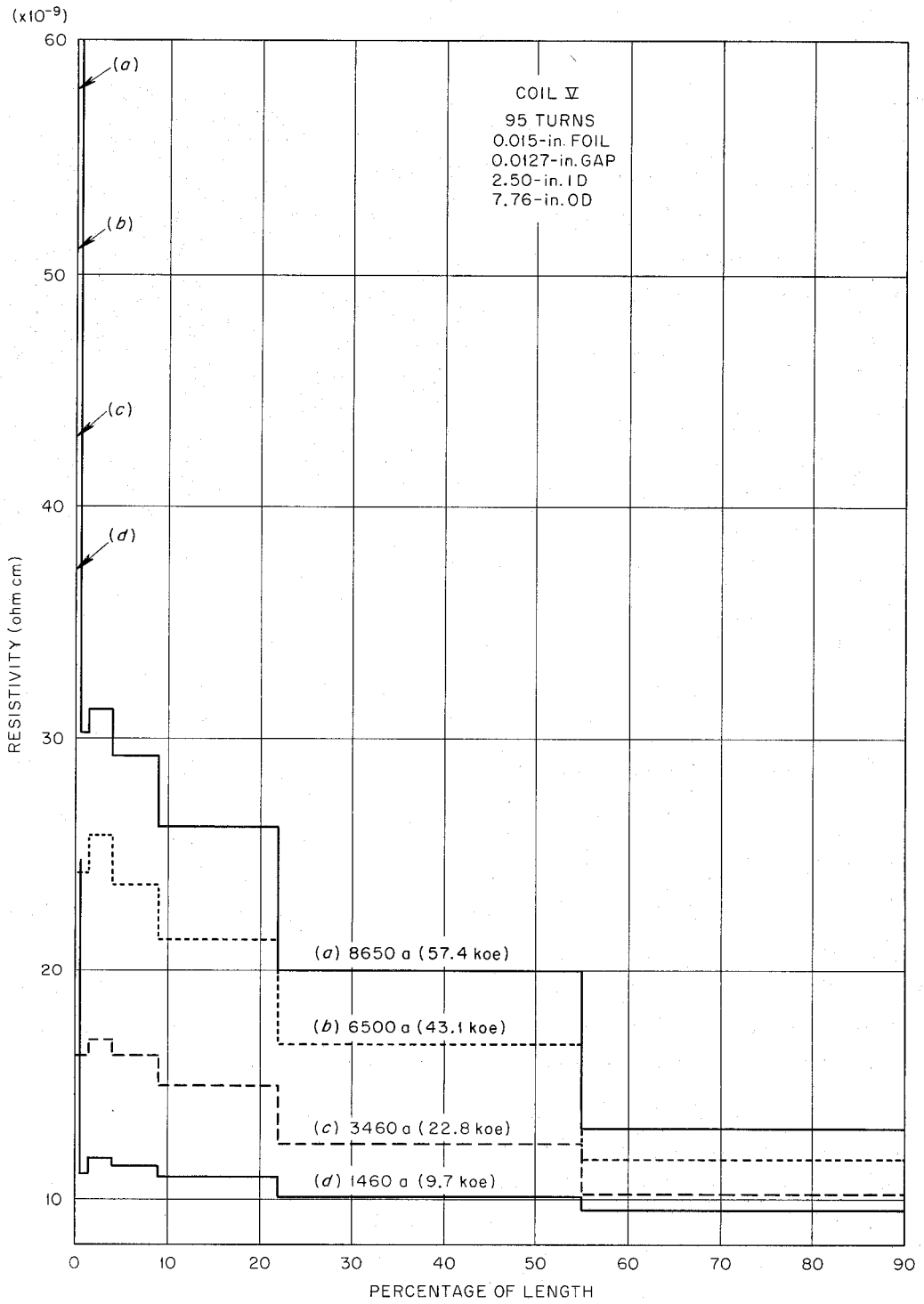


Fig. 27. Resistivity of Coil Section as a Function of Current.

15. THE PRODUCTION OF PULSED MAGNETIC FIELDS AT AFCRC

Morton A. Levine
Geophysics Research Directorate
Air Force Cambridge Research Center

For many applications, the use of pulsed currents to produce magnetic fields offers definite advantages over d-c methods. With pulsed currents one can produce larger fields of many varied shapes more simply and with considerably less equipment.

In all that follows it should be understood that all dimensions are large compared with the skin depth in any metal conductor. That is to say, when one first produces a magnetic field with a conductor the eddy currents are such as to exclude the magnetic field from the conductor — though in time the currents penetrate farther into the metal. The conditions under which our pulsed fields are produced are such that the current and field do not have time to penetrate appreciably into the conductor by diffusion; and currents may be treated, at least for the first approximation, as being surface currents alone.

Given an unlimited power supply, the maximum pulsed magnetic field that one can produce is limited by two factors:¹ the strength of the structure (this limitation can be calculated from the magnetic stress tensor) and the melting and destruction of the coil form by high currents.

It is not always necessary that a pulsed coil structure be as massive as one designed to operate under direct current. It is possible to design a coil so that the impulse that is transferred, $\int \nabla(H^2/2) dt$, to the momentum, mv , of the coil can be absorbed and dissipated in the stressing of the coil structure. (In bending or stressing a structure the energy absorbed can be calculated as the integral of the pressure times the deflection.) If the maximum allowable deflection is such that a coil in absorbing $\frac{1}{2} mv^2$ does not deflect beyond the elastic limit, then a coil can withstand corresponding $\int \nabla(H^2/2) dt$. Thus the coil can take large fields under pulse conditions when it might not necessarily be able to withstand such fields under d-c conditions.

While the d-c I^2R heating of metal conductors may be calculated rather straightforwardly, the situation is not quite so clear in the case where a single high-frequency component pulse is used. It can, however, be shown that in this case the energy (I^2R) dissipated per unit volume of the coil is approximately equal to or is at least of the same order of magnitude as the value of the quantity $H^2/2$ in that volume. This limits the value of the magnetic field to that corresponding to the melting and vaporizing of the metal.

The use of pulse methods to shape magnetic fields relies on the fact that magnetic fields lie along metal-vacuum interfaces. Thus, if one desires a curved field line it is only necessary to make a curved metal surface. It has been found in our laboratory that one of the most useful methods and most flexible apparatus that can be used for field shaping is provided by the flux concentrator first reported by Babat and Losinsky.² In this device metal eddy-current elements

¹H. P. Furth, M. A. Levine, and R. W. Waniek, *Rev. Sci. Instr.* **28**, 949–58 (1957).

²G. Babat and M. Losinsky, Concentrator of Eddy Currents for Zonal Heating of Steel Parts, *USSR, Jour. of Appl. Phys.* (1940).

are placed within a solenoid for the purpose of shaping and concentrating the magnetic field lines. Figure 28 shows a cross section of one conceivable design for such a device. Eddy currents flow along the outer surface of the copper slug by virtue of the magnetic field produced by the primary solenoid. The slot running parallel to the z-axis forces this current also to flow along the inner surface of the slug. The concave shaping of the copper inner surface gives a magnetic field on the inside which is curved as shown. Because the magnetic field varies from point to point along the inner wall of the copper slug the current density along this wall must vary correspondingly. Since the integrated current flow on the outer wall is equal to the integrated current along the inner wall, and the current density along the inner wall is not uniform, the current density at the central region is necessarily higher than that on the outside of the slug. This leads to a correspondingly larger magnetic field on the inside than on the outside. Thus the field can be both shaped and intensified. One of the major sources of energy loss of such a device is in the slit which feeds the current to the central region. This can be minimized, it has been found in this laboratory, by slanting the slot at an angle, θ , to the z-axis. The energy loss is then lowered by the cosine θ . This device has the added advantage of distributing the forces such that the coil can be made intrinsically stronger.

As an illustration of the flexibility and use of the flux concentrator in producing specialized magnetic fields, Fig. 29 shows a high-field betatron design. It will be recalled that a betatron gives a stable orbit when (1) the magnetic field at orbit is $\frac{1}{2}$ the average field through the orbit and (2) the field index number, n , takes on certain specified flux between 0 and 1. The field index number is the ratio of the radius of the orbit to the radius of curvature of the field line at the

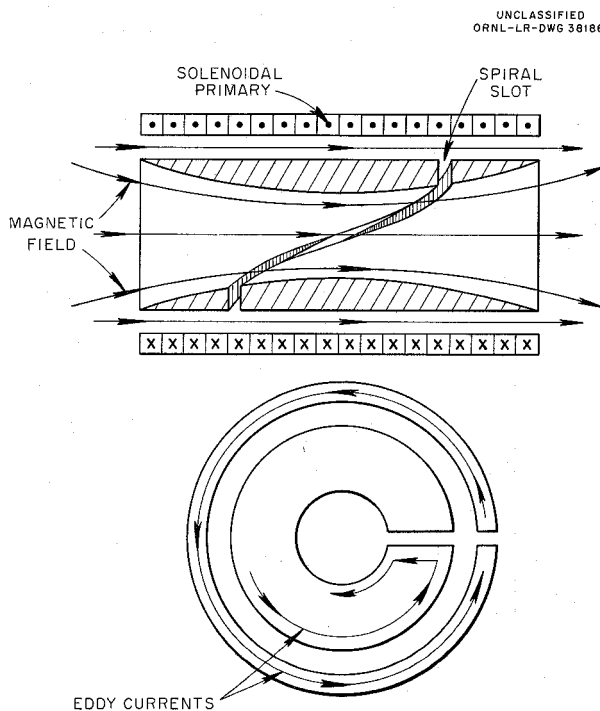


Fig. 28. Flux Concentrator.

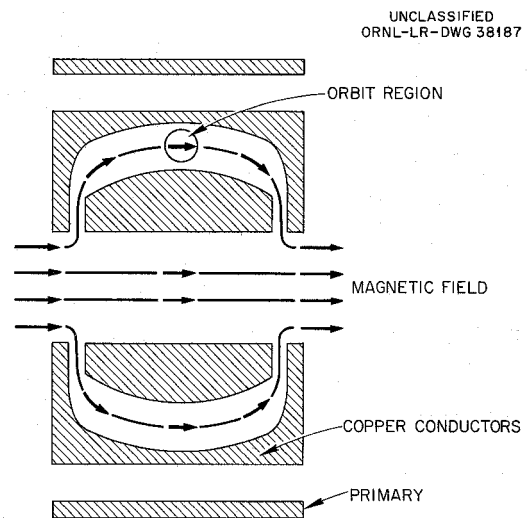


Fig. 29. High-Field Betatron.

orbit, and the curved walls of the cavity give the curved field lines corresponding to the proper n number. A simple device that may be used to understand the field shaping shown in Fig. 29 is the analogy that magnetic field lines will lie along the same lines as the flow lines for non-viscous fluid. Thus the magnetic field is of the same shape as a fluid flowing through a pipe into which an obstruction had been inserted, as shown in Fig. 29. The small entry crack into the orbit region cuts the average field in this region down to the desired value. The slightly curved walls surrounding the orbit region give the desired field shape. The open central region permits the field through the center to be as large as possible. A possible variation of this device is shown in Fig. 30. Here the field lines in alternate sections are bent in alternate directions corresponding to the Christofilos alternate gradient focusing.

UNCLASSIFIED
ORNL-LR-DWG 38188

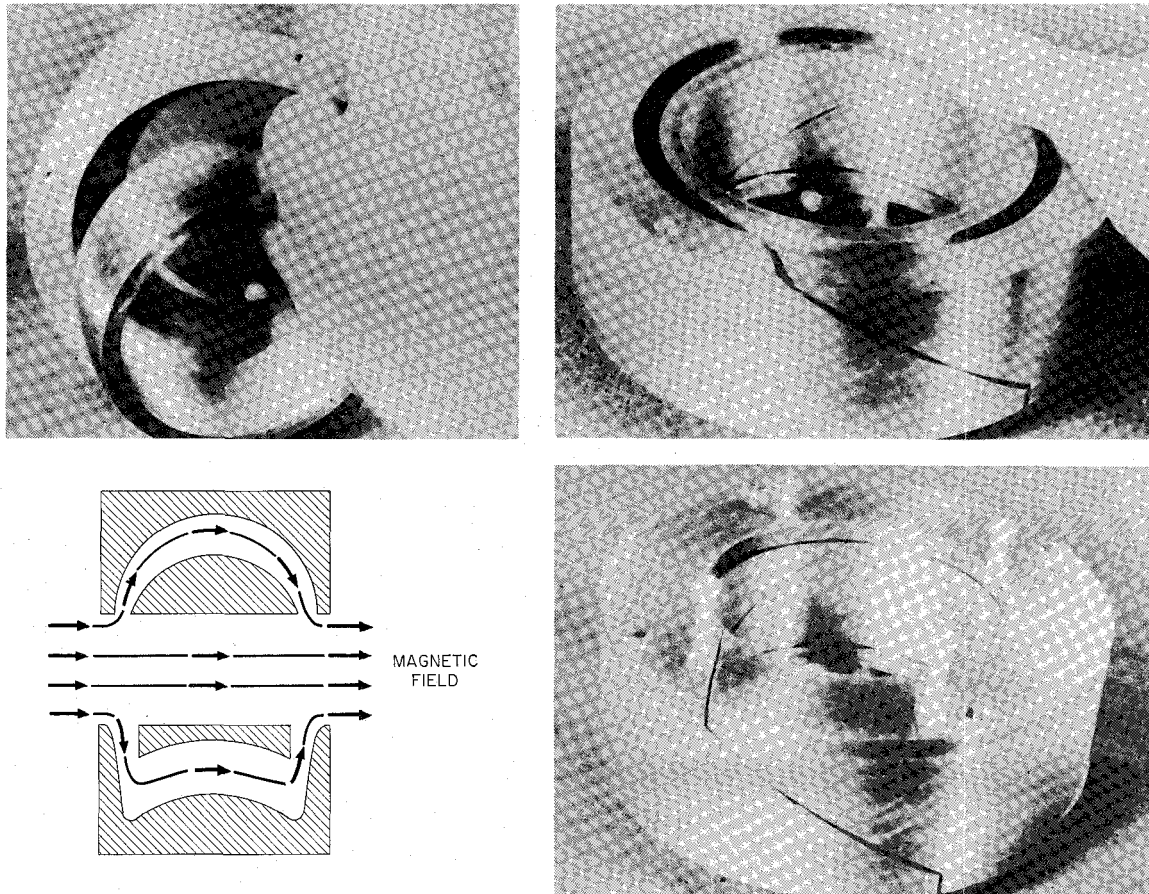


Fig. 30. Alternate Gradient Betatron.

16. MAGNETIC FIELD DESIGN AND CONSTRUCTION EXPERIENCE AT PRINCETON

R. G. Mills

Project Matterhorn, Princeton University

The Princeton program is the development of the stellarator type of thermonuclear machine. This type of equipment should eventually require continuous solenoidal fields of densities greater than 50,000 gauss in a device in which the location and direction of each line of the field is accurately positioned. The experimental program so far has largely been restricted to the investigation of phenomena which are completed within a few msec. This allows the fields in small experimental machines to be pulsed rather than continuous and enables the use of high fields in small machines without exceeding the capacities of a practical cooling system. Pulsing also saves a great deal of power, but in small devices the power is usually quite low although the energy storage requirements may be costly. The pulsed field in our devices should remain near peak value for a few msec, which means that the important frequency components to which the coils will be subjected lie in the range of hundreds of cycles per second rather than the much higher frequencies required by some other types of experiments. We have used capacitive storage as our source of energy. Further complication arises from the fact that parts of some coils must be very close to a vacuum system which must be baked out at approximately 450°C. This usually leads to cooling problems more severe than those associated with the dissipation of the electrical energy needed to generate the field. A problem always confronted in the design of high-strength fields is the mechanical support needed for the high forces. The hoop stresses induced by the tendency of a coil to expand and the collapsing force tending to shorten a segment of a solenoid are well known and treated in the literature. Two aspects of the mechanical force problems, however, which have been occasionally neglected in the design of equipment are "bounce" forces and fault condition problems. Suppose we have a solenoid bent into a closed torus. Under normal operation there is hoop stress and there is also a force on any segment toward the center. There are no large collapsing forces along the axial direction of the field. However, should there be a double arc to ground or failure in the exciting circuits so that only part of the coil carries current, then axial collapsing forces will appear. These collapsing forces which tend to shorten the coil must be adequately supported by an appropriate structure which is also capable of absorbing the "bounce" force. These come into play whenever the current in the coil is reduced suddenly in a length of time short compared to the natural period of the mechanical structure. This can happen in systems designed for short pulses or in a fault situation where the coil's current has been suddenly reduced. In this case the strain energy of the structure is released by acceleration in the opposite direction of the coil winding and large forces in the opposite direction are developed on other portions of the supporting structure. We are therefore faced with five problems in designing and constructing field systems:

1. determination of a physically realizable set of currents to produce the desired field shape,
2. design of coils to make efficient use of the stored energy available,
3. mechanical structure to support the forces produced,

4. cooling to remove electrical energy consumed,
5. cooling of coils closely associated with baked-out components.

Item 1 possibly represents the only area in our work where truly new engineering procedures have been developed. The engineering of the location of all the lines of a magnetic field for their entire length has been a new problem. Methods of treating this problem have been developed by K. E. Wakefield, as described in Paper 18. Item 5 is a very difficult one and we have no satisfactory answers. H. G. Johnson has done preliminary work on this which is discussed in Paper 12. We hope to learn a lot on this subject from the experience of other laboratories.

To present the history of our treatment of Items 3 and 4 and to illustrate the problems involved, a number of photographs are included. Our oldest operating machine, model B-1, has flat strap copper coils wound and potted against a Textolite center board. These are adequate for 50,000 gauss under normal conditions with the center board under compression but they are inadequate for fault conditions and/or bounce forces. In July 1955 a failure at 30,000 gauss occurred, which is shown in Fig. 31. Failure of a bond resulted in an accordion-like collapse failure of about ten coils. To prevent recurrence, stainless steel caps were placed on the coils

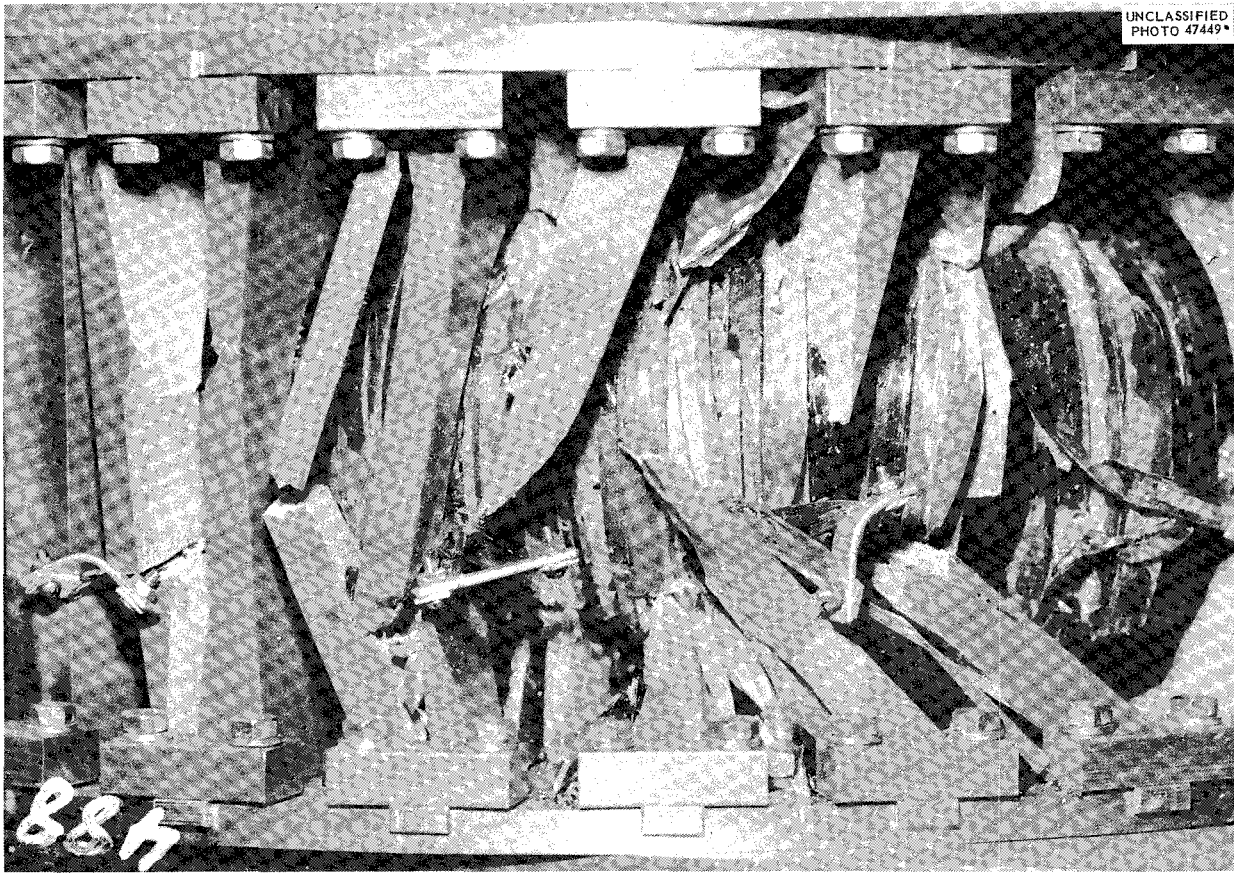


Fig. 31. Failure of Model B-1 Stellarator Magnetic Field Coils.

to hold bounce forces and prevent multiple coil failures in the event of a single failure. Figure 32 shows the coil designed for B-3, the next machine in this series. In this case we have strong K-Monel holders bolted together with twelve $\frac{1}{2}$ -in. bolts. The heavy case prevents convective cooling and these coils are cooled by internally circulating water. The case is designed to operate under fault conditions of 50,000 gauss with a safety factor of 2. This implies that the yield point should be reached at 70,000 gauss and actual failure prevented below 86,000 gauss. Tests have verified this, and the coil has been very satisfactory mechanically. The assembled B-3 machine is shown in Fig. 33.

Electrically, however, we have had several failures due to at least two causes. These have always been turn-to-turn insulation failures at points of maximum voltage. One cause, the only one we have identified, was our failure to anticipate the transmission-line effect of the machine.

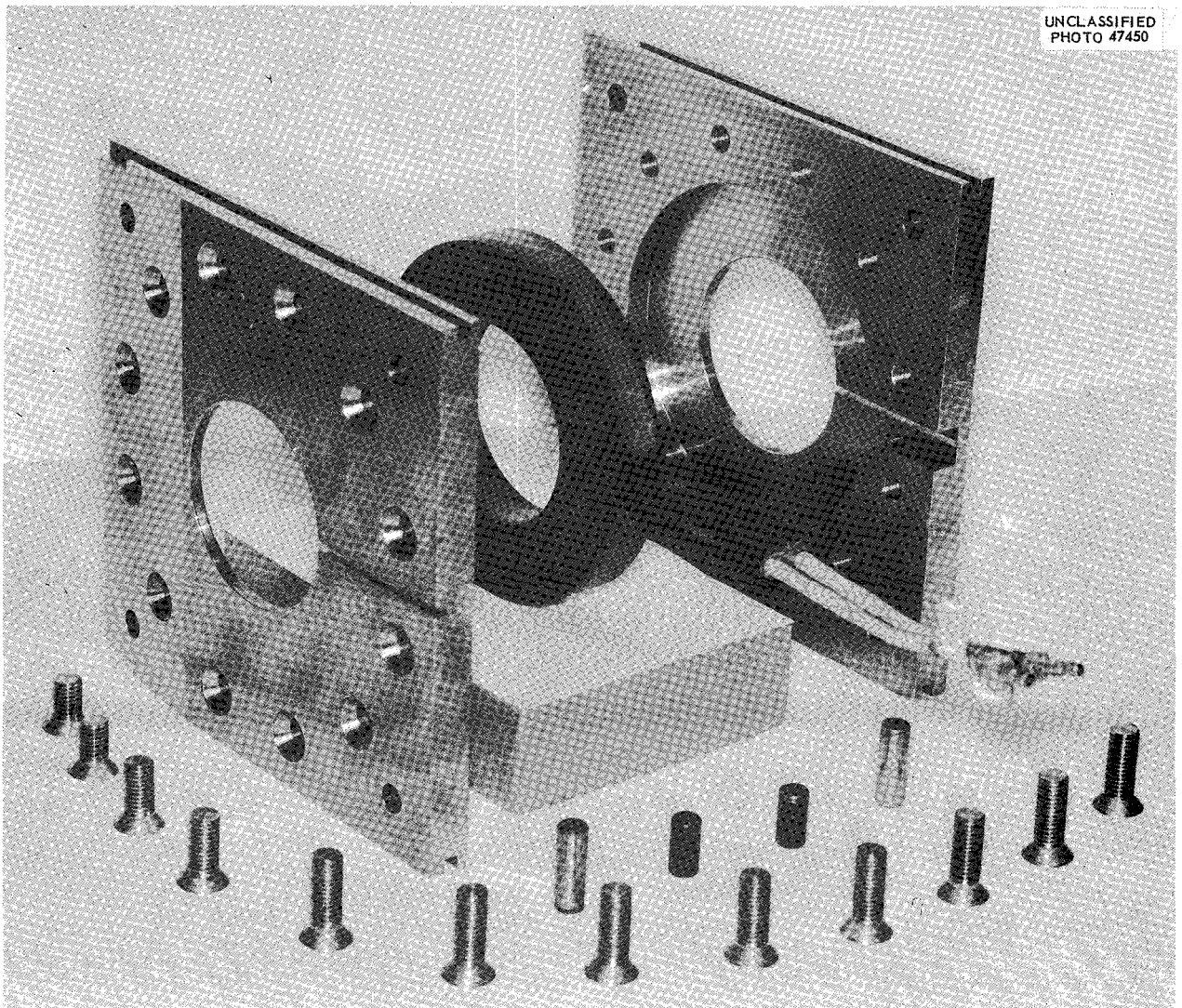


Fig. 32. Magnetic Field Coil for B-3 Stellarator.

UNCLASSIFIED
PHOTO 47451

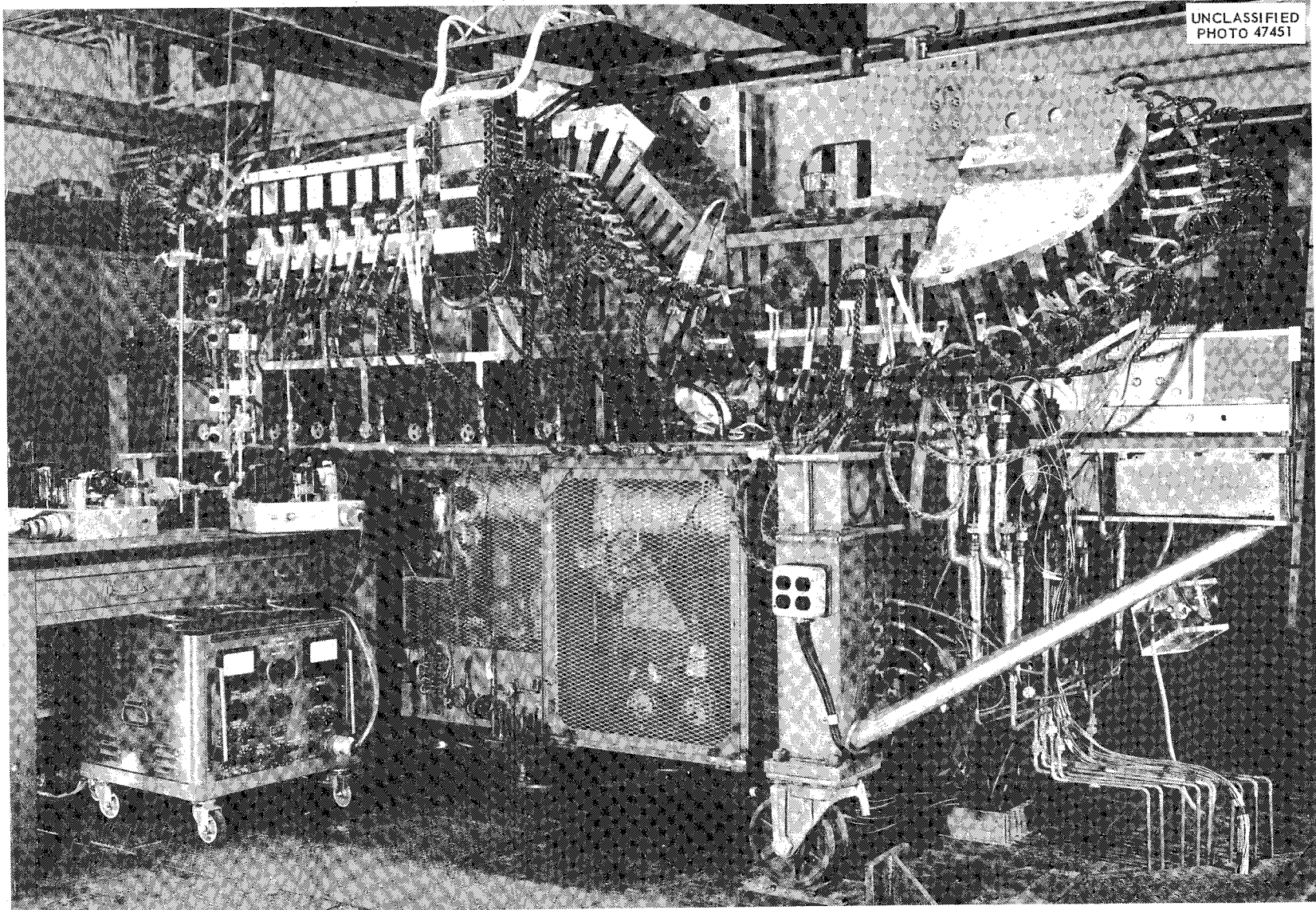


Fig. 33. B-3 Stellarator.

The coil system is a long inductance, and the metal cases constitute a set of shunt capacities to ground. When the switch is closed the voltage front propagates along the machine and an appreciable fraction of the total voltage can appear across one coil. Therefore, in spite of the fact that the normal operating voltage will never exceed about 70 v across 12 mils of insulation, one can get a transient of 50 times that much. Several coils failed under such treatment before we inserted a network between the capacitor bank and the machine designed to prevent changes of voltage at the input terminals more rapid than the transit time of the machine. Nevertheless we still experience an occasional insulation failure in spite of the fact that the coils operate at less than 10 v per turn and are tested at 25 v per turn before acceptance. The cross section of one coil is shown in Fig. 34. The conductor is $\frac{3}{16}$ in. square with a $\frac{3}{32}$ -in. hole. Insulation is 6 mils of Daglas. In later units two layers of 2-mil Mylar have been inserted between each layer of copper. The winding is wrapped with glass and potted in epoxy resin of $\frac{1}{10}$ -in. nominal thickness. A few miscellaneous types of coils are shown in the following figures. The Etude machine (Fig. 35) is a d-c machine with water-bath cooling used to maximize cooling efficiency. It will generate a 10,000-gauss field continuously. Experience with this machine has emphasized the importance of

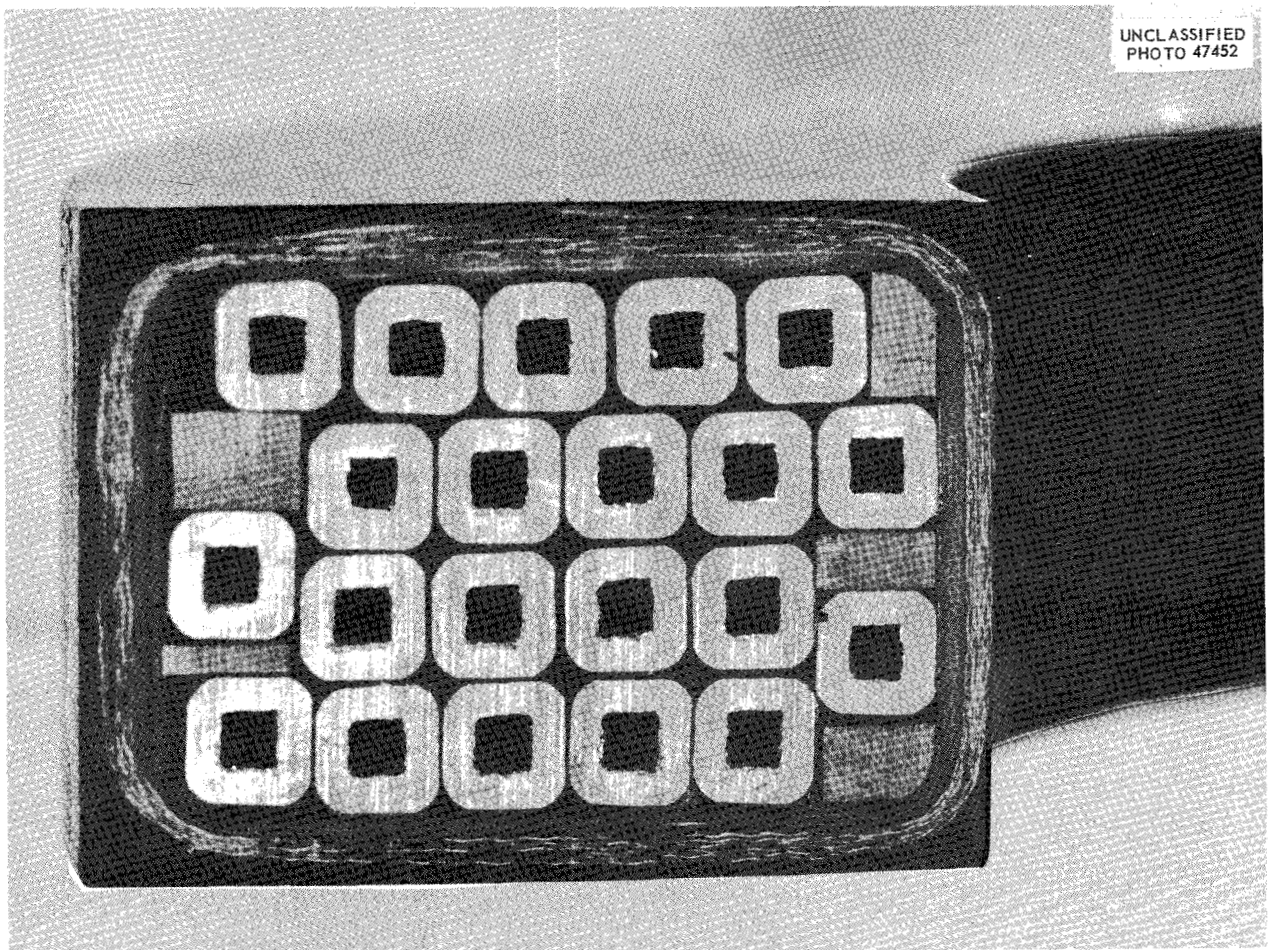


Fig. 34. Cross Section of Magnetic Field Coil for B-3 Stellarator.

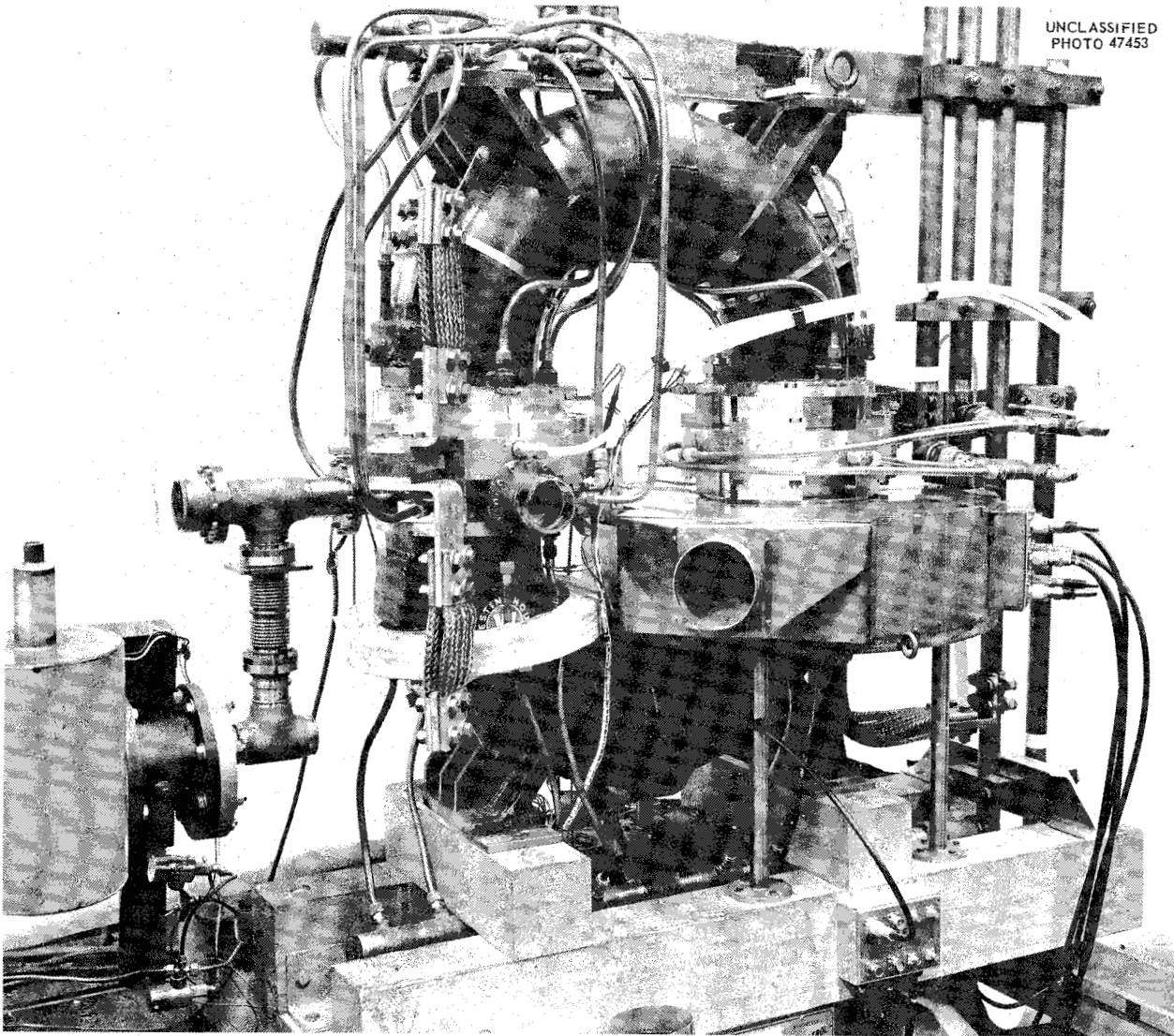


Fig. 35. Etude.

operating only when the deionized water has high resistivity. Otherwise electrolytic action will transfer considerable copper and can lead to shorts. Figure 36 shows a cross section of a coil designed to produce a field of constant field strength in a portion of the machine devoted to cyclotron resonance heating experiments. The methods described by K. E. Wakefield in Paper 18 were used to specify the location of each turn and the coil was embedded in epoxy glass cloth. Field strength is uniform within $\frac{1}{2}\%$. Figure 37 shows a model C test coil which has been sectioned for inspection and exhibit. These coils were pulsed to the 50,000-gauss level for times longer than a second. We had one failure of a different unit similar to the B-3 failures in that turn-to-turn insulation breakdown occurred at a high-voltage stress point. This probably was due to a low-pressure gas pocket left between turns during the vacuum impregnation process.

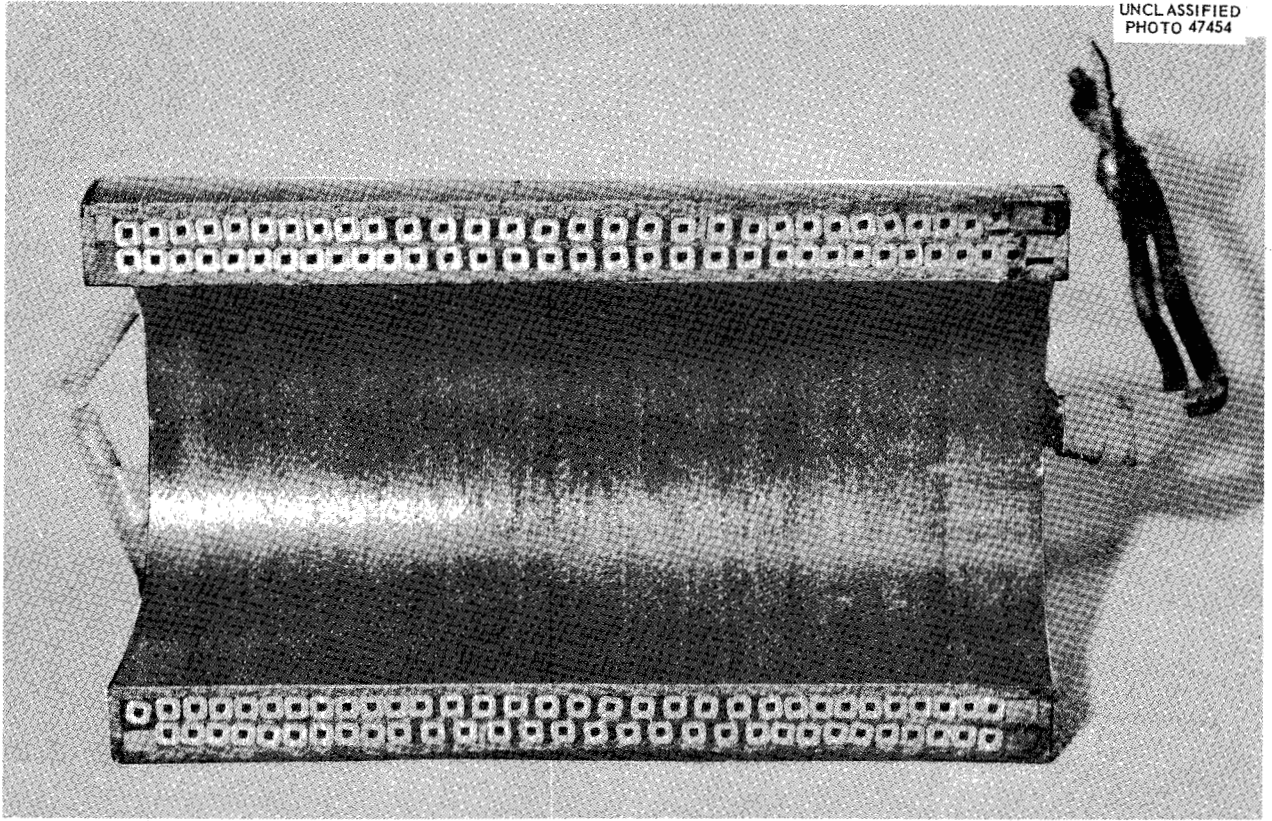


Fig. 36. Cross Section of Magnetic Field Coil of Constant Field Strength.

Item 2 is of great importance and merits discussion. Assume that we store our energy in capacitors and we wish to use this energy to produce a pulsed magnetic field in air or vacuum. The energy situation is this:

$$\frac{1}{8\pi} \iiint B^2 d\Omega = \eta \left(\frac{1}{2} CV^2 \right) ,$$

where B is the field strength, $d\Omega$ an element of volume, η is some number less than one and represents the transfer efficiency of this system, C is the capacitance of the energy storage capacitor, and V is the voltage to which it is charged. In practice, transfer efficiencies of greater than 90% can sometimes be achieved. The result of this is that the peak field available from a fixed amount of energy storage is

$$B_{\max} \sim (\eta/\Omega)^{1/2} ,$$

where Ω is the effective volume of the region to contain the magnetic field. If ω is the resonant frequency, $[(1/LC) - (4R^2/L^2)]^{1/2}$, of the system and Q is defined as $\omega L/R$, then

$$\eta = e^{-(\arctan 2Q)/Q} .$$

This should always be calculated in considering a proposed system.

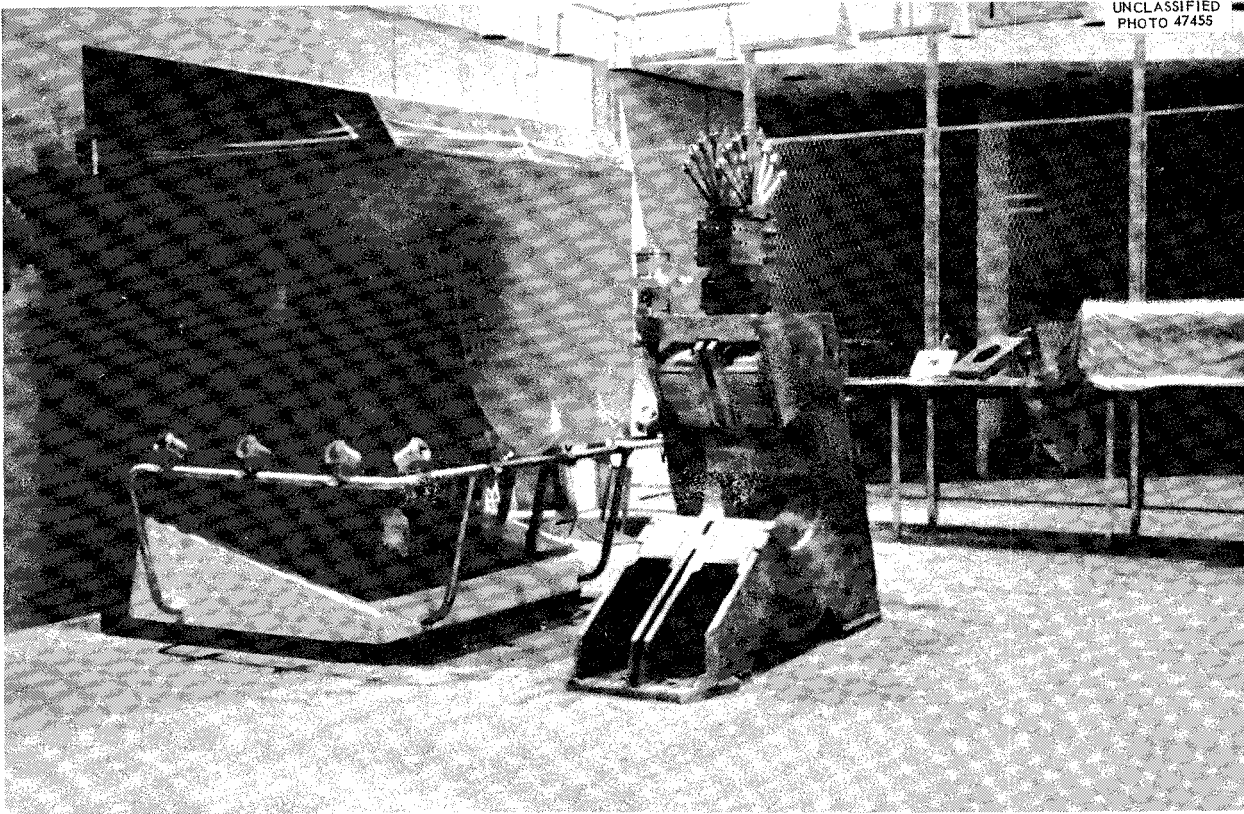


Fig. 37. Section of Model C Test Coil.

Figure 38 shows some design curves of a proposed design. The ordinate is the peak field achieved and the abscissa represents the OD- to-ID ratio of the magnet. Notice that if the peak field is the only consideration, one should not raise η excessively by oversize coils. This will merely increase the volume in which the field is produced and lower the maximum field strength to which it will go. If the duration of the field is important, then one should increase the size of the coil to increase the time constant L/R . The cost in peak field is not excessive. In applying this design approach one must be extremely careful about the value of resistance used in computing ω , Q , and η . The correct d-c value may be very seriously in error even at a frequency that is very low, for example, a few cycles per second. Failure to check this point carefully may result in a peak field only one-third of what the designer may have anticipated. As a practical matter the designer should use as small a cross-section wire as practical questions of cooling and voltage limit dictate. Paper 17 presented at this conference by D. R. Wells and F. Tenney concerns this question of a-c resistance.

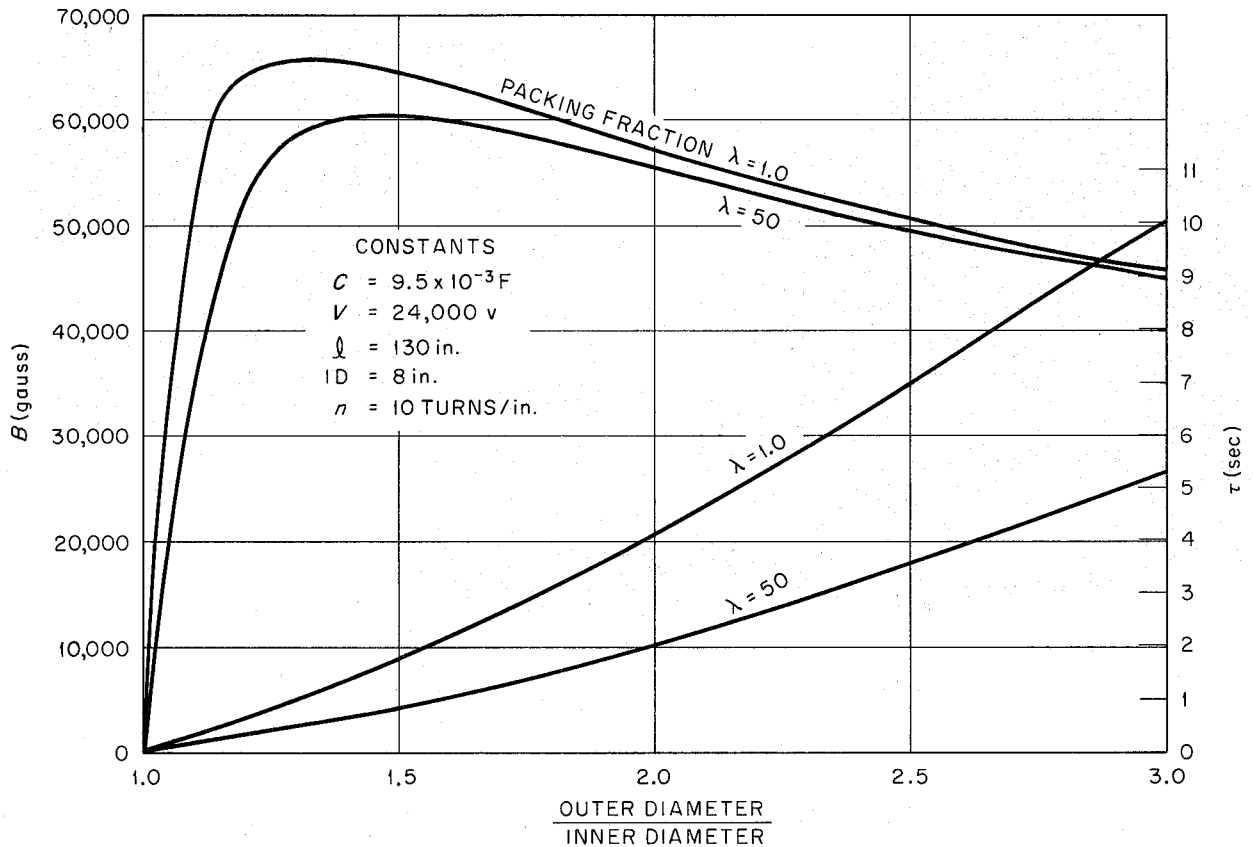


Fig. 38. Time Constant and Magnetic Field vs OD/ID Ratio of Magnet.

17. PROXIMITY EFFECT AND ITS IMPORTANCE TO THE PULSED FIELD DESIGNER

F. Tenney and D. R. Wells
 Project Matterhorn, Princeton University

ABSTRACT

A method is illustrated for computing the a-c resistance of infinitely long single and multiturn solenoids.

With the design of the axial confining field coil system of stellarators in mind, we consider the a-c impedance of long solenoids. More exactly, we consider the a-c impedance of a typical "pancake" of such a solenoid as illustrated in Fig. 39. We neglect the displacement current in Maxwell's equations and assume the magnetic field to be everywhere parallel to the axis of symmetry.

Hence the boundary conditions for the magnetic field are the usual ones for a solenoid. We consider the various layers of the "pancake" to be connected in series and take the applied emf in any one turn to be independent of the radius. We then relate the total emf applied to the pancake to the

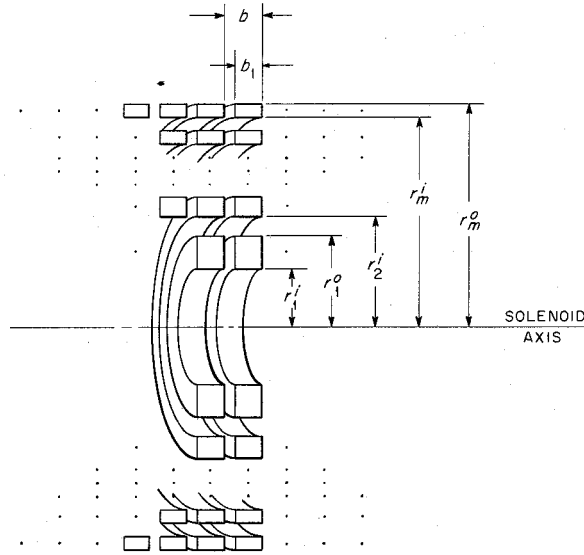


Fig. 39. Some Units Used in Solenoid Design Calculations.

series current flowing in order to find the impedance. The calculation is straightforward. Our results are:

$$Z \equiv R + i\omega L = i\omega \frac{4\pi^2}{b} \left[m^2 r_1^{i2} + \sum_{n=2}^m (m-n+1)^2 (r_n^{i2} - r_{n-1}^{o2}) \right] + \frac{\omega}{i} \sum_{n=1}^m T_n,$$

where

- $\omega = 2\pi \times \text{frequency},$
- $m = \text{number of layers in the pancake},$
- $R = \text{total pancake resistance},$
- $L = \text{total pancake inductance};$

and

$$T_n = \frac{8\pi^2}{bki^{1/2}} \left(\frac{2(m-n+1)(m-n)}{ki^{1/2}\Delta_n} - \frac{1}{\Delta_n} \left\{ r_n^i (m-n+1)^2 [K_o(u_n^o)I_1(u_n^i) + I_o(u_n^o)K_1(u_n^i)] + r_n^o (m-n)^2 [K_o(u_n^i)I_1(u_n^o) + I_o(u_n^i)K_1(u_n^o)] \right\} \right),$$

where

- $u \equiv kri^{1/2} = i^{1/2}(r/\delta_1),$
- $k^2 \equiv \frac{4\pi\omega}{\rho} \cdot \frac{b}{b_1} = \frac{b}{b_1} \cdot \frac{1}{\delta^2} = \frac{1}{\delta_1^2},$
- $\rho \equiv \text{resistivity},$
- $\delta \equiv \text{"skin depth"} \equiv (\rho/2\pi\omega)^{1/2},$

I and K are modified Bessel functions of the first and second kind, respectively,¹ and where

$$\Delta_n \equiv I_0(u_n^o)K_0(u_n^i) - I_0(u_n^i)K_0(u_n^o) .$$

For $(r/\delta_1) \gg 1$, asymptotic expressions for the Bessel functions may be used, and the expression T_n becomes a function of $[(r_n^o - r_n^i)/\delta_1] \equiv (t_n/\delta_1)$. In the limit of high frequencies where $(t_n/\delta) \gg 1$ (e.g., for copper at 100 cps, $\delta \sim 0.675$ cm), we find:

$$R \rightarrow \frac{2\pi\rho}{b\delta_1} [r_1^i m^2 + r_1^o (m-1)^2 + r_2^i (m-1)^2 + r_2^o (m-2)^2 + \dots + r_{m-1}^i (2^2) + r_{m-1}^o (1^2) + r_m^i (1^2)] ,$$

$$L \rightarrow \frac{4\pi^2}{b} \left[m^2 r_1^i + \sum_{n=2}^m (m-n+1)^2 (r_n^i - r_{n-1}^o) \right] .$$

¹We use the notation of McLachlan, *Bessel Functions For Engineers*, 2nd ed., Oxford, 1955.

18. THE USE OF ANALOG COMPUTERS IN THE DESIGN OF MAGNETIC FIELD SYSTEMS

K. E. Wakefield

Project Matterhorn, Princeton University

ABSTRACT

Analog devices used in the design and study of magnetic field configurations at Project Matterhorn are described briefly. The mathematical basis for each of these analogs is discussed. Other aids used in field calculations are digital computers (used primarily as a check) and flux charts.

USE OF RESISTANCE ANALOGS

Axially Symmetric Systems

In early 1955 the stellarator people were faced with the problem of how to design a divertor. At that time, it was felt that a divertor was feasible, but no clear approach was known. Hand calculations, flux plotting, and measurements on models were all too slow and costly. Some attempts had been made to use digital computers to solve the problem on a trial and error basis, but here again cost and time considerations presented a dreary picture.

In order to provide a quick and inexpensive means for obtaining solutions to this problem, a resistance network was devised which was capable of reasonably accurate solutions to axially symmetric magnetic field problems. This network was different from axially symmetric networks suggested and built previously by others in that the flux function (heretofore represented by currents in the network) was represented by the electric potential appearing at the nodes.

In the axially symmetric electromagnetic system, the flux function ϕ is defined:

$$\frac{\partial^2 \phi}{\partial R^2} - \frac{1}{R} \frac{\partial \phi}{\partial R} + \frac{\partial^2 \phi}{\partial Z^2} = -2\pi R \mu j \quad (\text{mks rationalized}) .$$

If a two-dimensional conducting sheet has the property that the conductivity of the sheet at any point is inversely proportional to the distance from the point to one boundary, the potential function V can be written as follows:

$$\frac{\partial^2 V}{\partial r^2} - \frac{1}{r} \frac{\partial V}{\partial r} + \frac{\partial^2 V}{\partial z^2} = -\frac{rj}{c} ,$$

where j = source current density, c = conductivity constant, and $\sigma = c/r$.

These equations are obviously similar in form, and are exactly equivalent if the following identity is used:

$$\phi = \frac{2\pi c \mu p}{S} V ,$$

where

p = current scaling factor, ampere turns/board ampere,
 S = dimensional scaling factor, board units/meter.

From one of the basic equations used to derive $f(\phi)$, one finds

$$\begin{aligned} |B| &= \left| \frac{c \mu p S}{r} \nabla V \right| , \\ F_n &= 2\pi c \mu p (\nabla \nabla V_n) , \\ L_m &= \frac{2\pi c \mu N}{S i} \sum_{n=1}^{n=m} N_n V_n . \end{aligned}$$

Current sources are provided through high resistance feed-in resistors, which carry almost constant current, regardless of board potential.

Although originally devised to aid in the design of divertors, the resistance analog has since been applied to many other axially symmetric field problems, including those in which magnetic materials, permanent magnets, or eddy currents are present.

The original network represented a "half space" 15 units long and 35 units in radius in which points were uniformly spaced, and contained expanded regions (in which points were spaced at ever-increasing intervals) extending 62 units farther out in each direction. Although serving its immediate purpose, it soon became apparent that the device was not large enough. Consequently, in the spring of 1956 we built a much larger, better designed, analog using 1% carbon deposited resistors, in which the region of uniformly spaced points extended 40 units in the axial direction and 80 units radially. The expanded regions extended the effective volume by 254 units radially in each direction

along the axis. This network, however, was constructed so that the axial expansions could be removed at will, enabling one to provide reflecting boundaries at 0, 20, or 40 units as well as at the extreme boundaries. The network also was designed to use feed-in resistors equipped with springs for attachment to the network nodes and spade lugs for easy connection to feeder lines consisting of lengths of spiral springs similar to the springs used on screen doors. These were substantial improvements over the soldering method used on the first network.

As time passed, however, we began to run into problems in the design of some of the heating sections, which were quite long compared with the components previously studied. Consequently, this spring, we built two more smaller analogs, each representing a uniformly spaced region 30 units long and 24 units in radius, and featuring expanded regions extending only in the radial direction, out to 86 units. Using multiconductor cable and quick-disconnect plugs, these units are capable of being interconnected to each other and to the large analog just described. Each of the three units is capable of being operated independently, or in any combination with or without axially expanded regions.

In using these analogs to solve particular field problems, the approach used depends on the accuracy desired and the type of information available. Determining the magnetic field configuration, local flux densities, forces on coils, and inductances of given coil configurations is straightforward. One merely supplies the appropriate currents to the network at the equivalent coil locations and calculates the desired information from the network potentials.

In designing a divertor, however, one must use a trial and error technique, in which past experience obviously plays an important part. One sets up a trial coil configuration and adjusts the current in two of the coils to satisfy two of the major specifications the divertor must meet. One then examines the properties of the system to determine how well it meets other requirements. The manner and degree with which the trial system fails to meet these requirements are used as a basis for modification of the trial coil system. It is in this area that the analog most vividly proves its usefulness, since the operator very quickly acquires a "feel" for the problem by making numerous small adjustments and noting the effect of each.

In designing systems in which the constancy of the field over a relatively long axial span is important, such as the confining field for a resonant heating section, one can superpose a second coil system which consists of a uniform solenoid producing a constant negative field. This enables one to measure the variation in the field directly with extremely good accuracy since errors in the network tend to cancel. The method also enables one to control the input currents more accurately. Using this technique, we were able to design one system of spaced coils in which the field on the axis was constant within 0.2%. The absolute value of flux density was not determined to accuracies even approaching this, however, being limited to the normal one or two per cent achievable with the network.

Representing magnetic material or permanent magnets is accomplished by introducing current couples in the network which are equivalent to the magnetic moment of the material. If the magnetic material covers not too large a volume, the iterative procedure required to adjust these moments

according to the local strength of magnetic field is not difficult. If one contemplated a steady diet of this type of problem, however, it is recommended that a special network be constructed using variable resistors, which can also be used to represent permeable materials.

Eddy currents can be represented by the addition of capacitive elements to the network or to the feed-in circuit. If the resistance of a shorted turn is very small compared to its inductive reactance, however, one can represent these shorted elements by shorting the appropriate pins to each other or to the axis, depending on the conditions present.

Two-Dimensional Systems

We have also used methods similar to those used on the analogs just described to feed current into a uniform conducting sheet.

The conducting sheet used is called "Teledeltos" and is manufactured by Western Union Telegraph Co. The paper can be painted with silver paint to represent surfaces of zero permeability and can be cut with a knife or scissors to represent infinitely permeable surfaces. Care must be taken in representing conductors of large cross section. The method we found most suitable was to punch a hole in a piece of Scotch tape with a paper punch and stick the Scotch tape on the surface of the paper. The hole would then be covered with silver paint and the current fed into the area through a pin or nail driven into the plywood on which the paper was mounted. The area covered by the silver paint was too small to affect the field distribution, yet was large enough to ensure that the voltage at the base was small. Large conductors were split up into a number of sections, the current in each section being controlled independently.

Although readily available and easy to work with, the uniformity of the conducting paper was poor, varying by as much as 8% in its conductivity over a 30 × 30-in. sheet. A further disadvantage is the inability to move the boundaries away from the region of interest, a feat so readily accomplished in the networks.

Helically Invariant Fields

When helical stabilizing fields were first envisioned, analytical solutions were obtained using certain current distributions enabling relatively easy calculation of the characteristics of the system. However, as design of the C stellarator progressed, it became evident that these assumptions might not be sufficiently accurate; and in addition, some coil arrangements were being suggested for which it would be extremely difficult to predict performance accurately. As a result, in the spring of 1957, a resistance analog, suggested by E. Frieman of the Matterhorn theoretical group, was built.

In a helically invariant system, one can show

$$-\frac{1}{\mu} \left[\frac{1}{r} \frac{\partial}{\partial r} \left(\frac{r}{1+K^2 r^2} \frac{\partial \psi}{\partial r} \right) + \frac{1}{r^2} \frac{\partial^2 \psi}{\partial u^2} \right] = -\frac{2Kf}{\mu(1+K^2 r^2)^2} + \frac{J_z}{1+K^2 r^2} + \frac{KrJ_\theta}{1+K^2 r^2},$$

where ψ is the flux per unit length crossing a helical ribbon extending from the center of the system to any point, r , u , and having a pitch K radians per unit distance traveled in the z direction; u is

defined as $\theta - Kz$, which is constant as one moves along a helix with pitch K . The function f is defined as $f = B_z + KrB_\theta$. In this system, magnetic surfaces are defined by $\psi = \text{constant}$.

If one postulates a conducting sheet (polar coordinates) in which $\sigma_u = \sigma$, and $\sigma_\rho = \sigma/1 + \rho^2$, one finds:

$$-\frac{\sigma}{\rho} \left[\frac{\partial}{\partial \rho} \left(\frac{\rho \partial V / \partial \rho}{1 + \rho^2} \right) + \frac{1}{\rho^2} \frac{\partial^2 V}{\partial u^2} \right] = \nabla \cdot i ,$$

where $V = \text{electric potential}$.

Since the left-hand sides of both these equations are similar in form, one may make them identical if one uses the relations:

$$\rho = Kr ,$$

$$\psi = \sigma \mu p V ,$$

where $p = \text{scaling factor, coil current/source current}$; hence

$$\nabla \cdot i = - \frac{2f}{p\mu K(1 + \rho^2)^2} + \frac{J_z}{pK^2(1 + \rho^2)} + \frac{\rho J_\theta}{pK^2(1 + \rho^2)} ,$$

and

$$S = - \frac{2fA}{p\mu K(1 + \rho^2)^2} + \frac{J_z A}{pK^2(1 + \rho^2)} + \frac{\rho J_\theta A}{pK^2(1 + \rho^2)} ,$$

where

$$A = \rho \Delta u \Delta \rho ,$$

$$S = \text{source current per pin, representing an area } \rho \Delta u \Delta \rho .$$

This source function is made up of a distributed source, indicated in the first term, and sources associated with currents in conductors, indicated by the remaining terms. Since it can be shown that f is constant in regions not occupied by coil currents, one can build the distributed source into the network using fixed resistors, and adjust the value of the voltage across these resistors according to the value of f . If we let:

$$E_f = \frac{-f}{p\mu K} a_1 ,$$

then

$$R_f = \frac{(1 + \rho^2)^2}{2A} a_1 ,$$

and

$$i_{\text{coil}} = \frac{1}{p(1 + \rho^2)} \left(\frac{j_z A}{K^2} + \frac{\rho j_\theta A}{K^2} \right) = \frac{1}{p} (I_H) .$$

We chose σ to produce reasonably sized resistors in the network itself, then chose p to produce workable voltages in this network, and finally chose a value of a_1 requiring reasonably high voltages to represent expected values of f , compared to the voltages appearing in the network.

In order to represent systems having various values of Kr with about the same relative mesh size, we chose a logarithmic scale in ρ in the region of main interest in which $\Delta\rho$ and $\rho\Delta u$ were about equal. The logarithmic region extends from $\rho = 0.09$ to $\rho = 2.5$; since ρ is the tangent of the angle the helical conductor makes with the axis, one can represent helical systems in which the conductor angle is between 5° and 65° with good accuracy.

The physical arrangement of the board, which represents a half circle with resistors on radial lines and on lines around the circumference at each radius, can of course be altered to suit one's fancy. We chose to arrange the pins in a rectangular pattern, with the R_f resistors being brought out to pins in the middle of the squares thus formed. These intermediate pins were equipped with spade lugs protruding about $\frac{1}{2}$ in. from the surface. The nodes, or normal pins, were insulated with hollow sleeves about $\frac{5}{16}$ in. in diameter and $\frac{7}{8}$ in. long, being cemented in place. The constant f regions could now be interconnected with the same type of coil springs that we use to carry current to the feed-in resistors. They lie along the surface of the board and are well out of the way, avoiding interference with other operations.

When the distributed and local currents, representing helical conductors, are fed into the network, one can then plot $V = \text{constant}$ lines to determine the location and shape of the magnetic surfaces.

If desired, one can determine the magnitudes of the components of the field in r , z , and θ directions from the potentials on the pins and the value of f , which would always be known.

Properties of the stabilizing field, such as the transform, are readily determined from the shape of the magnetic surface, or if more accuracy is desired, by numerical operations using data from the network.

OTHER AIDS IN FIELD COMPUTATION AND DESIGN

Digital Computers

Since the accuracy of the resistance analog is limited by accuracy of board components and meters, we have checked some of our solutions using the IBM-704. For example, this was done for the complete coil system for the C stellarator, operating without divertor and without r-f heating section.

We calculated the field produced by all the coils in the machine at 232 points on the centerline of the vacuum system. Two components were determined, the component parallel to the axis of the tube, and the component perpendicular to this axis and in the plane of the stellarator.

The component parallel to the axis should be constant within a few per cent, equivalent to maintaining a tube of flux whose outside dimensions do not greatly vary.

The component perpendicular to the axis should be small, and should be such that a flux line which starts out at any given point on the centerline would traverse the whole machine without deviating very far from this centerline.

This transverse field ordinarily does not meet the requirement set forth above, but can be altered by tilting individual coils about an axis normal to the plane of the stellarator. We are using the field values calculated on the IBM-704 for the entire machine with untilted coils, and the calculated effect of tilting individual coils, to determine the tilts which will give the most satisfactory results. Similar work will be undertaken for machine arrangements containing divertors and heating sections.

Flux Charts

Other tools we have found to be useful in axially symmetric systems are devices called "flux charts." Each chart consists of a large transparent sheet ruled off into $\frac{1}{2}$ -in. squares, with a reference line along the bottom edge, referred to as the axis. A point at some radial distance is prominently marked at one edge of the chart. Each square on the chart contains a number designating the total flux for one ampere turn at the reference point linking the circle formed by rotating the center of the square around the axis. However, since mutual flux between two coils must be the same no matter which is energized, one can just as well regard the number in each square as representing the total flux linking the *reference point* if one ampere turn exists at the particular square chosen.

In practice, the chart is laid on a drawing or sketch of a coil system under study so that the axis line corresponds to the axis of the coil system and the reference point is at the point where flux values are desired. In order to find the total flux within the reference circle, one merely adds up the numbers within the outlines of the coils, seen through the transparent sheet. For fractions of squares, which can be estimated by eye, the number in the square is multiplied by the corresponding fraction. The total flux is equal to this sum times the coil ampere turns divided by the total number of squares occupied by the coil cross section, taking fractions into account as they were estimated. The coil drawing may be made to any convenient scale.

In order to make the system more flexible, we are planning charts whose reference points are at a number of radii, so that one may determine roughly the field pattern of a simple coil system without redrawing the system to different scales. The data for all these charts were calculated on the UNIVAC.

We have used these charts to determine forces on coils in long, rather complex, systems. One chooses a chart (or a scale for the drawing) to correspond to the center of gravity of the ampere turns on one coil. The forces on the other coil are very easily determined by reading the chart values at the boundaries of the second coil, and applying one of the basic equations for force.

These charts are reproducible and are available on request.

19. OPTIMIZATION OF D-C COIL DESIGN WITH RESPECT TO COIL FABRICATION COST AND COST OF INSTALLED D-C POWER

A. F. Waugh

Lawrence Radiation Laboratory, University of California
Livermore

About two years ago the Project Sherwood experimental program at Livermore required an ample supply of relatively high field strength, modular, d-c magnet coils of several sizes. Since the design of these coils might become somewhat of a standard and the number to be ordered was fairly large with a good possibility of reorder in the future, it appeared worth while to try to optimize the design from an economic point of view, taking into account the cost of the d-c power installation required as well as the fabrication costs of the coils themselves. The following derivation came out of this design study.

Starting with the basic equation for the field strength at the center of an air-core solenoid:¹

$$B = \eta_0 \frac{NI}{L} \cos \beta, \quad (1)$$

where (in the mks system of units)

$B =$ webers/m²,

$N =$ total turns,

$I =$ amps,

$\eta_0 = 4\pi \times 10^{-7}$,

and β is as shown in Fig. 40.

Since (see Fig. 40)

$$\bar{r} = \frac{r_1 + r_2}{2} = \frac{(\alpha + 1)r_1}{2},$$

Eq. (1) can be written in the form

$$B = \eta_0 NI \frac{1}{r_1 \sqrt{\delta^2 + (\alpha + 1)^2}}, \quad (2)$$

by expressing $\cos \beta$ in terms of the parameters inner radius r_1 , α , and δ , where $\alpha = r_2/r_1$ and $\delta = L/r_1$. The net winding cross section is S , the winding space factor, times the gross winding section, $S(r_2 - r_1)L = S(\alpha - 1)\delta r_1^2$. The cross section of a single conductor is the above expression divided by the number of turns, $A = S(\alpha - 1)\delta r_1^2/N$. The total length of conductor is the number of turns times the mean circumference, $L_c = N2\pi\bar{r} = N\pi(1 + \alpha)r_1$. The coil resistance can now

¹G. W. Carter, *The Electromagnetic Field in Its Engineering Aspects*, p 113, Longmans, Green, New York, 1954.

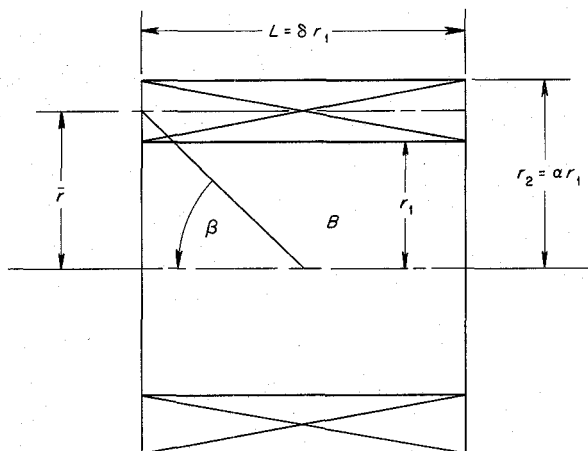


Fig. 40. Some Units Used in Field-Strength Equation, $B = \eta_0 (NI/L) \cos \beta$.

be stated as:

$$R_c = \frac{L_c}{A} \rho = \frac{\pi N^2 (1 + \alpha)}{S r_1 (\alpha - 1) \delta} \rho, \quad (3)$$

with ρ in ohm-meters.

Now solving Eq. (1) for N and substituting in Eq. (3) yields

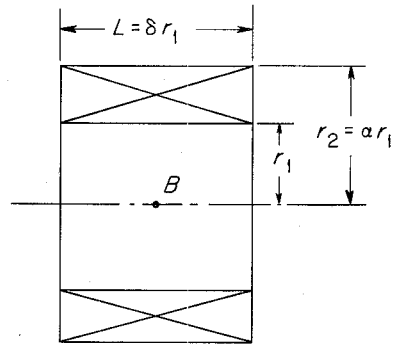
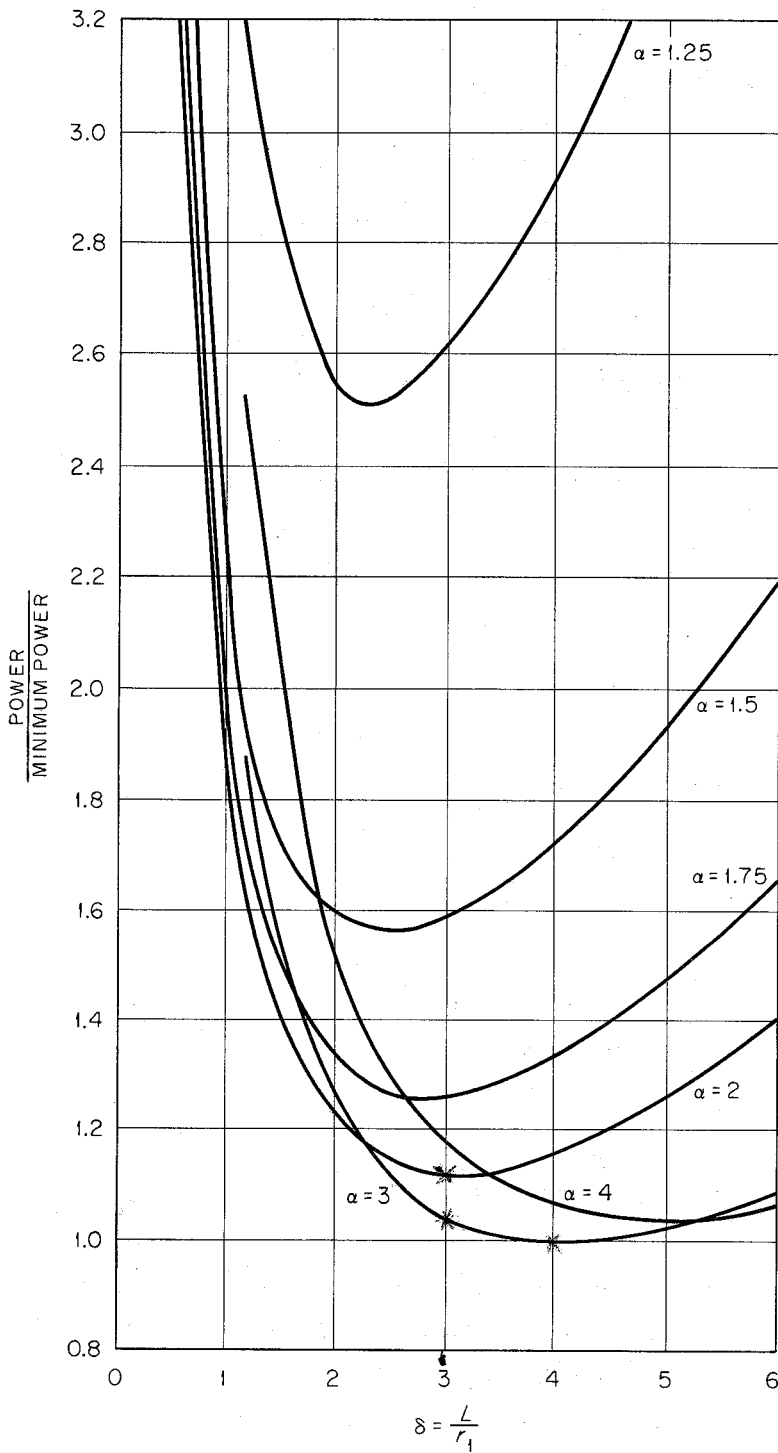
$$R_c = \frac{\pi B^2 r_1 \rho (\alpha + 1) [\delta^2 + (\alpha + 1)^2]}{\eta_0^2 I^2 S (\alpha - 1) \delta}. \quad (4)$$

The power dissipated in the coil is $I^2 R_c$; therefore, multiplying both sides of Eq. (4) by I^2 obtains Eq. (5), the power required to produce a central field strength B in terms of the basic parameters resistivity of the conductor, space factor of the winding, and the dimensions of the coil:

$$P = \frac{\pi B^2 r_1 \rho (\alpha + 1) [\delta^2 + (\alpha + 1)^2]}{\eta_0^2 S (\alpha - 1) \delta}. \quad (5)$$

It is evident that the power required varies directly as the square of the field strength, directly as the inner radius and resistivity of the conductor and inversely as the winding space factor.

If the function of α and δ contained in Eq. (5) is differentiated partially with respect to these two variables and the simultaneous equations obtained are set equal to zero and solved, you will obtain the well-known optimum values of $\alpha = 3$, $\delta = 4$ for the coil requiring minimum power. For these values of α and δ the function in Eq. (5) has a numerical value of 16. Figure 41 is a plot of this function of α and δ which shows the ratio of power required over minimum power plotted against δ . A family of curves is shown for different values of α .



POWER REQUIRED
FOR B AT CENTER
ON AXIS $\approx \frac{\delta^2(\alpha+1)+(\alpha+1)^3}{\delta(\alpha-1)}$

$$P(\text{WATTS}) = \frac{\pi B^2 r_1 \rho}{\eta_0^2 S} \frac{\delta^2(\alpha+1)+(\alpha+1)^3}{\delta(\alpha-1)}$$

B = WEBERS/M²
 r_1 = METERS
 ρ = OHM-METERS
 S = SPACE FACTOR
 $\eta_0 = 4\pi \times 10^{-7}$

Fig. 41. Ratio of Power Required/Minimum Power vs α and δ .

Making the simple but reasonable assumption that the coil cost (cost of copper plus fabrication costs) is proportional to the coil volume, if $C_c = \text{dollars/meter}^3$, then the coil cost can be written as

$$C_c \pi(r_2^2 - r_1^2)L = C_c \pi(\alpha^2 - 1)\delta r_1^3 . \quad (6)$$

The total cost of the coil and required installed d-c power capacity is then:

$$C_T = C_p \frac{\pi B^2 r_1 \rho (\alpha + 1) [\delta^2 + (\alpha + 1)^2]}{\eta_o^2 S} + C_c \pi(\alpha^2 - 1)\delta r_1^3 , \quad (7)$$

where $C_p = \text{dollars/watt}$ of d-c power installation. For known values of $C_p, C_c, B, r_1, \delta, \rho,$ and S , Eq. (7) can be simplified to:

$$C_T = K_p \frac{(\alpha + 1)\delta^2 + (\alpha + 1)^3}{(\alpha - 1)\delta} + K_c(\alpha^2 - 1)\delta . \quad (8)$$

To find the minimum total cost differentiate Eq. (8) with respect to α , set equal to zero, and solve for α . The differentiation is simplified if the change of variable $u = (\alpha + 1)$ is used.

Then

$$du = d\alpha \text{ and } (\alpha + 1) - 2 = u - 2 ;$$

also

$$(\alpha^2 - 1) = (\alpha + 1)(\alpha - 1) = u(u - 2) .$$

Then Eq. (8) takes the form

$$C_T = K_p \frac{\delta^2 u + u^3}{(u - 2)\delta} + K_c u(u - 2)\delta , \quad (9)$$

and

$$\frac{dC_T}{du} = (K_p + K_c \delta^2)u^3 - (3K_p + 5K_c \delta^2)u^2 + 8K_c \delta^2 u - (K_p + 4K_c)\delta^2 = 0 . \quad (10)$$

The following is an example of the application of the above criterion.

For:

$$r_1 = 18 \text{ in.} = 0.46 \text{ meter,}$$

$$L = 6 \text{ in. } (\delta = \frac{1}{2}),$$

$$B = 2 \text{ kilogauss, } S = 0.65, \rho = 1.86 \times 10^{-8} \text{ ohm-meter,}$$

$C_p = 0.1 \text{ dollar/watt}$ (obtained from known costs of 300 kw, d-c supplies, substation, and installation costs),

$C_c = \$24,000/\text{meter}^3$ (or about \$1.50/lb of coil),

optimum α was found to be 1.5. Therefore, $r_2 = 1.5 r_1 = 27 \text{ in.}$

Of course most coil designs, especially for controlled thermonuclear research work, cannot be based solely on the economics of the design. More often space limitations, impedance matching to available supplies, and the power-dissipation capacity are the governing factors.

20. SOME ASPECTS OF HEAT DISSIPATION FROM ALUMINUM-FOIL COILS

A. F. Waugh

Lawrence Radiation Laboratory, University of California
Livermore

Some time ago we at Livermore became interested in aluminum-foil coils for use as d-c field coils, primarily because of the inherent relatively high impedance of this type of coil.

The conductor of an aluminum-foil coil is, as its name implies, a thin aluminum ribbon one-half to several mils thick. The surface and edges of the foil are treated so that a thin coating, 5 to 10 μ in. thick, of aluminum oxide is formed on them. This oxide coating provides turn-to-turn dielectric strength of about 10 v, which is adequate for most applications. The treated foil is tightly wound on a form. The completed winding is nearly a solid ring of aluminum.

The space factor of a well-made aluminum-foil coil should be in the range of 95 to 97%. It is this high space factor that enables this aluminum conductor coil to compete with a coil wound with copper conductor. The power required to produce a given central field strength with a coil of a given size and shape is, among other things, proportional to the ratio:

$$\frac{\text{conductor resistivity}}{\text{coil space factor}}$$

The space factor of a coil wound with insulated round copper wire or insulated hollow copper bar would be about 65%; therefore, the ratio of resistivity to space factor for the aluminum-foil coil is very nearly the same as the value of this ratio for the copper conductor coil. Or, in other words, the higher space factor of the aluminum-foil coil just offsets the higher resistivity of aluminum.

Another feature of this type of coil is that since no organic insulating material is required in the interior of the coil winding for insulation, the midpoint hot-spot temperature is limited only by the safe working temperature of the aluminum foil itself. This temperature is believed to be about 400°C.

An experimental coil was ordered. The inside diameter of foil winding was 31 in., the outside diameter 43 in. The coil contained about 1200 turns of 5-mil, $4\frac{3}{4}$ -in.-wide foil in the 6-in. radial buildup. The total length of foil was 11,600 ft. Nominal resistance of the coil is 8 ohms. The coil is to be enclosed by, but insulated from, an aluminum spool composed of the $\frac{3}{8}$ -in.-thick inner ring and annular end plates. The outside of the spool is held rigidly with a $\frac{1}{4}$ -in. buildup of Fiberglas cloth and epoxy resin which is molded and bonded to the aluminum end plates. This lamination forms part of the cooling water channel and encapsulates the plastic water tubing. Cooling

is to be done by circulating low-conductivity water on the end faces of the coil. The flow is to spiral into the center, through a corrugated path under the coil and back out on the other face in another spiral. The water channels are formed by a silicon rubber strip that is bonded to the aluminum end plates with epoxy resin. The coil was to be able to dissipate 50 kw of power (80 amp at 630 v) producing 96,000 ampere-turns and a central field strength of about 1.3 kilogauss.

It was the opinion of the developer and fabricator of this type of coil, Jobbins Electronic Enterprises of Menlo Park, California, that heat could be removed adequately from the outside- and inside-diameter surfaces, assuming fairly good thermal conductivity radially from the interior of the winding to these outer faces. A big advantage of such a system is that the coolant would flow over an essentially unipotential surface. A test was made to determine the thermal conductivity in the radial direction, using a small sample coil which had a 2-in. buildup of foil on a 4½-in. ID. This thermal conductivity was found to be about $\frac{1}{50}$ that of aluminum. This result was to be expected since the thermal conductivity of Al_2O_3 is $\frac{1}{50}$ that of aluminum and also the heat must pass across all the layer-to-layer interfaces of the winding. If heat removal from the outer- and inner-diameter surfaces alone was to be relied upon in the case of the big coil running at 50 kw, the temperature at the mean radius would go to about 900°C.

The above-mentioned test confirmed our belief that the heat must be removed from the end faces of the coil, there being good thermal conductivity to these faces from the interior of the winding along, rather than across, the aluminum foil. However, it was decided that the edges of the oxidized foil could not be relied upon for adequate dielectric strength. An additional barrier layer was needed between the edges of the winding and the cooling water. Ideally such a barrier should have fairly good thermal conductivity as well as good dielectric strength. As an attempt to achieve, at least to some degree, these incompatible properties, the addition of fine aluminum and copper powder as a filler to epoxy resin was investigated. The results of these tests are generalized as follows:

The addition of a highly conductive filler to a cast epoxy resin results in only a slight increase in the thermal conductivity of the system. The effect does not appear to be directly proportional to either the volume or weight concentration of the filler, nor does it bear an obvious relationship to the conductivity of the filler itself. If the thermal resistivity of aluminum is taken as unity, then the thermal resistivity of epoxy is about 1000. The addition of about 50% by weight concentration of a high-conductive filler results in a thermal resistivity for the mixture of about 100, a factor of 10 lower than that of epoxy but still a factor of 100 higher than aluminum. Unfortunately, the 50% weight addition of filler required to produce even this improvement in thermal conductivity also produced a material which had practically no usable dielectric strength. However, probably the most interesting finding to come out of this experimental work was that the addition of aluminum oxide as a filler resulted in a mixture that had a thermal conductivity only about 10% less than the mixture containing pure aluminum powder and had adequate dielectric strength for the application at hand. A 15- to 20-mil coating exhibited a dielectric strength of 75 to 100 v/mil after being thermally cycled from ice water to boiling water 250 times. It was

decided to apply a 20- to 30-mil coating of the aluminum oxide-epoxy mixture to the end faces of the coil.

There is a temperature rise of only 10°C from the end face to the midplane of the coil. This was calculated using the thermal conductivity of solid aluminum for heat flow in this axial direction and a uniform power density of 15 w/in.³ which results from a total power input of 50 kw.

I was recently informed by the West Coast developer of this type of coil that aluminum foil can be obtained in widths from $\frac{3}{8}$ to 16 in. He has also developed the surface treatment technique so that the annular end faces of the coil can be machined to a smooth surface or holes can be bored through the winding. The machined surfaces are then treated to remove the turn-to-turn shorts produced by the machining operation. Also, a different water-cooling design than the one previously described has proved quite successful. Instead of building a water cooling jacket onto the end faces of the coil, a copper plate with cooling water tubes soldered to it is bonded to the end faces with the aluminum oxide-epoxy mixture.

While there are many things yet unproved about a large high-powered coil of this type, it is nevertheless interesting to consider, due to its high impedance characteristic and because the power-dissipation problem is primarily one of heat removal from an exterior surface rather than from the interior of the coil winding.

21. SYNTHESIS OF INHOMOGENEOUS MAGNETIC FIELDS¹

D. R. Whitehouse

Department of Electrical Engineering
and
Research Laboratory of Electronics
Massachusetts Institute of Technology

ABSTRACT

A complete analytic expression for the magnetic field of current-carrying coils is difficult to obtain. However, research in plasma physics has created a need for synthesizing specified inhomogeneous, magnetic fields with such coils. Several people at M.I.T. who have been associated with the Microwave Gas Discharge Group have done work on the design of electromagnets to produce a magnetic mirror field configuration. The purpose of this paper is to summarize both the theory and the experiments that have been completed.

THEORY

From magnetostatic theory, it is known that

$$\nabla \cdot \bar{B} = 0, \quad (1)$$

and further, in empty space one can describe a scalar magnetic potential, ψ , related to \bar{B} through

¹This work was supported in part by the U.S. Army, Air Force, Navy, and by AEC Contract AT(30-1) 1842.

the gradient operator

$$\bar{B} = -\nabla\psi \quad (2)$$

Substituting (2) into (1) gives Laplace's equation for the scalar magnetic potential

$$\nabla^2\psi = 0 \quad (3)$$

The allowable solutions for \bar{B} in any given configuration are easily obtained by first solving for the potential ψ in Eq. (3) and then obtaining \bar{B} from Eq. (2).

The problem of producing a specified field configuration within a simple, closed region of space was considered by L. J. Chu. He suggested that current sheets and magnetic shorts are sufficient boundary conditions to completely enclose the volume and establish the magnetic field. The suggestions of Chu break down into the following three postulates which are applicable to the design of a magnetic field:

1. Completely enclose the volume of interest with a surface that lies along constant flux contours or streamlines and magnetic equipotentials.
2. Establish current sheets along the constant flux contours of value given by $\bar{J} = \bar{n} \times \bar{H}$ where \bar{n} is a unit vector normal to the surface.
3. Establish magnetic shorts along the magnetic equipotential surfaces.

For magnetic fields of solenoidal symmetry, one must solve Laplace's equation for the magnetic potential in circular cylindrical geometry.

$$\nabla^2\psi = \frac{1}{r} \frac{\partial}{\partial r} \left(r \frac{\partial\psi}{\partial r} \right) + \frac{\partial^2\psi}{\partial z^2} = 0 \quad (4)$$

The solution of this equation is well known and given by

$$\psi = \sum_{n=1}^{\infty} [A_n J_0(k_n r) + B_n N_0(k_n r)] [C_n e^{k_n z} + D_n e^{-k_n z}] \quad (5)$$

where k_n can be both real and imaginary. The coefficients B_n must all be zero since both ψ and \bar{B} must be finite at $r = 0$. With the geometrical origin at the center of the symmetrical solenoid, ψ must be an odd function of z . Therefore, the general solution for the potential becomes

$$\psi = \sum_{n=1}^{\infty} A'_n J_0(k_n r) \sinh(k_n z) + \sum_{m=1}^{\infty} A'_m I_0(k_m r) \sin(k_m z) \quad (6)$$

and the magnetic field is given by

$$\bar{B} = \bar{a}_r \left[\sum_{n=1}^{\infty} A'_n k_n J_1(k_n r) \sinh(k_n z) - \sum_{m=1}^{\infty} A'_m k_m I_1(k_m r) \sin(k_m z) \right] - \bar{a}_z \left[\sum_{n=1}^{\infty} A'_n k_n J_0(k_n r) \cosh(k_n z) + \sum_{m=1}^{\infty} A'_m k_m I_0(k_m r) \cos(k_m z) \right] \quad (7)$$

Any desired field may now be expanded in the appropriate functions of (7). The solution of \bar{B} up to

this point is well-known, but further application to the design of solenoidal fields is one of personal choice.

DETERMINATION OF ψ AND \bar{B}

It was desired to obtain a solenoidal mirror magnetic field. There were further restrictions that the axial field should be uniform in the central region and that there should be a hill or "mirror" ratio of 5 to 1 at the ends of the solenoid. These requirements allow a considerable latitude in choosing an appropriate analytic expression from (7).

One possible solution is to use two terms of the hyperbolic cosine variation,

$$B_z = A_1 J_0(k_1 r) \cosh(k_1 z) + A_2 J_0(k_2 r) \cosh(k_2 z) . \quad (8)$$

The constants A_1 , A_2 , k_1 and k_2 can be chosen to match the specified variation of B_z at 3 points along the axis: at the center, at the edge of the uniform region, and at the magnetic mirror. A low-power solenoid was constructed to achieve the field of Eq. (8) by a graduate student, R. G. Meyerand, and the results proved encouraging.

More recently, D. C. White has designed a medium power solenoid by using a different expansion for B_z (ref 2):

$$B_z = Ak [J_0(kr) \cosh(kz) + I_0(kr) \cos(kz)] . \quad (9)$$

An expansion of (9) for $r = 0$ gives

$$B_z = Ak \left[2 + \frac{2(kz)^4}{4!} + \frac{2(kz)^8}{8!} + \dots \right] . \quad (10)$$

This expression for the magnetic field has analytic simplicity, excellent uniformity of B_z around $r = 0$, $z = 0$, and a very rapid increase in B_z for large z . The z component of B given by (9) can be obtained from the scalar potential

$$\psi = A [J_0(kr) \sinh(kz) + I_0(kr) \sin(kz)] . \quad (11)$$

EVALUATION OF MAGNET BOUNDARY CONDITIONS

The first step in designing the solenoid for the field of Eq. (9) is to draw the flux lines which, in this case, determine surfaces of revolution that are contours of constant flux. One of these flux contours must now be chosen for the physical boundary of the solenoid consistent with its desired size. Figure 42 shows a quarter-section drawing of our desired experimental solenoid where the boundary was chosen along a flux contour of $\Phi_s = 201,580$ lines. Next one determines the value of H_z along this boundary of constant flux from (9). This automatically determines the value of the azimuthal current density, J_ϕ , which is required along the contour Φ_s . Thus Fig. 42 shows that for an increase in z , the solenoid diameter should decrease and the current density should increase.

The design of a single layer coil was made to these specifications and is shown in Fig. 43. Copper rings are connected in series as shown and the current per unit length is increased by making

²D. C. White, "Inhomogeneous Magnetic-Field Design," *Quarterly Progress Report, M.I.T. Research Laboratory of Electronics*, p 16-24 (July 15, 1957).

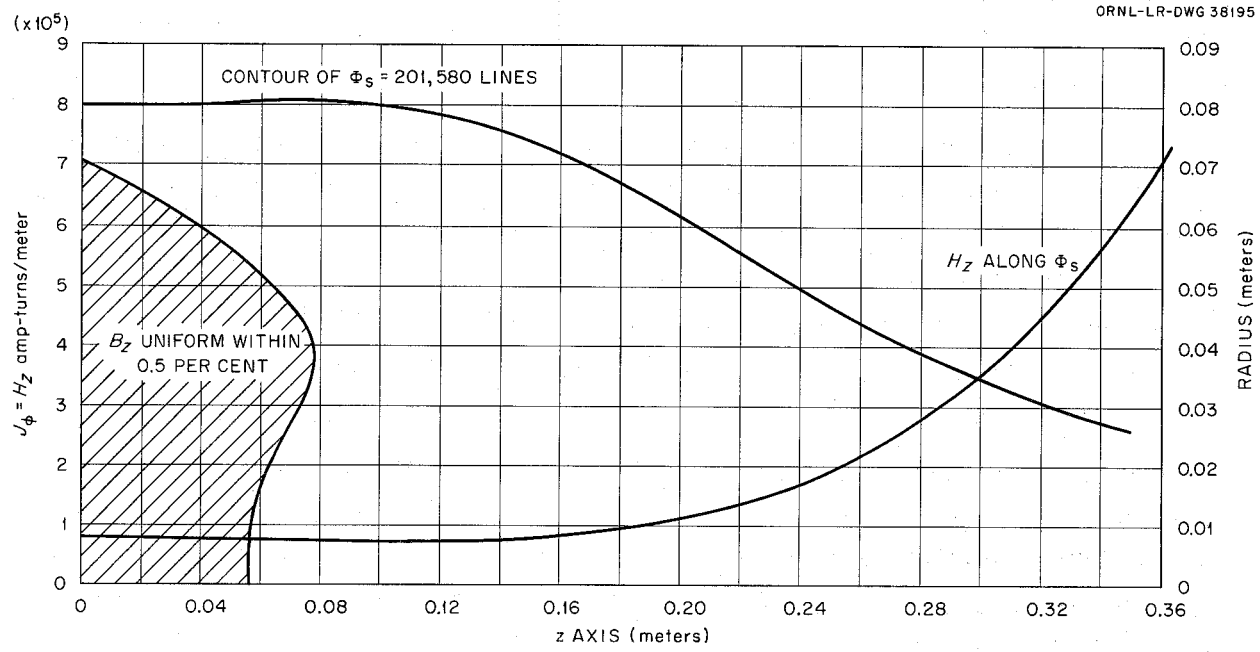


Fig. 42. Constant-Flux Contour and Axial Current Density Used in Solenoid Design.

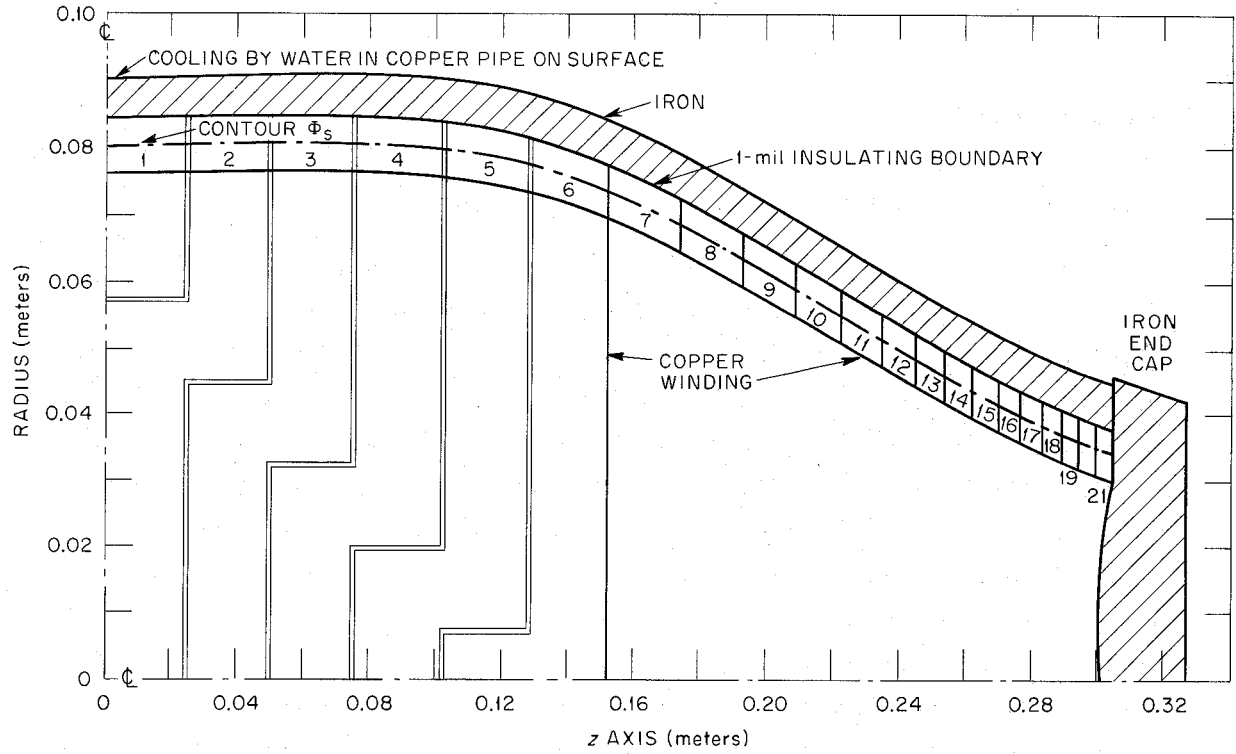


Fig. 43. Design of a Single-Layer Coil with Copper Winding and Iron Shell.

thinner rings at the end of the solenoid. An iron end-cap is shown with its surface machined to coincide with the surface of constant potential ψ . This completely satisfies the boundary conditions, but an additional iron shell is placed over the current in order to minimize the problems of leakage flux.

The coil is designed for 2000 amp at 8 kw with 1000 gauss at the center. Figure 44 shows a picture of the two halves of the solenoid in addition to a water cooling jacket which is placed inside the solenoid.

CONCLUSION

Ideally the prescribed synthesis procedure should give an exact reproduction of the desired field. However, there are several practical factors which will alter this situation.

1. The current sheets are not infinitely thin and the current density varies discontinuously as a function of z .
2. Careful consideration must be given to the axial currents which flow.
3. Iron is not a perfect magnetic short and there will be some leakage flux.
4. Port holes must be placed in the solenoid in order to run and instrument an experiment.

The magnitude of the error induced by these factors has not been evaluated. Measurements indicate, however, that the resultant field is useful for our purposes.

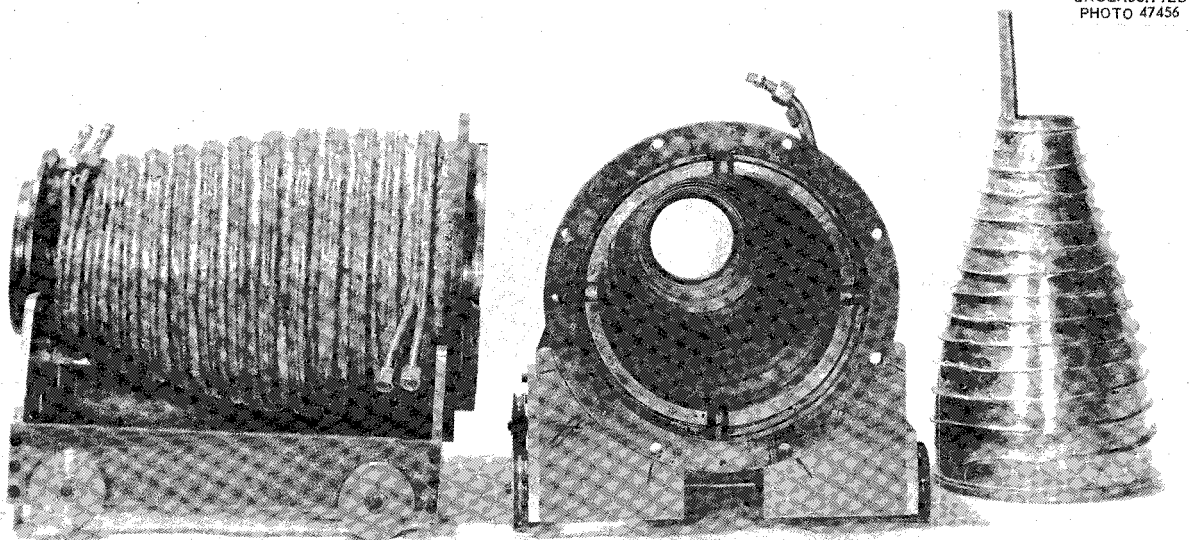


Fig. 44. Solenoid and Additional Internal-Cooling Water Jacket.

22. MAGNETIC FIELD PROBLEMS ASSOCIATED WITH THE LOS ALAMOS THERMONUCLEAR EXPERIMENTS

F. L. Ribe
Los Alamos Scientific Laboratory

INTRODUCTION

In the following a brief summary will be given of some of the magnetic field problems which have been encountered in connection with the Los Alamos experiments. It may generally be remarked that to date, nearly all of our field coils are pulsed, air cooled, and capacitor driven. Large d-c coils have not been much used, except in the case of a large 250-kw solenoid designed for plasma diffusion experiments. Some of the Los Alamos experiments will be identified and bits of related magnetic field experience noted.

SCYLLA

This is a fast plasma-compression apparatus in which the field at the center of a magnetic mirror (mirror ratio = 1.4) rises from zero to 60 kilogauss in 1.25 μ sec. Figure 45 shows the approximate shape of the magnetic lines (dashed curves), the cross section of the 5-cm cylindrical ceramic vacuum envelope, and also the cross section of the single-turn brass coil which provides the magnetic field. The field coil is also shown in Fig. 46. It is typically driven at 800 ka by ten 0.88- μ f capacitors charged to about 80 kv. In this coil the skin effect of the brass is almost

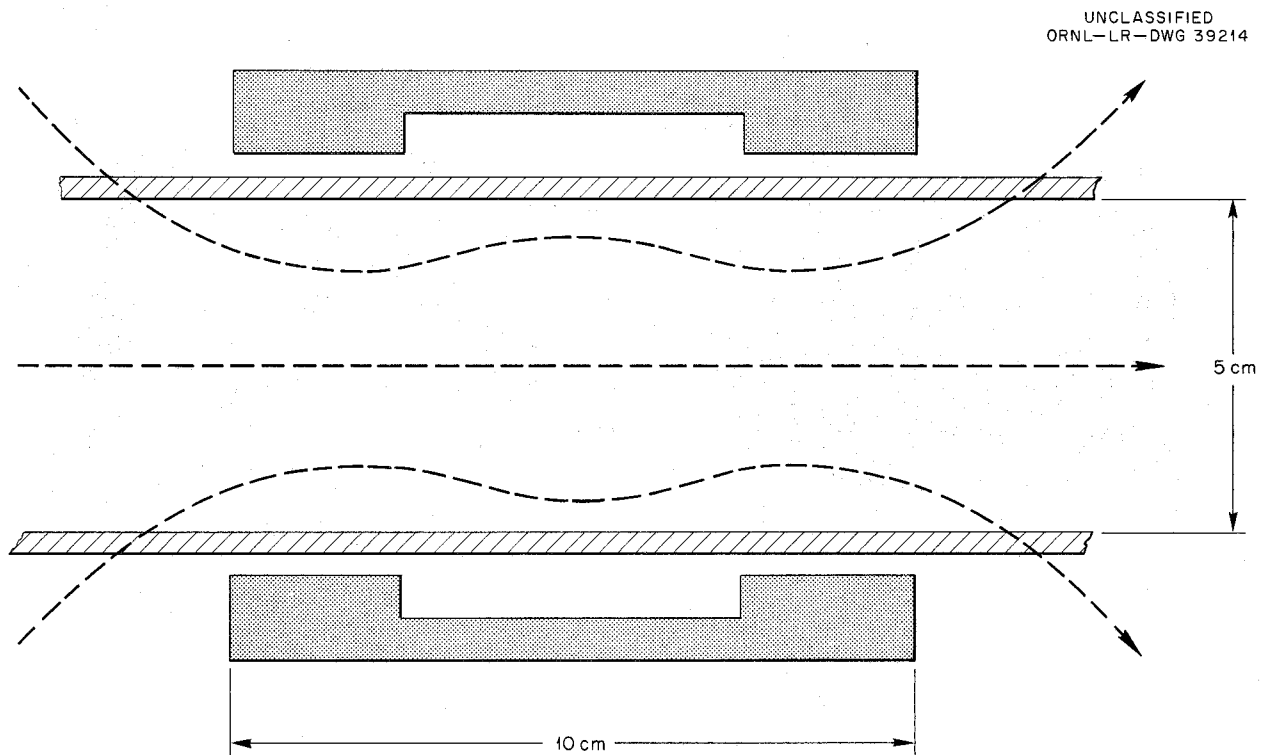


Fig. 45. Scylla Magnetic Field Shape.

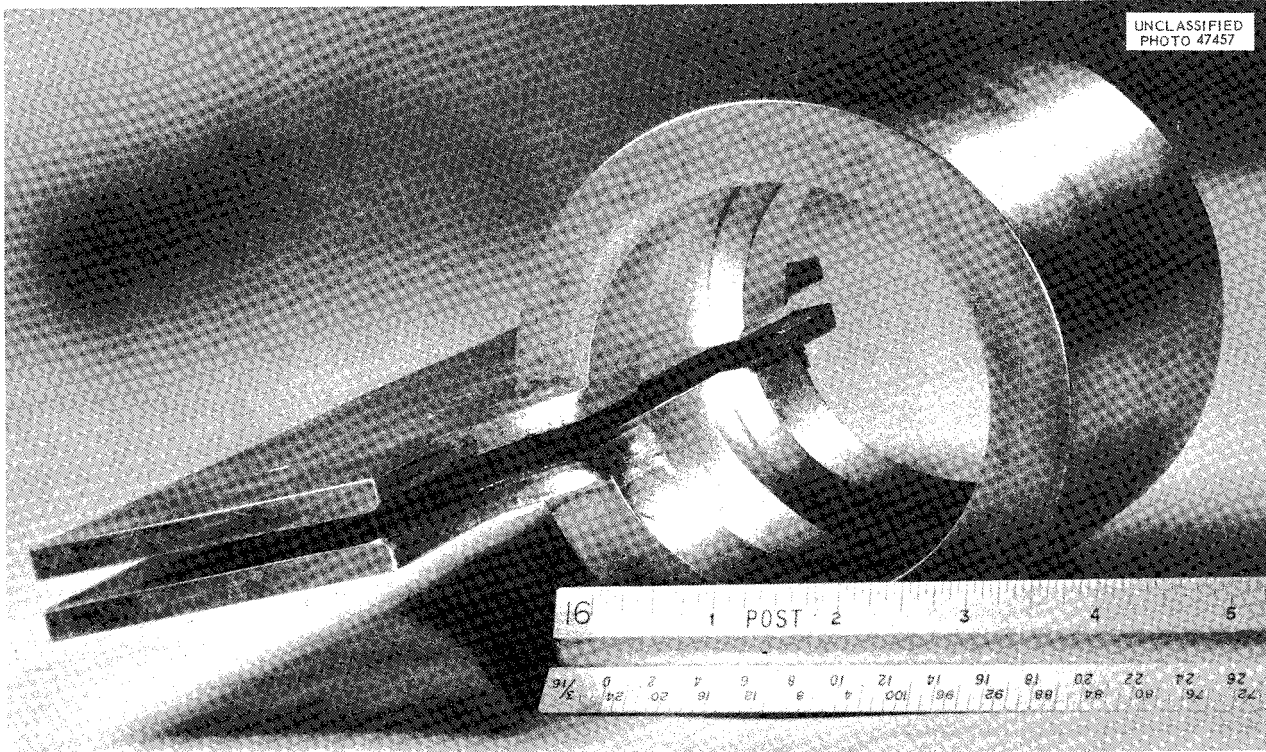


Fig. 46. Scylla Magnetic Field Coil.

complete, and the inner surface is a magnetic flux surface. The magnetic mirror is obtained simply by shaping this surface.

The problems of obtaining high magnetic fields in this manner were first discussed by Furth, Levine, and Waniek.¹ They noted that at 500 kilogauss, copper melts because of heating caused by penetration of the magnetic field. The "sawing" effect of the strong magnetic field at irregularities produced by the silver solder joints in the Scylla coils has been observed. One must take care to shield such joints from the strong magnetic field as much as possible.

In a new machine being built – Scylla II, the magnetic field will be power crowbarred at one of its 60-kilogauss peaks, and allowed to rise to about 330 kilogauss at the center of the mirror and 500 kilogauss at its ends. One is faced with a problem of material strength here. (The static strength of copper is 300 kilogauss.) The coils are being constructed of heavy beryllium copper, reinforced with steel and massively clamped.

IXION

This is an $E \times B$ rotating plasma apparatus in which a generally radial electric field is imposed upon a slowly pulsed magnetic mirror field. In the present machine the magnetic field on the central plane has a maximum strength of 10 kilogauss, and the mirror ratio is 2.2.

¹H. P. Furth, M. A. Levine, and R. W. Waniek, *Scientific American* 198, 28 (1958).

In designing this coil, care was taken to choose a magnetic mirror with a central region of fairly uniform magnetic field and fairly large length-to-diameter ratio in order that the drift orbits about the axis change adiabatically as the mirrors are approached. It is desirable to know the positions of the flux surfaces with reasonable accuracy.

In designing the present coil, we used a Wakefield resistance analog board.² The principle of such a board (see Paper 18) is illustrated in Fig. 47. The lower horizontal line corresponds to the z axis of symmetry of the magnetic field and is divided into a number of segments by means of terminal pins between which resistors are soldered. Each vertical column is similarly divided by terminal pins, dividing the radii correspondingly. Thus the analog of an r - z plane marked off by lattice points separated by a distance Δ is a board of terminal pins connected by resistances which are integral and half-integral multiples of a fundamental value R . (R has the value 100 ohms on the Los Alamos board.) Figure 47 also shows the differential equation for the flux function ψ in terms of current density j , as well as the corresponding difference equation at some lattice point denoted by $(0, 0)$. The analog quantities measured on the resistor board are the voltages V_{ij} and the pin currents I_B .

The Ixion coil was designed by trial and error and built in close physical approximation to the arrangement of pin currents of the analog board. After its construction, the coil was excited with 60-cycle alternating current, and measurements were made by means of "flux" coils. Two such

²K. E. Wakefield, *A Resistance Analogue Device for Studying Axially Symmetric Magnetic Fields*, NYO-7313 (1956).

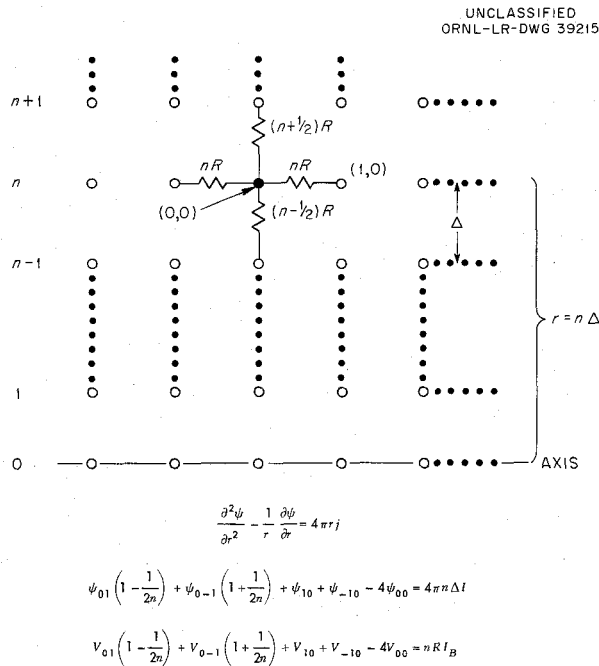


Fig. 47. Principle of the Wakefield Resistance Analog Board.

coils are shown in Fig. 48, mounted concentrically for simultaneous measurements at two radii. A number of coils of accurately known radii were used, and their induced voltages were measured as functions of axial position z . Curves of constant induced voltage per coil turn (i.e., constant flux) were plotted on the r - z plane and represented the B lines of the coil.

Figure 49 shows a quadrant of the Ixion coil, drawn on the r - z plane. The curves are the B lines derived from the analog board for a current distribution indicated by the solid black squares. The actual windings are shown in cross section as open rectangles. Measured fluxes corresponding to the values of the analog curves are indicated by the solid circles. The values of coil inductance and its sensitivity, in gauss per ampere of excitation, were also found to be in good agreement with those derived from the analog board.

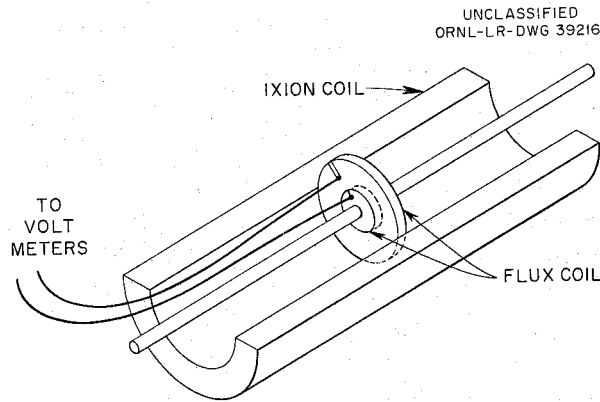


Fig. 48. Flux Coils Used to Determine the Shape of the Ixion Mirror Field.

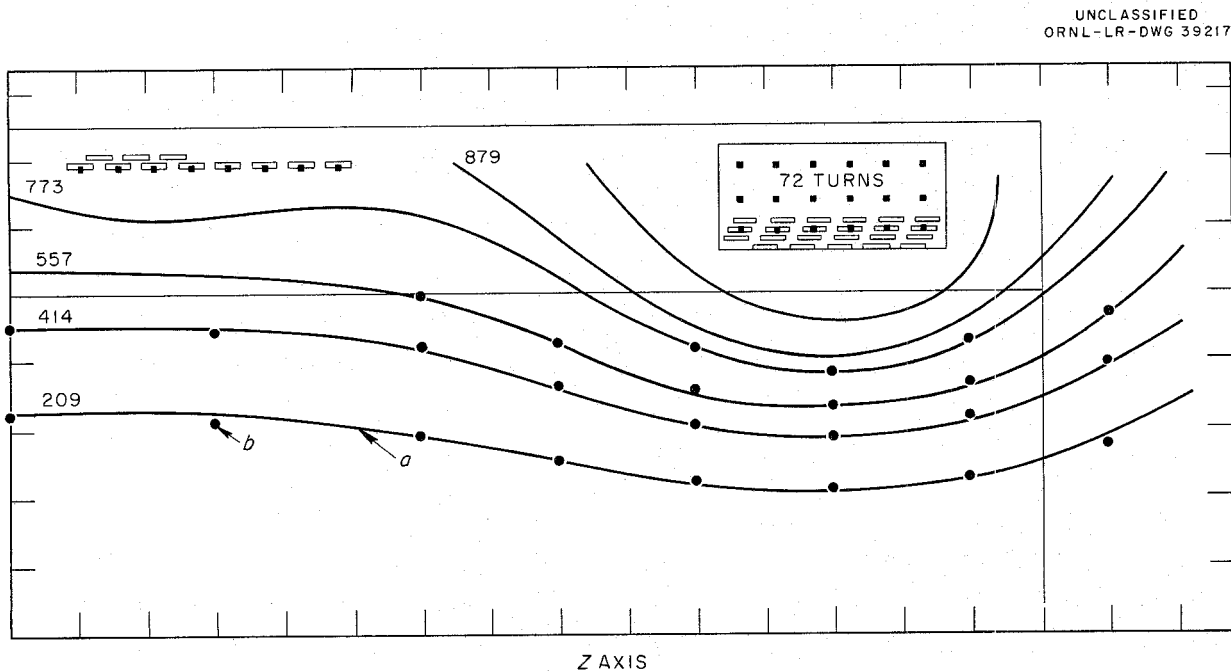


Fig. 49. Shape of One Quadrant of the Ixion Mirror Field. (a) As derived from the resistance analog board; (b) as determined by voltage induced in flux coils.

Much experimental work at Los Alamos has been concerned with pinch machines, both toroidal (Perhapsatron) and straight (Columbus). The letter S in their designations refers to the fact that their plasma and conductor configurations are such as theoretically to stabilize them against growing hydromagnetic surface disturbances.

PERHAPSATRON S-4 AND S-5

In the S-4 machine, a quartz torus of 14-cm minor diameter and 70-cm major diameter is surrounded by a hollow toroidal aluminum primary 0.5 in. thick. The plasma itself forms the secondary of the transformer which is driven at two feed points by two 20-kv, 45,000-joule capacitor banks. In order to increase the coupling between primary and secondary, the torus is linked by two iron cores made up of 2-mil laminations, weighing a total of two tons.

The 2-mil laminations of the S-4 core were chosen rather conservatively on the basis of the skin depth of the iron ($\mu \approx 600$) at the frequencies expected to be involved in the discharge. As a result of suggestion by Stirling Colgate that considerably thicker laminations could be used, the subject of required lamination thickness was investigated.³ This was particularly important in designing the cores of the new and larger S-5 machine, since their cost could be reduced by a factor of 2.5 by using 4-mil, instead of 2-mil, laminations.

In designing the laminations of a transformer core, the thickness should be chosen as that which can just be penetrated by the magnetic fields during the times they exist. One is first led to visualize a diffusion type of field penetration like that indicated for $\mu = 600$ in Fig. 50 (upper left). However, owing to leakage there is usually plenty of magnetic field to saturate the iron. Under this condition, its permeability approaches unity, and the field penetrates faster. At a given time the field distribution is more nearly like that shown by the curve with the flat horizontal portion.

The experimental arrangement for testing core laminations is shown in the upper right-hand portion of Fig. 50. The volt-second product VT of the input signal was kept constant at the value which saturated the core at 60 cps. The ratio ϕ/VT of the core flux to the input volt-seconds was then plotted vs the duration of the input pulse as indicated in the lower graphs of Fig. 50. It was found that a 12-mil lamination actually became filled with flux in a considerably shorter time, compared with a 4-mil lamination, than would be expected on the basis of magnetic field diffusion at full permeability. Figure 51 shows the Perhapsatron S-5 torus with its four linking cores.

COLUMBUS S-4

This is a straight pinch apparatus having a 13-cm inner diameter and a length of 61 cm. It is driven by a 20-kv capacitor bank of 15,000 joules. In such an apparatus stabilization of the plasma is sought by applying an axial magnetic field B_z , which is most almost entirely swept inward with the plasma as the pinch is formed. Stabilization of hydromagnetic disturbances is

³We are indebted to R. Carruthers for pointing out that this subject was investigated in connection with the British radar program. Cf. TRE Journal *ca.* 1954.

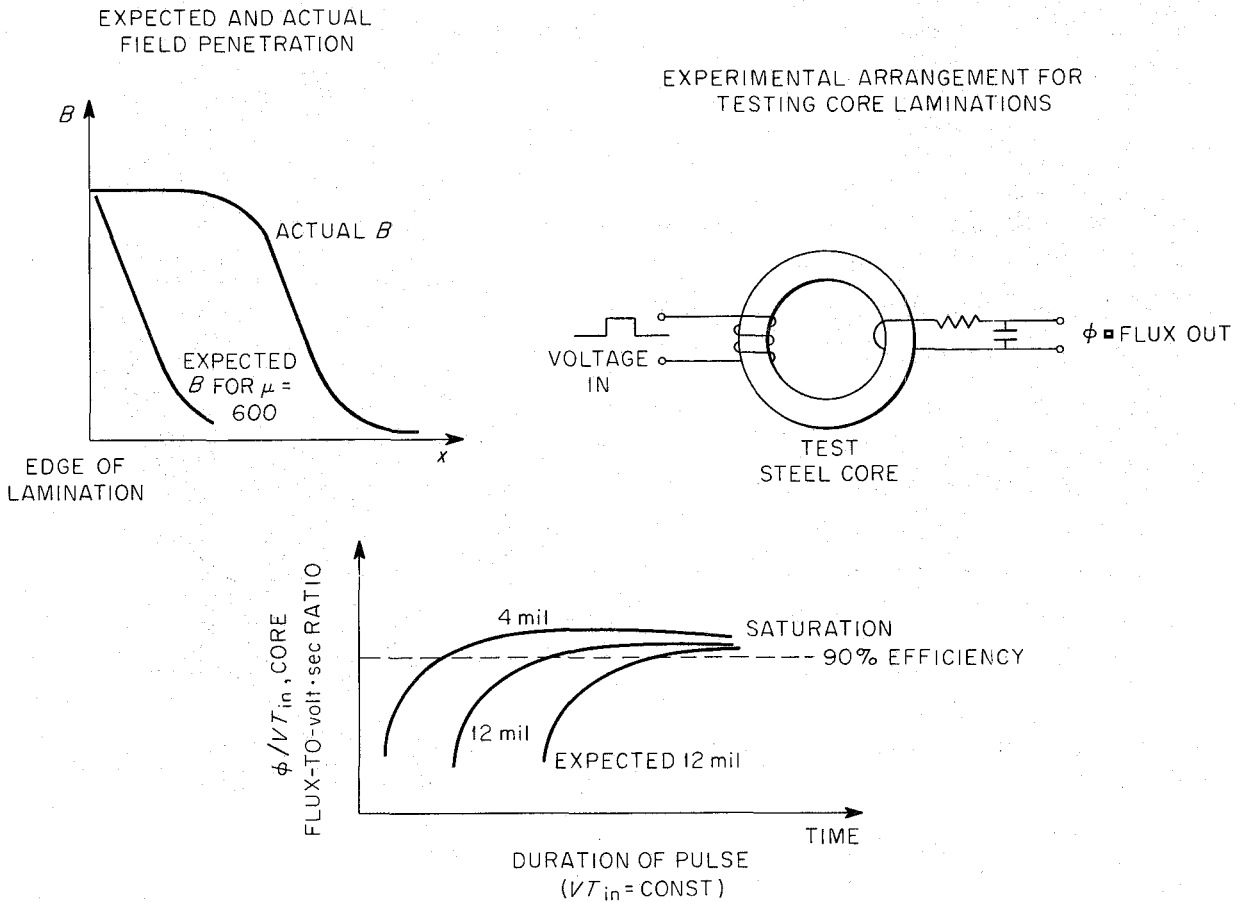


Fig. 50. Magnetic Field Penetration of Transformer Core Laminations.

brought about largely by the "shear" of the magnetic field as its direction varies from axial, inside the pinch, to azimuthal ($B_z = 0$), outside the pinch surface.

In order to increase the magnetic shear it was desirable further to decrease the outer B_z field, so that its direction outside the pinch was the reverse of that inside the pinch. This required operating a fast " B_z " capacitor bank capable of driving a solenoid which would generate the reverse field after the pinch was formed. A schematic diagram of the slow 3-kv capacitor bank for generating the initial B_z , as well as the fast 20-kv bank for reverse B_z , is shown in the upper portion of Fig. 52. In the lower portion is shown an oscillogram indicating reversal of the current in the B_z winding in about 3 μ sec.

In a stabilized pinch machine the discharge is usually surrounded by a thick conducting metal current return which is slotted to admit B_z . The B_z solenoid is wrapped around the metal return shell as shown in Fig. 53 (upper left).

In the case of a rapidly changing magnetic field, the skin effect is nearly complete, and the presence of the conducting return leads to the interesting field distortion shown in the top view

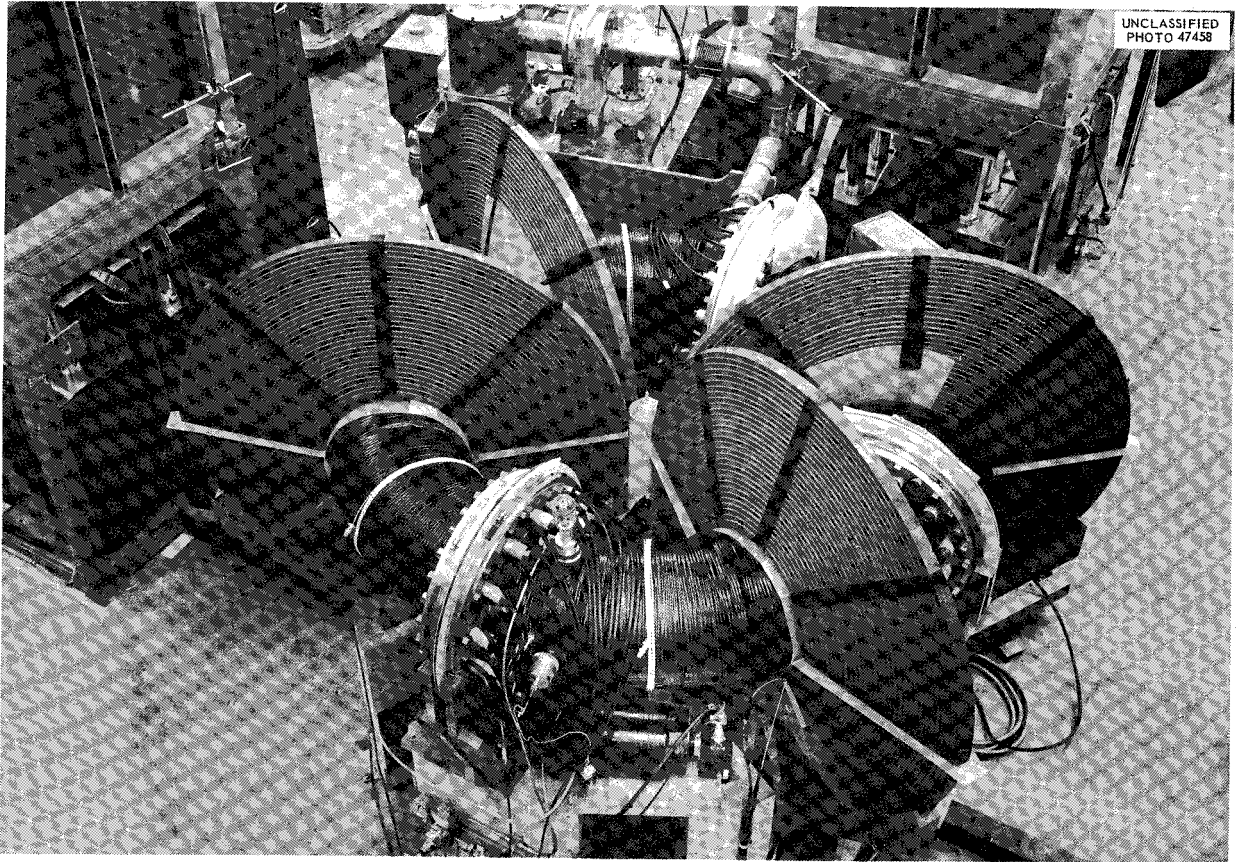


Fig. 51. Perhapsatron S-5 Torus Showing Its Four Linking Cores.

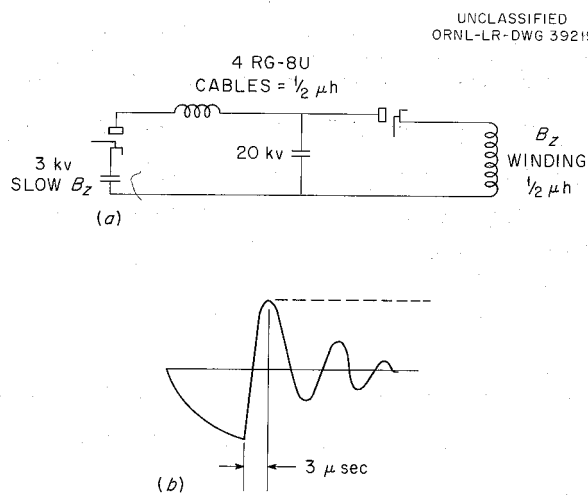


Fig. 52. (a) Circuits for Generating Initial Slow (3-kv) and Reverse Fast (20-kv) B_Z in Columbus S-4; (b) Oscillogram Showing Reversal of Current in B_Z Winding.

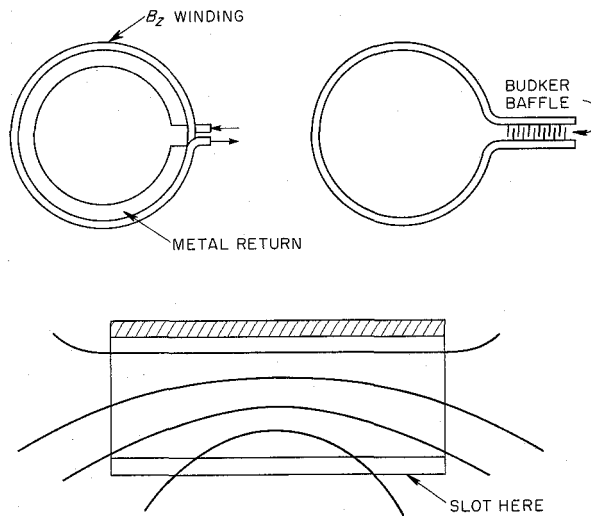


Fig. 53. Columbus S-4 Solenoid Winding and Field Distortion.

section in the lower part of the figure. The magnetic lines can bend out through the slot but must be parallel to the conductor wall at the opposite side of the cylinder. Such distortion could have the undesirable effect of connecting the pinch discharge to the walls at the slotted side of the conductor. One interesting solution of such distortion might be the "Budker baffle" (Fig. 53, upper right), which passes only straight B lines through its teeth. Another approach is to decrease the field weakening at the ends of the B_z solenoid by concentrating the ampere turns at the ends. In doing this, one must take account of the fact that in a fast B_z solenoid the coils are paralleled across a bus of constant voltage in order to obtain a low solenoid inductance. Thus the flux per coil is nearly constant, and one increases the field at the ends by providing coils of fewer, rather than more, turns as in a constant current arrangement.

In practice it seems that the distortion effects of fringing are minimized by the pinch itself which seems to hold the B lines parallel to the axial direction.

INTERNAL DISTRIBUTION

1. L. G. Alexander
2. R. G. Alsmiller
3. C. F. Barnett
4. M. C. Becker
5. P. R. Bell
6. C. E. Bettis
7. E. S. Bettis
8. D. S. Billington
9. E. P. Blizard
10. C. W. Blue
11. R. L. Brown
12. C. E. Center (K-25)
13. R. A. Charpie
14. R. E. Clausing
15. D. L. Coffey
16. F. L. Culler
17. R. A. Dandl
18. R. C. Davis
19. S. M. DeCamp
20. R. R. Dickison
21. J. L. Dunlap
22. H. O. Eason
23. R. S. Edwards
24. L. B. Emler (K-25)
25. J. L. Fowler
26. T. K. Fowler
27. J. E. Francis
28. J. H. Frye, Jr.
29. W. R. Gambill
- 30-32. W. F. Gauster
33. J. H. Gibbons
34. R. A. Gibbons
35. W. R. Grimes
36. E. Guth
37. D. P. Hamblen
38. C. S. Harrill
39. C. C. Harris
40. A. Hollaender
41. A. S. Householder
42. H. C. Hoy
43. R. P. Jernigan, Jr.
44. W. H. Jordan
45. C. P. Keim
46. M. T. Kelley
47. G. G. Kelley
48. R. J. Kerr
49. R. L. Knight
50. F. A. Knox
51. J. A. Lane
52. N. H. Lazar
53. G. F. Leichsenring
54. T. A. Lincoln
55. S. C. Lind
56. R. S. Livingston
57. J. S. Luce
58. J. N. Luton
59. J. R. McNally, Jr.
60. R. J. Mackin
61. W. D. Manly
62. F. T. May
63. C. Michelson
64. K. Z. Morgan
65. O. B. Morgan
66. J. P. Murray (Y-12)
67. R. V. Neidigh
68. J. H. Neiler
69. M. L. Nelson
70. J. Neufeld
71. C. E. Normand
72. C. E. Parker
73. D. Phillips
74. J. F. Potts
75. M. Rankin
76. H. Postma
77. R. G. Reinhardt
78. P. M. Reyling
79. M. T. Robinson
80. P. W. Rueff
81. W. K. Russell
82. H. E. Seagren
83. E. D. Shipley
84. A. Simon
85. M. R. Skidmore
86. M. J. Skinner
87. A. H. Snell
88. W. L. Stirling
89. R. F. Stratton, Jr.
90. R. A. Strehlow
91. J. A. Swartout
92. E. H. Taylor
93. A. Tell
94. R. E. Toucey

- | | |
|----------------------------------|---|
| 95. R. M. Warner | 109. E. G. Harris (consultant) |
| 96. H. L. Watts | 110. H. Lewis (consultant) |
| 97. A. M. Weinberg | 111. F. E. Low (consultant) |
| 98. E. R. Wells | 112. H. S. Snyder (consultant) |
| 99. T. A. Welton | 113. Sherwood Reading File (P. R. Bell) |
| 100. G. K. Werner | 114. Sherwood Reading File (V. Glidewell) |
| 101. G. C. Williams | 115. Biology Library |
| 102. C. E. Winters | 116. Health Physics Library |
| 103. W. L. Wright | 117. Reactor Experimental Engineering Library |
| 104. O. C. Yonts | 118-119. Central Research Library |
| 105. A. A. Blank (consultant) | 120-139. Laboratory Records Department |
| 106. W. R. Chambers (consultant) | 140. Laboratory Records, ORNL RC |
| 107. M. W. Garrett (consultant) | 141. ORNL - Y-12 Technical Library,
Document Reference Section |
| 108. O. G. Harrold (consultant) | |

EXTERNAL DISTRIBUTION

- 142-143. Massachusetts Institute of Technology (1 copy each to H. H. Kolm and D. R. Whitehouse)
- 144-145. Los Alamos Scientific Laboratory (1 copy each to F. L. Ribe and H. L. Laquer)
- 146-151. Princeton University (1 copy each to R. G. Mills, H. G. Johnson, F. H. Tenney, K. E. Wakefield, U. Christensen, and F. J. Arnaud)
- 152-153. Lawrence Radiation Laboratory, University of California, Livermore (1 copy each E. I. Hill and A. F. Waugh)
- 154. Air Force Cambridge Research Center, Geophysics Research Directorate, Bedford, Mass. (M. Levine)
- 155. Lincoln Laboratories, Lexington, Mass. (S. Foner)
- 156. Division of Research and Development, AEC, ORO
- 157-750. Given distribution as shown in TID-4500 (15th ed.) under Controlled Thermonuclear Process (75 copies - OTS)



